

**ELEMENTARY THEORY OF THE UNIFIED FIELD©**

2011

R. H. Dishington

## ACKNOWLEDGEMENT

The author thanks, for help in many forms over a span of years,

R. L. Kirkwood                      D. J. Margaziotis  
L. O. Heflinger                      T. Hudspeth  
B. H. Meuller                      G. Ialongo  
R. S. Margulies

## I. INTRODUCTION

Since 1989, a rigorous unified field theory that combines *classically* corrected electromagnetism and gravitation has been available.<sup>1</sup> However, for obvious reasons, the rigor required to achieve acceptance is far greater than that needed for a clear understanding of its day to day use. The following is an attempt to offer a reduced version that illustrates the simplicity of the underlying physics. Those who need more rigor, should consult PHYSICS 2001Rev (2009).

Taking guidance from Einstein, who pursued a *deterministic*, unified field theory<sup>2</sup> through the last years of his very productive life, and taking advantage of 100 years of *new* experimental data, Einstein's belief in the necessity to base the General Theory on an ether is accepted here and furthered by gleaning the ether's properties from the old and new data. *The simplicity of the ether concept rests in the idea that there is only one, single substance filling all space.* In all regions of space an enormous amount of ether is present. Where particles and waves are observed, they represent tiny dimples, ether distortions, in the great overall ether average. The ether's equations of motion yield everything in the universe, and *the whole of physics is contained in the ether's properties.*

You have been told by "modern" physicists and their written word that *there is no ether.* You have also been told, by Lorentz, Einstein and others that *there is an ether.* Surprisingly, you yourself perform an experiment every day that demonstrates the ether's existence.

Experiments are conducted with equipment (eg. rods and clocks) used to measure, among other things, length and time intervals. These rods and clocks, as well as *the investigators, themselves, are made of particles that are quite flexible.* Lorentz and others have shown that the particles *change shape when accelerated with respect to the ether;* although, *at any constant speed, they maintain the particular distorted shape that corresponds to that speed.* This affects the length of real rods and the time intervals indicated by real clocks in motion with respect to the ether, so that the rods shorten and the clocks run slower.

- 
1. R.H.Dishington, PHYSICS, Beak Publications, Pacific Palisades, CA (1989).  
....., PHYSICS 2001, Beak Publications, Pacific Palisades, CA (2001).  
....., PHYSICS 2001 Rev, <http://www.lafn.org/~bd261> (2009).
  2. A.Einstein, "Ether and the Theory of Relativity" an address delivered at Leyden in 1920; Translation printed in Sidelights on Relativity, p1, Dover Publications, N. Y.  
....., "Uber den Aether", Verh.Schweiz.Naturf.Ges., **105**, p85 (1924).

*Even more important is the fact that a lab worker (or you in your car) can know immediately if there is acceleration with respect to the ether, because one feels the acceleration as his body particles are changing shape. Acceleration with respect to the ether is **absolute**, for if several observers are accelerating towards or away from each other, there is no question as to who is accelerating with respect to the ether. Any one who is, can measure just how much, using a plumb bob and spring scale or any other form of accelerometer. Acceleration with respect to the ether is the most direct way to verify the ether's existence.*

On the other hand, in a lab moving at *constant* speed with respect to the ether, a worker *cannot* sense the ether or his motion, *since his body particles are not changing shape*. Furthermore, a plumb bob and spring scale will not indicate his motion or the ether's presence. It was to these constant velocity *inertial* labs that Einstein's 1905 statement that the ether is superfluous made reference. But, even in inertial labs, many physical phenomena require the ether as a cause for observed effects, unless one is willing to accept the miracle working space-time. All this is familiar to anyone who has driven a car (a personal lab) at constant speed on a straight freeway, and then has put on the brakes or stepped on the gas.

A *classical* physicist's tools include intuition, visualization, cause-and-effect, theory, experiment and measurement, mathematics and determinism. Armed with these, during the past 400 years a partially complete picture of the world has been found in *descending layers of abstraction*, starting with the galaxies, going down to the standard, molecular, atomic, sub-atomic and sub-particle levels, below which is an unexplained *metaphysical base*. The highest and the lower few levels are the frontiers of physics. Early in the 20<sup>th</sup> century, "modern" physicists traded determinism for statistics and gave up visualization and cause-and-effect. In their own words, visualizing the atomic and particle levels in the same way as the levels above is "**impossible**". This is simply not true. By avoiding "point particles", applying statistics only to *ensembles* and correcting several errors still written in all present textbooks on electromagnetism and gravitation, a *deterministic* visualization of the lower levels is available.<sup>1</sup>

## II. THE METAPHYSICAL BASE

In principle, an ideal theory of the world would answer all questions with no remaining metaphysical base, an unlikely possibility. The next best goal is a theory with a minimum of unanswered questions, and that is achieved by pushing the unanswered questions lower and lower in the layers of abstraction. No attempt will be made here to choose a metaphysical base and argue in its defense. That is not the job of physics. The job of physics is to explain the various levels of abstraction

in such a way that the metaphysical base is pushed down to the lowest possible level. Whatever metaphysical base then results will be accepted. If properly done, that metaphysical base will be as unexplainable as the beginning and end of time; but all the levels above will be intuitive and simple, and no paradoxes will extend up into those levels of abstraction. The metaphysical base that resulted from preparing the present work is:

1. The existence of the *real* world is *assumed*.
2. Measurement, carried out by experimenters, is in no way necessary for the real world's *existence* or *functioning*.
3. Space is absolute - a place.
4. Time is the sequence of events, not as they are measured, but as they occur.
5. Space is filled with a substance called ether, whose properties are unknown except for the few to be discussed in this work.

Here, space is Newton's absolute space<sup>3</sup>, an uncurved, euclidean place of large extent; exactly as the intuition indicates. Time is Newton's absolute time<sup>3</sup>, the sequence of events, not as they are measured but as they occur; again in agreement with the intuition. The *fact* that space is filled with ether is part of the metaphysical base, but the ether's properties are not. They are clearly part of the theory; since, until they are correctly specified there could be alternative ways to describe the ether. In the present theory, the ether is the lowest level of abstraction. Speculation beyond its equations of motion, questions related to its sub-structure, will not be dealt with here, being regarded as meaningless. Certainly, no description of its nature using the words particle, mass, charge, energy or momentum is permissible. All of these properties are derivable from the ether itself. The five items listed earlier, then, *represent the total metaphysical base that results from the specific theory developed here*.

### III. THE UNIFIED FIELD

Looking out, the world gives the impression of being a vast empty room in which, at a few scattered places, something special exists. This something special appears to take on various forms, sometimes as waves moving at high speed, sometimes as particles, moving or at rest, generally following an observable sequence of events. Early on, these configurations were given separate names, such as mass or energy, although finally it was realized that they were all just energy in different forms, conserved in passing from one form into another. Ultimately, because one form of energy seemed to be purely wave-like, the feeling

---

3. I. Newton, Principia Mathematica, (1686); translated by F. Cajori, University of California Press, p6 (1946).

developed that there was a more fundamental substance called the *ether* in which energy was a configuration or a form of motion. This concept will be accepted here, and will be the basis for the development of the unified field theory.

In the great blank regions, between the specks where energy is located, the ether has essentially a constant density  $\phi_d$  (ether/cm<sup>3</sup>), defined here as the *datum*. Where there appear to be particles (energy bundles) or waves, the ether is *distorted* into specific kinds of patterns. Early physicists pictured the ether as the datum with waves and solid objects moving in it; but by the end of the 19<sup>th</sup> century they were trying to show that there is only ether in space, constant or distorted. That is the visualization developed here. Where the ether is distorted away from  $\phi_d$ , the absolute density (ether/cm<sup>3</sup>) is defined as  $\phi_a$ ; and, for particles at rest relative to the datum ether, there are several *implicit* distortions such as  $\phi_a$  itself, or  $\frac{1}{2}(\nabla\phi_a)^2$ , or  $\nabla^2\phi_a$ , or others. Some of these produce such important effects in particle or field interactions that they are given specific names such as "energy" or "charge", etc. However, the important thing to understand is that *there is nothing in space but the ether density  $\phi_a$* . All the other "named" quantities are just implied in the shape of the  $\phi_a$  field.

Once the properties of the ether are specified, the unified theory is complete; i.e. the theory and a statement of the ether's properties are synonymous. A complete description of the ether has two parts; visualizable definitions of certain of its physical characteristics, and a few formal equations giving a shorthand description of the relationships between those physical properties. The *equations* are listed in APPENDIX A, but the main thrust here is in the *visualization*, which will be described in the following.

### Units

Unless the visualization is made quantitative, it is just speculation; so it is necessary to choose a system of units. The units closest to the physics are called Heaviside-Lorentz. However, they have all but disappeared. Rather than have readers relearn the old names, in this series of write ups the unit names are the same as in the common systems (mks, esu, emu, etc.) with hl appended. For example, the table in APPENDIX B converts hlvolts to mksvolts and vice versa.

### The Ether's Properties

To start, some of the ether's important properties are:

- a. The ether is an invisible, conserved, compressible *fluid*.
- b. At any one absolute time t, at each absolute space point x,y,z, the ether has a positive absolute density  $\phi_a$  (ether/cm<sup>3</sup>) that varies from point to point.
- c. Over large volumes, the average, datum ether density is  $\phi_d$ .

- d. The incremental ether density  $\phi$  at each point is defined as  $\phi_a - \phi_d$ , and can be positive or negative.
- e. At any one absolute time  $t$ , at each absolute space point  $x, y, z$ , the ether has three velocity components  $V_x, V_y, V_z$ .
- f. In regions of space far from energy (matter),  $\phi_a = \phi_d$  and  $\phi = 0$ .
- g. An observer considering a large region free of energy is called an absolute observer if the datum ether has zero velocity everywhere as seen by him.
- h. Questions related to other observers moving at constant velocity relative to the absolute observer are dealt with later under rods and clocks.
- i. If energy in the form of waves or particles is introduced into the region, the absolute observer sees a four variable field  $\phi_a, V_x, V_y, V_z$  varying with  $x, y, z$  and  $t$  ( $\phi = V_x = V_y = V_z = 0$  at  $\infty$ ).
- j. The laws of physics can be written as non-linear, partial differential field equations relating the field variables and  $x, y, z$  and  $t$  (see APPENDIX A).

The *mathematical* theory of fields involves functions that are single valued (uniform), finite, continuous, and have continuous derivatives. None of the examples of physical fields (fluids, gasses, etc.) usually discussed in textbooks satisfies these requirements rigorously because of the *particulate* structure of matter. However, the match between the field mathematics and the physics in the case of the ether is exact; because the ether is a perfect continuum. *It is not composed of elements of the periodic table, it is basic.* It is a *frictionless* fluid, of great compressibility, but has no mass, i.e., it has no inertia or linear momentum per se and is not directly affected by gravitation. Therefore, it does not obey Newton's laws or any of their derivatives such as the Navier-Stokes equation, etc. Dynamically it will remain unspecified until later, kinematically it behaves as a perfectly compressible fluid, a continuum.

Later, the ether will be described primarily by its absolute density  $\phi_a$  and its velocity  $\mathbf{V}$ . The incremental density  $\phi$  is an alternative representation for the density because of the assumption that the average density over all space is a constant  $\phi_d$ . Far out from all matter and energy, the ether density is visualized as actually having the datum value  $\phi_d$ . Consequently, at any point where ether has space and time variations it is possible and often considerably more convenient to use the incremental density,

$$\phi = \phi_a - \phi_d \quad . \quad (1)$$

The fact that  $\phi_d$  is a constant ensures that space and time derivatives of  $\phi$  and  $\phi_a$  are equal. An important difference between  $\phi$  and  $\phi_a$  is that  $\phi_a$

has only positive values, representing the actual density in space, whereas  $\phi$  can be positive or negative as  $\phi_a$  is greater or less than the average value  $\phi_d$ . When referring to the ether, the word *density* (ether/cm<sup>3</sup>) will be applied to both  $\phi_a$  and  $\phi$  throughout, and it will be left to the reader to keep in mind the difference between them.

It is clear from the preceding, that the ether has only a few simple properties, each of which is *visualizable*. All that is required to complete its description is a set of formal relationships that connect these various properties. However, before presenting the details of the unified field, a few corrections to the usual textbook description of the failure of "classical" Electricity and Magnetism will be useful later on.

#### IV. CORRECTED CLASSICAL E&M

Modern physics textbooks describe the failure of "classical" E&M. Yet, except for a few incorrect results, classical physics makes up a large part of the present theory in the form of Maxwell's equations. There were three principal things classical E&M did wrong:

1. It ended up with "point" particles.
2. It defined electric and magnetic energy incorrectly (often attributing a particle's kinetic energy to its magnetic field).
3. The Poynting theorem failed to correctly describe energy flow except for radiation.

At present, all of these problems are carried over into Quantum Mechanics. Fortunately, they have the simple solutions presented here.

There are no "point" particles

By the 1870's Maxwell had completed his equations for electromagnetic fields in labs *at rest in the ether*, but he questioned their applicability in labs *moving through the ether* (e.g. earth labs). In 1905, Einstein published a clock setting technique that allowed Maxwell's equations to be used in moving labs. In the following, when Maxwell's equations are used, it is the potential form (Heaviside-Lorentz units),

$$\nabla^2\phi - \frac{1}{c_0^2} \frac{\partial^2\phi}{\partial t^2} = -\rho \quad , \quad \nabla^2\mathbf{A} - \frac{1}{c_0^2} \frac{\partial^2\mathbf{A}}{\partial t^2} = -\frac{\mathbf{J}}{c_0} \quad , \quad \nabla\cdot\mathbf{A} = -\frac{1}{c_0} \frac{\partial\phi}{\partial t} \quad , \quad (2)$$

that is referred to. Any solution of Eq.(2) provides a unique solution of the **E** and **B** form of Maxwell's equations as well. The two sets of equations are completely equivalent in that respect. However, although **E** and **B** correctly represent forces acting on charged particles, for moving particles and waves they give erroneous visualizations of electric and magnetic energy density contributions. In Eq.(2),  $\phi$  is related to the *measured* incremental ether density and **A** is related to the *source* of the magnetic field. For this reason, in ether discussions, Eq.(2) is preferred.

At present, the most commonly used solution of these equations for a spherically symmetrical, charged particle at rest is,

$$\phi = \frac{q}{4\pi r} \quad , \quad (3)$$

where  $q$  is the total "charge" on the particle. The distributed charge density  $\rho$  that matches the solution is found by substituting Eq.(3) in Eq(2), with the result (at rest, spherical coordinates),

$$\rho = -\nabla^2\phi = -\frac{1}{r^2} \frac{d}{dr} \left( r^2 \frac{d\phi}{dr} \right) = \left( \frac{q}{2\pi r^3} - \frac{q}{2\pi r^3} \right) = 0 \quad . \quad (4)$$

The *electric* energy density in the field of this particle at rest is,

$$\epsilon_e = \frac{1}{2}(\nabla\phi)^2 = \frac{1}{2} \left( \frac{d\phi}{dr} \right)^2 = \frac{q^2}{32\pi^2 r^4} \quad , \quad (5)$$

which, when integrated from any sphere of arbitrary radius  $r_0$  to  $\infty$  gives a total energy  $E_0$  *outside*  $r_0$ ,

$$E_0 = \frac{q^2}{16\pi r_0} \quad . \quad (6)$$

This is clearly not a "physical" solution of Maxwell's scalar equation, because, from Eq.(4), *there is no charge anywhere in the field*, just a mysterious something that is concentrated at the "point" center, although it influences other particles all the way out. Meanwhile, if the "classical" electron radius is entered for  $r_0$  in Eq.(6), the result is the *measured total rest energy* of the electron, all outside  $r_0$ , leaving the *infinite* energy found between  $r = 0$  and  $r_0$  to be explained away. The process used in quantum mechanics for dealing with this, introduced by Feynman, is to just ignore the infinity. He expressed dissatisfaction with what he called *normalization*, but offered no alternative. Dirac wrote a diatribe against it. Here the conclusion is, there are no "point particles."

#### A finite particle solution of Maxwell's scalar equation

A solution of Maxwell's scalar equation,

$$\nabla^2\phi = -\rho \quad , \quad (7)$$

that eliminates the infinities of the "point" charge is required. That simple, at rest, finite spherical solution is,

$$\phi = \phi_0(1 - \psi^2) \quad , \quad (8)$$

where  $\psi$  is the shape factor,  $\psi = e^{-r_i/r}$ . Figure 1 indicates that *this potential has only two significant features*, the center value  $\phi_0$  (positive or negative) and the radius  $r_i$  of the inflection point.



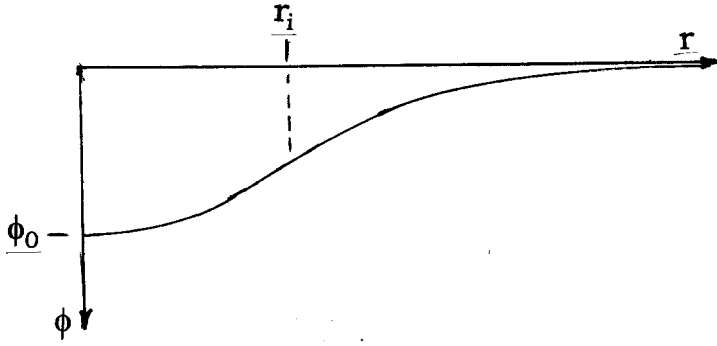


Figure 1

The corresponding charge density distribution required to complete the solution is found by substituting the solution Eq.(8) in Eq.(7) to yield,

$$\rho = 4 \frac{\phi_0 r_i^2}{r^4} e^{-2r_i/r} \quad , \quad (9)$$

a smooth shell of charge distortion that peaks at half  $r_i$ . Integrated over all space, the total charge is  $q = 8\pi\phi_0 r_i$ .

Similarly, the at rest *electric* energy density distribution is found from,

$$\epsilon_e = \frac{1}{2}(\nabla\phi)^2 = 2 \frac{\phi_0^2 r_i^2}{r^4} e^{-4r_i/r} \quad , \quad (10)$$

a smooth shell of energy distortion that peaks at the inflection radius  $r_i$ . If  $\epsilon_e$  is integrated over all space, the resulting finite energy is  $E_0 = 2\pi\phi_0^2 r_i$ .

Just to get some idea of the magnitudes involved, if the potential in Eq.(8) is assumed to represent an electron, then using  $E_0 = 8.18711 \times 10^{-7}$  ergs (0.511 MeV) and  $q = -e = -1.7027 \times 10^{-9}$  hcoul ( $-1.6022 \times 10^{-19}$  C), the center potential and inflection point radius are  $\phi_0 = -1.9233 \times 10^3$  hlvolts (approx.  $-2 \times 10^6$  V) and  $r_i = 3.522 \times 10^{-14}$  cm.

#### The "point charge" electron "measurement"

In the *finite* solution, any potential level is always closer to the center than the corresponding potential in the "point" charge field, i.e., the finite particle has a smaller diameter. It is also important to notice that the expansion of the gradient of Eq.(8),

$$\frac{d\phi}{dr} = -2 \frac{\phi_0 r_i}{r^2} \left( 1 - 2 \frac{r_i}{r} + 2 \frac{r_i^2}{r^2} - \dots \right) \quad r > r_i$$

reduces to  $d\phi/dr \cong e/4\pi r^2$  (for  $r > 200r_i$ ), the Coulomb field of the "point charge". This explains why the well known collision experiments<sup>4</sup> that appear to support the "point charge" electron model are also in complete agreement with the present, finite solution. At low collision energies, the principal interaction is out in the Coulomb region. As the collision energy is increased, the Lorentz contraction of the gradient causes the inner, non-Coulomb volume to shrink, and the interaction never catches up with that inner region.

4. D.P. Barker, et. al., Phys. Rev. Lett., 43, 1915 (1979); Phys. Rev. Lett., 45, 1904 (1980).

### The finite particle in motion

So far, the finite particle solution is satisfactory; but it still must be shown to give the *constant velocity* total energy  $\gamma E_0$ , where  $u$  is the velocity and  $\gamma$  is defined as,

$$\gamma = 1 / \sqrt{1 - \frac{u^2}{c_0^2}} \quad . \quad (11)$$

The calculation begins by going back to Eq.(2) and looking for a finite solution of the full changing field scalar equation,

$$\nabla^2 \phi - \frac{1}{c_0^2} \frac{\partial^2 \phi}{\partial t^2} = -\rho \quad . \quad (12)$$

Paralleling the derivation of Eqs.(8) and (9), the potential of the constant velocity field, moving in the  $x$  direction at velocity  $u$ , is,

$$\phi = \gamma \phi_0 (1 - \varepsilon^{-2r_i/r'}) \quad , \quad (13)$$

where,  $r' = \sqrt{\gamma^2 x^2 + R^2}$  in cylindrical coordinates. Eq.(13) differs from the spherical case of Eq.(8) mainly in that the equipotentials are oblate spheroids; *not because of any longitudinal contraction*, but because *the potential  $\phi$  expands laterally*. The longitudinal contraction of  $\mathbf{E}$  is always emphasized, but *the lateral expansion of  $\phi$  is more significant in relation to energy and charge*.<sup>5</sup>

Substituting Eq.(13) in Eq.(12), the charge density distribution is,

$$\rho = 4\gamma \frac{\phi_0 r_i^2}{r'^4} e^{-2r_i/r'} \quad . \quad (14)$$

The solution in Eq.(13) can be checked by using a Lorentz transformation on the rest solution of Eq.(8). Furthermore, if Eq.(14) is *integrated over all space*, the total moving electron charge is found to be  $q = 8\pi\phi_0 r_i$ , *the same as for the charge at rest*, a well established fact.

### The electric energy density correction

This is the second point at which the classical E&M theory of particle structure breaks down. Conventionally the expression for *electric energy density* is commonly written,

$$\varepsilon_e = \frac{1}{2} \mathbf{E}^2 = \frac{1}{2} \left( -\nabla\phi - \frac{1}{c_0} \frac{\partial \mathbf{A}}{\partial t} \right)^2 \quad . \quad \text{WRONG} \quad (15)$$

This form works for radiation propagation (where  $\nabla\phi$  is zero), but in other applications (in association with the Poynting theorem) it has led to a long, confusing literature of strange paradoxes and suggested alternatives<sup>6</sup>. If Eq.(15) is integrated over all space, it fails to give a total energy  $\gamma E_0$ . Combinations of Eq.(15) and the  $\mathbf{B}$  field also fail.

---

5. P. Lorrain, D. R. Carson, Electromagnetic Fields and Waves, 2<sup>nd</sup> Ed., W. H. Freeman and Company, San Francisco, p.266, (1970).

6. J.W. Butler, Amer. J. Phys., **36**, 936 (1968); **37**, 1258 (1969).

There are several hints as to why this is so. For example, the conventional definition of *magnetic* energy density is,

$$\varepsilon_m = \frac{1}{2} \mathbf{B}^2 \quad , \quad (16)$$

where  $\mathbf{B}$  is *defined as the magnetic field*,

$$\mathbf{B} = \nabla \times \mathbf{A} \quad . \quad (17)$$

Both the definition of  $\mathbf{B}$  as the magnetic field and  $\mathbf{B}^2/2$  as the magnetic energy density have problems similar to those of  $\mathbf{E}$  and  $\varepsilon_e$ . For example, the  $\mathbf{E}$  field of Eq.(15) and the  $\mathbf{B}$  field of Eq.(16) are so called "force" fields, because, in principle they are measured by inserting a "test" charge at any space point and observing the charge's behavior, i.e. the "force" on it. But, the vector  $\mathbf{B}$  does not point in the direction of either the test charge reaction or that of the current source of the field, but instead points in a non-physically motivated direction that is determined by several conventions. On the other hand,  $\mathbf{A}$  always points in the general direction of the motion of the sources of the field.

Several subtleties appear in the process of defining a magnetic field. Usually the  $\mathbf{B}$  field is regarded as basic, but the Aharonov-Bohm experiment<sup>7</sup> clearly indicates that, even in some situations where  $\mathbf{B}$  is zero, an  $\mathbf{A}$  field can produce magnetic effects on charged particles. Thus, it makes sense to *define the presence of  $\mathbf{A}$  as the magnetic field*. Here  $\phi$  and  $\mathbf{A}$  are considered to be the *fundamental* fields. This leads to an important observation related to Eq.(2). *The equations for  $\phi$  and  $\mathbf{A}$  are completely separate. The solution of the scalar equation just found is purely electric and a solution of the vector equation is purely magnetic.* So Eq.(15) fails because it *mixes* electric and magnetic effects.

Another hint as to the failure of Eq.(15) relates to the *success* of Eq.(12) in defining moving microscopic charge density, for there is an alternative picture of elementary particle structure that gives *insight into the basic nature of microscopic charge and electric energy densities*. If it is assumed that *the potential  $\phi$  is the only physical entity in the electric field*, then the construct in Figure 1 is *the total essence of an elementary particle's bulk nature*, i.e. a specific distortion in the ether. In the "point charge" model, charge is "something" *at the point producing* the field. Electric energy density is even more evanescent.<sup>8</sup> However, as mentioned in Sec.III, the nature of  $\phi$  in the preceding allows a different approach. The microscopic Eqs.(7) and (10) can be considered to *define two secondary implicit distortions*,  $\frac{1}{2}(\nabla\phi)^2$  and  $-\nabla^2\phi$ , *automatically present if  $\phi$  is present. They do **not** cause the field, they are the result of it.*

---

7. Y. Aharonov, D. Bohm, Phys. Rev. **115**, 485 (1959). R. G. Chambers, Phys. Rev. Lett. **5**, 3 (1960).

G. Moellenstedt, W. Bayh, Naturwiss. **45**, 81 (1962).

8. R. P. Feynman, R. B. Leighton and M. Sands, *The Feynman Lectures on Physics I*, (Addison -Wesley, Reading, MA 1963) p. 4-1, 4-2 (last paragraph).

An *erroneous* assumption, adopted almost unanimously around 1900 and still held today, is *that, in the microscopic case, the elements of distributed charge  $\rho$  inside a single particle, for example, individually obey Coulomb's law just as whole charged particles do in the macroscopic case.* Lorentz had doubts,<sup>9</sup> but they did not prevail. However, there is no direct experiment to support this assumption, and electrons, for example, do not fly apart. Thus, *microscopically, there is no reason to expect the distributed "elements" of the  $\phi$  field to produce distant actions on each other such as the Coulomb force, which, macroscopically, results from two **whole particle** fields interacting.* That Eq.(12) gives the correct moving microscopic charge density bears this out.

Now that the physical nature of  $\rho$  and  $\varepsilon_e$  as *secondary* implicit distortions *dependent* upon  $\phi$ , rather than as sources of  $\phi$ , has been indicated, the path to the correct form of *moving* electric energy density  $\varepsilon_e$  is clear. *It should be formulated in exactly the same way that moving charge density  $\rho$  was.*

In going from the rest Eq.(7) to the moving Eq.(12), because of the finite rate of propagation, *the charge density in time variable fields is assumed to change as,*

$$\rho = -\nabla^2\phi \quad \rightarrow \quad \rho = -\square^2\phi = -\left(\nabla^2\phi - \frac{1}{c_0^2} \frac{\partial^2\phi}{\partial t^2}\right) . \quad (18)$$

That this is true is a well verified fact. Considering the *similar* natures of  $\rho$  and  $\varepsilon_e$  as auxiliary distortions implicit in the shape of  $\phi$ , it would be surprising if electric energy density did not have the simple definition, *parallel to Eq.(18),*

$$\varepsilon_e = \frac{1}{2}(\nabla\phi)^2 \quad \rightarrow \quad \varepsilon_e = \frac{1}{2}(\square\phi)^2 = \frac{1}{2}\left((\nabla\phi)^2 - \frac{1}{c_0^2}\left(\frac{\partial\phi}{\partial t}\right)^2\right) , \quad (19)$$

for changing fields. Thus,

$$\boxed{\varepsilon_e = \frac{1}{2}\left((\nabla\phi)^2 - \frac{1}{c_0^2}\left(\frac{\partial\phi}{\partial t}\right)^2\right)}$$

*is offered here as the correct, **complete** definition of electric energy density.* It deserves serious attention, because it not only resolves the many paradoxes, but also leads to Lorentz invariance like Eq.(18). Its success in providing the correct energy of the constant velocity particle

---

9. H. A. Lorentz, *The theory of Electrons*, 2nd Ed. (Dover Publications, Inc., New York 1952) p.215.

warrants its adoption. This can be seen as follows: the implication is that, in addition to spreading out laterally, at each point in the moving field the *rest* electric energy density distortion found from Eq.(10) has increased to,

$$\varepsilon_e = 2\gamma^2 \frac{\phi_0^2 r_i^2}{r'^4} e^{-4r_i/r'} \quad , \quad (20)$$

and when integrated over all space gives a *total* electric energy  $\gamma E_0$ , a well established fact. Thus, a reasonable finite charged particle description has been demonstrated, and the correct form of the moving electric energy density has been derived.

#### Energyless magnetic fields

The correction to the Poynting Theorem can now be developed. It involves some surprising insights into the nature of magnetic fields. Even to this day, the incorrect form of  $\varepsilon_e = \frac{1}{2} \mathbf{E}^2$  and the idea that *all* magnetic fields have energy density  $\varepsilon_m = \frac{1}{2} \mathbf{B}^2$  are used to imply that the magnetic energy in a moving charged particle is in some way responsible for its kinetic energy; but this is not the case. *A particle's kinetic energy is due entirely to the increase of the electric distortion in the laterally expanded  $\phi$  field*, as borne out by the total energy  $\gamma E_0$  integrated above. *A constant velocity charged particle carries no magnetic energy due to its  $\mathbf{A}$  field.* This is similar to the  $\mathbf{A}$  field due to the electron's spin, which is an energy-less magnetic field, i.e. no energy can be added to or removed from it.

The electron's spin and magnetic moment are established when the electron is formed (e.g. in pair production) and are *intrinsic* properties that never change until the electron is annihilated. Because the spin field cannot take on or give off energy, it is essentially an energy-less field. It is true that an electron placed in an external magnetic field can be torqued, and the combined fields will store the interaction energy; but that energy also can be recovered. Neither the electron's spin nor magnetic moment changes during the torquing process, so the stored interaction energy cannot be regarded as part of the spin field energy. The constant velocity electron, then, has two energy-less magnetic fields; its spin field and the one generated by constant velocity motion. These can be ignored in many energy flow calculations, although they can still exert forces on other charged particles, and then the interaction energies (torques, etc.) must be considered.

Because the total moving electron energy  $\gamma E_0$  is 100% electric (i.e. produced only by  $\phi$ ), any energy density associated with the quantity  $\frac{1}{2}(\partial \mathbf{A} / \partial t) / c_0$  that appears in Eq.(14) must be considered as part of the *magnetic* energy density  $\varepsilon_m$ . To emphasize this, the Lorentz force

equation is written,

$$\mathbf{F}_L = q \left[ -\nabla\phi + \left( \frac{1}{c_0} \mathbf{u} \times \nabla \times \mathbf{A} - \frac{1}{c_0} \frac{\partial \mathbf{A}}{\partial t} \right) \right] , \quad (21)$$

where the first RHS term is the *electric* force component and the second and third terms are the *magnetic* force component. Again, this complete separation of electric and magnetic effects is to be expected from Maxwell's Eqs.(2), which show the separation clearly. In light of Eq.(21), the most reasonable way to define magnetic energy density is to assume that each term involves a separate form of energy storage that is not necessarily influenced by the presence of the other forms, so that  $\varepsilon_m$  can be defined as,

$$\varepsilon_m = \varepsilon_v + \varepsilon_t , \quad (22)$$

where  $\varepsilon_v$  and  $\varepsilon_t$  are called the *vortex* and *transformer* components of  $\varepsilon_m$ , represented by,

$$\varepsilon_v = \frac{1}{2} (\nabla \times \mathbf{A})^2 \quad \text{and} \quad \varepsilon_t = \frac{1}{2c_0^2} \left( \frac{\partial \mathbf{A}}{\partial t} \right)^2 . \quad (23)$$

Written out in full,

$$\varepsilon_m = \frac{1}{2} \left( (\nabla \times \mathbf{A})^2 + \left( \frac{1}{c_0} \frac{\partial \mathbf{A}}{\partial t} \right)^2 \right) , \quad (24)$$

where the subscript r indicates that there are serious restrictions in applying Eq.(24). These are the result of there being *two different types of A fields, one that stores energy and one that is energy-less*. Eq.(24) *does not apply to energy-less A fields, even though A is not zero*.

#### Propagating transverse waves

Although layered particles involve only *electric* energy, propagating antenna radiation involves only *magnetic* energy. Radiation comes in two forms, antenna and photon radiation. The latter is not, as yet, understood; but antenna radiation is well described. Except in rare cases, a system of charges and currents, varying in time and confined to a region of dimensions  $d \ll \lambda$ , radiate energy which, at distance  $r \gg \lambda$ , is essentially plane wave. Figure 2 shows this transverse radiation. The

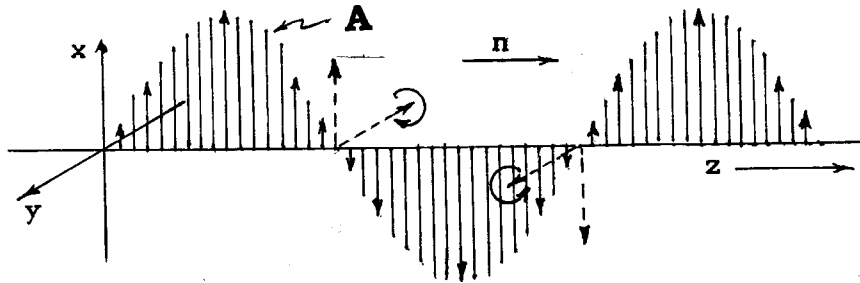


Figure 2. The field pattern of plane wave radiation.

wave propagates in the z direction with velocity  $\mathbf{u} = c_0 \mathbf{n}$ ,  $\mathbf{n}$  being a unit vector. The vector  $\mathbf{A}$  is constant over any x,y plane, and varies sinusoidally along the axis of propagation. Where  $\mathbf{A}$  is maximum, there is no energy density; but  $\varepsilon_m$  increases towards the null regions, where the vortex and transformer energy densities are maximum. At each plane along the wave, the energy is half vortex and half transformer. It also is possible to generate waves that corkscrew circularly polarized.

This picture of wave propagation differs from the conventional, because the position is taken here that *antenna radiation is solely a magnetic phenomenon*, requiring only one magnetic vector field  $\mathbf{A}$  to describe it. The scalar potential  $\phi$  is zero, and the above description says that the amplitudes of the vortex and transformer components of the wave are equal, i.e.,

$$(\nabla \times \mathbf{A})_a = \left( \frac{1}{c_0} \frac{\partial \mathbf{A}}{\partial t} \right)_a . \quad (25)$$

The two components are also perpendicular to each other and to  $\mathbf{n}$ .

#### The old Poynting theorem

The conventional Poynting theorem is written,

$$\frac{\partial \varepsilon}{\partial t} = -\nabla \cdot \mathbf{S}_o - \rho \mathbf{u} \cdot \mathbf{E} \quad , \quad (26)$$

where,

$$\mathbf{S}_o = c_0 \mathbf{E} \times \mathbf{B} \quad , \quad \text{and} \quad \varepsilon = \frac{1}{2} (\mathbf{E}^2 + \mathbf{B}^2) \quad .$$

Eq.(26) supposedly describes the change in energy density at each point in the field as a result of the energy flow away from the point and the work done by the field on the free charge at that point.  $\mathbf{S}_o$  is the old Poynting vector. *Eq.(26) represents a rigorously correct, macroscopic identity derived directly from Maxwell's equations.* However, only in cases of transverse wave radiation propagation do  $\mathbf{S}_o$  and  $\varepsilon$  actually represent energy flow and density.<sup>6</sup> In such cases,  $\phi = 0$ , and the Poynting vector and energy density are,

$$\mathbf{S} = -\frac{\partial \mathbf{A}}{\partial t} \times (\nabla \times \mathbf{A}) \quad , \quad \varepsilon_m = \frac{1}{2} \left( (\nabla \times \mathbf{A})^2 + \left( \frac{1}{c_0} \frac{\partial \mathbf{A}}{\partial t} \right)^2 \right)_r . \quad (27)$$

#### A modified Poynting theorem

In Eq.(27),  $\varepsilon_m$  is not the conventional magnetic energy density but the one newly defined. Then the question arises immediately as to whether there might be another equation, rigorously derivable from Maxwell's Eqs.(2), that would replace the old Poynting theorem with a new magnetic one that works in all cases. Such an equation will be presented here for energy carrying magnetic fields described by Eq.(24).

The rate of change of  $\epsilon_m$  is found from Eq.(24) to be,

$$\frac{\partial \epsilon_m}{\partial t} = (\nabla \times \mathbf{A}) \cdot \frac{\partial(\nabla \times \mathbf{A})}{\partial t} + \frac{\partial \mathbf{A}}{\partial t} \cdot \left( \frac{1}{c_0^2} \frac{\partial^2 \mathbf{A}}{\partial t^2} \right) .$$

Substituting from Maxwell's vector Eq.(2), replacing  $\nabla^2 \mathbf{A}$  with an identity and using the divergence equation in Maxwell's Eq.(2) to convert the third RHS term resulting gives,

$$\frac{\partial \epsilon_m}{\partial t} = (\nabla \times \mathbf{A}) \cdot \frac{\partial(\nabla \times \mathbf{A})}{\partial t} - \frac{\partial \mathbf{A}}{\partial t} \cdot (\nabla \times \nabla \times \mathbf{A}) - \frac{1}{c_0} \frac{\partial \mathbf{A}}{\partial t} \cdot \frac{\partial \nabla \phi}{\partial t} + \frac{\rho \mathbf{u}}{c_0} \cdot \frac{\partial \mathbf{A}}{\partial t} .$$

From here it is easy to show that,

$$\boxed{\frac{\partial \epsilon_m}{\partial t} = -\nabla \cdot \mathbf{S}_m - \frac{1}{c_0} \frac{\partial \mathbf{A}}{\partial t} \cdot \frac{\partial \nabla \phi}{\partial t} + \frac{\rho \mathbf{u}}{c_0} \cdot \frac{\partial \mathbf{A}}{\partial t}} , \quad (28)$$

where,

$$\mathbf{S}_m = -\frac{\partial \mathbf{A}}{\partial t} \times (\nabla \times \mathbf{A}) . \quad (29)$$

Eq.(28) is a *new* Poynting theorem that is rigorously derivable from Maxwell's Eqs.(2) and appears to correctly describe *magnetic* energy flow. Not too surprisingly, the new flow vector  $\mathbf{S}_m$  is exactly the same as the one that has always worked correctly for radiation propagation, i.e. Eq.(27). However, *the magnetic energy density  $\epsilon_m$  is quite different from the one in the old theorem.*

In Eq.(28), the last RHS term describes the work done by the magnetic field  $\mathbf{A}$  on the free charge at each point. A commonly found statement in present textbooks is that the magnetic field does no work on free charges (only turning their paths), but the inclusion of the transformer  $\mathbf{A}$  field as a *magnetic* field changes that. Only the vortex field does no work on free charges.

The second RHS term in Eq.(28) represents the transfer of energy from the magnetic field to an electric field (or radiation).

#### Electromagnetic energy flow

The *new* Poynting theorem appears to give the correct picture of energy flow in all cases so far examined. It does, however, require a significant shift of viewpoint. The fact that *no electric energy appears anywhere, except in the field structure of particles*, is hard to reconcile with already learned conventional thinking. The fact that *all antenna radiation is purely magnetic*, and has no *electric* component is also difficult to become accustomed to. Even more bothersome is the idea of *two kinds of magnetic fields*, energy carrying and energy-less; although the electron's spin field has been known for over 80 years. The best way



to overcome these prejudices is to look at a few examples.

### The Charging Capacitor

A simple example of *electric* energy transport is shown in Figure 3. It consists of an uncharged capacitor connected to a battery by a twisted pair of wires. At the instant the battery is connected to the wires, all their conduction electrons start to drift away from the positive plate and toward the negative plate of the capacitor at an average speed as low as a

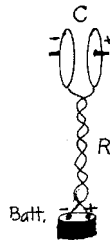


Figure 3. Charging capacitor

fraction of a centimeter per second. For each electron that pops onto the (-) plate, another electron leaves a nucleus on the (+) plate and enters the wire; and during the drift, each electron adds to its rest energy a minute amount of kinetic energy which it draws from the potential field inside the wire. When it arrives at the (-) plate, it stops drifting and stores the minute kinetic energy as interaction energy with the (+) plate nuclei, but it still retains its much larger rest energy. Only the small interaction energies are recoverable from the capacitor. As the process continues, the voltage across the capacitor increases until it equals the battery voltage. Then the current stops.

The total number of electrons moved to the (-) plate is very large. Each electron's rest energy is held inside a sphere of radius roughly  $7 \times 10^{-12}$  cm. Clearly, the recoverable energy stored in the capacitor came through the wires with the electrons. It did not come in through the field outside the capacitor as the old Poynting theorem suggests. Since electric energy only exists in the fields of particles, this is always the case. The use of a twisted pair of wires eliminates any *magnetic* effect due to the changing current, so the experiment is totally *electric* in nature.

### The Long Straight Conductor

A simple example discussed in the literature is that of a long, straight conducting wire through which current is steadily driven by a battery (see Fig. 4). If the leads between the wire and the voltage source have negligible resistance, then the potential, neglecting end effects, is uniform across the wire's interior and the electric field inside and just outside the wire is uniform, with equipotentials perpendicular to the wire's axis.

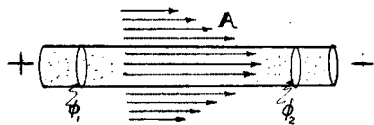


Figure 4. Long, straight conductor

As long as the current is *steady state*, the magnetic **A** field inside and outside the wire and the electric field  $\phi$  are constant with time, so no energy from the battery goes into the magnetic or electric fields after they are established. The energy that goes into heat (collisions of conduction electrons with

atoms) is carried by the electron's individual electric kinetic energies. It is stored in a sphere about each electron that is less than  $10^{-11}$  cm in radius and *none of it gets near the region outside the wire*. Clearly, in this case, the old Poynting theorem is wrong; since it indicates that the steady state energy from the battery doesn't go directly into the wire with the electrons, but leaves the source and travels through the space around the wire, entering it radially through its long cylindrical surface.

#### Further corrections of classical E&M

The three major corrections have now been made. There are several others that are not as general as these three. They will be discussed where they fit into the applications.

### V. THE ETHER AS THE UNIFIED FIELD

Although the final ether equations could be written for an arbitrarily moving laboratory (even accelerating), they are far simpler if written by an observer whose laboratory is not accelerating, i.e. whose laboratory's speed and direction of motion, relative to the ether, are not changing. All constant velocity laboratories, moving at arbitrary speeds, are defined as *inertial* systems, in which observers standing still in each room feel no acceleration. While, today, it is fashionable to formulate field equations using the theory of transformations between the various inertial systems, *all of physics can be discovered by a single observer in any one inertial laboratory*. Later on, it will be shown that identical experiments have the same results in any two inertial laboratories; but the *derivation* and *visualization* of the physics is far simpler for one particular inertial observer called the *absolute* observer.

The absolute observer is one whose laboratory is at rest relative to the datum ether, so that before particles and fields are introduced inside, the ether in the laboratory is homogeneous, isotropic, and at rest. The laws of physics are discovered by introducing a particle, such as an electron; or an electric field, such as that between the plates of a charged capacitor; or two small masses suspended close to each other; etc. Then the generalization of all the experiments is synthesized using the well known mathematics of field representation (see Appendix A). This consists of simple forms that describe spatial changes with time.

Although the forms used to represent the fields are usually quite simple, the actual experiments or calculations related to them, using the equations, usually require the establishment of a coordinate system inside the laboratory. This is done by visualizing three sets of imaginary surfaces, fixed relative to the laboratory walls, ceiling and floor, so that a different set of three numbers identifies each point in the room. For the ether, the density  $\phi_a$  and fluid velocity  $\mathbf{V}$  are specified at each space point; but also, other quantities, related to  $\phi_a$  and  $\mathbf{V}$ , can be written in the form of scalars, vectors or dyadics and specified at each point.

Most experiments of interest involve fields that are changing with time, so, in several places about the room, the laboratory has clocks that have been set by one of several possible methods. *The time is considered to be the same at every point in the laboratory, whether or not a clock is located there.* Choice of the method of clock setting involves certain subtleties that are discussed in detail later on.

Once a coordinate system and a laboratory time have been established, the field can be described by equations for the field variables like  $\phi_a$ ,  $\mathbf{V}$ , etc. in terms of the independent variables  $x$ ,  $y$ ,  $z$ , and  $t$ . The ether field equations for the absolute observer's system, as obtained through the preceding process, will now be discussed.

## VI. THE CONSERVATION LAW

The study of fluid motion is logically divided into two parts, kinematics and dynamics. Kinematics is a *geometrical* description of the possible motions resulting from the fact that any fluid occupies space as it moves about, and a particular part of it cannot be in two places at once. Dynamics deals with the laws of cause and effect governing a *particular* fluid's motion. *Kinematics is, therefore, the same for all fluids, whereas the dynamics of each different fluid can be different.*

The most fundamental *kinematic* equation of motion of a conventional fluid is the continuity equation, which relates the change in density at a point to the flow of the fluid towards or away from that point. Defining the ether *flow* vector as  $\phi_a \mathbf{V}$  and  $\nabla \cdot (\phi_a \mathbf{V})$  as the divergence of the flow vector at the point in question, the continuity equation is written,

$$\frac{\partial \phi_a}{\partial t} = -\nabla \cdot (\phi_a \mathbf{V}) \quad . \quad (30)$$

It says that the time rate of increase of density  $\phi_a$  at a fixed point is equal to the negative of the divergence of the flow vector  $\phi_a \mathbf{V}$  at that point.

The intuitive meaning of the continuity equation is perfectly clear. If the divergence of the flow away from a point is net positive, then the density of the fluid at that point must be decreasing and vice versa. Only if fluid is being created or destroyed at a point is it possible to violate this relationship. Therefore, Eq.(30) is *the formal expression for the conservation of ether.*

## VII. LONGITUDINAL WAVES

### Static ether concentrations

The ether can be distorted into particles, and propagates both transverse,  $t$ , and longitudinal,  $\ell$ , waves. However, the concept that certain particles are composed of regions of condensed and rarefied ether

is complicated by the frictionless fluidity of the medium, which would immediately flow to thin the condensed regions and fill in the attenuated regions. So, it is clear that no truly static ether configurations exist. In the case of so called "static" fields, the stability is the result of a combination of bulk displacements held together by some dynamic action in the ether. Thus, the designation "static" field, as commonly used, implies both bulk displacements and active, dynamic ether motion.

### Longitudinal waves

Motion of *transverse* ether waves is well understood. These *t*-waves are generated by moving charges, and they carry *energy* in two forms; antenna and photon radiation. No *longitudinal* radiation appears in E&M theory. Nevertheless, *l*-waves are more prevalent than *t*-waves. The sometimes strange physical effects they produce are not yet recognized as caused by *l*-waves; and the theory of *l*-waves is lacking any large *experimental* base. Since all energy transfer by waves is presently seen to be carried by *t*-waves, *l*-waves appear to be *energyless*; which accounts for their lack of observability.

The generation of *l*-waves is impossible to avoid. Just as a stone dropped into a quiescent pool of water causes a set of circular waves to leave the point of impact, *any disturbance of the ether at any point immediately produces high frequency, spherical l-waves that move outward*. These waves are essentially like those visualized by Huygens<sup>10</sup>. When they come in contact with particles, more waves are generated; so that the ether, everywhere, is traversed by *l*-waves, moving in all directions, caused by all the interacting particles in the universe. Unlike waves in elastic media, the velocities of ether *l*-waves and *t*-waves are the same, and equal to the velocity of light.

Non-linearity is a major factor in the ether's behavior and for this reason the equations that establish the energyless *l*-wave amplitudes are different from those giving the bulk flow properties involving energy in one way or another. Thus, in writing the field equations, the bulk ether distortions must be distinguished from the *l*-waves, so the incremental density and velocity are separated into two components,

$$\phi_a = \overline{\overline{\phi_a}} + \dot{\phi} \quad , \quad \mathbf{V} = \overline{\overline{\mathbf{V}}} + \mathbf{V} \quad , \quad (31)$$

bulk *l*-wave                      bulk *l*-wave

where the double bar indicates a constant (time average) or slowly varying bulk ether deformation or a *t*-wave, and the sub-dot indicates a rapidly oscillating, periodic, *zero time average*, longitudinal wave. Typical *l*-wave examples are,

$$\mathbf{V} \cdot = \hat{\mathbf{r}} f(r) C \quad , \quad \phi \cdot = g(r)(C - h(r) S) \quad , \quad (32)$$

$$C = \cos \omega(t - \frac{\mathbf{r}}{c_0}) \quad , \quad S = \sin \omega(t - \frac{\mathbf{r}}{c_0}) \quad .$$

---

10. C.Huygens, Treatise on Light, (1690); translation by S.P.Thompson, Dover Publications, p16 ff (1962).

In some situations, a problem can be solved using either the bulk or the  $\ell$ -wave equations separately; but more often than not, a close meshing of both is required to explain the physical phenomena.

### Separation equations

Eqs.(31) represent two of a set of *separation* equations that allow working with one or the other of the two components, bulk or  $\ell$ -wave. As an example, consider the flow vector  $\phi_a \mathbf{V}$ , i.e. the density, velocity product that specifies the ether *flow density* at each point in space. If separated into time average and periodic components, it is written,

$$\phi_a \mathbf{V} = \overline{\overline{\phi_a \mathbf{V}}} + \{\phi_a \mathbf{V}\}_\cdot \quad . \quad (33)$$

Its components can be found simply by using Eqs.(31) in,

$$\phi_a \mathbf{V} = (\overline{\overline{\phi_a}} + \phi_\cdot)(\overline{\overline{\mathbf{V}}} + \mathbf{V}_\cdot) \quad .$$

Carrying out the multiplication,

$$\phi_a \mathbf{V} = \underbrace{\overline{\overline{\phi_a}} \overline{\overline{\mathbf{V}}}}_{\text{bulk}} + \underbrace{\overline{\overline{\phi_a}} \mathbf{V}_\cdot + \phi_\cdot \overline{\overline{\mathbf{V}}}}_{\text{periodic}} + \phi_\cdot \mathbf{V}_\cdot \quad , \quad (34)$$

where the first RHS term is non-periodic, the next two terms are periodic, and  $\phi_\cdot \mathbf{V}_\cdot$  can have both periodic and non-periodic components given by,

$$\phi_\cdot \mathbf{V}_\cdot = \overline{\overline{\phi_\cdot \mathbf{V}_\cdot}} + \{\phi_\cdot \mathbf{V}_\cdot\}_\cdot = \hat{\mathbf{r}} \text{fg}(C^2 - hCS) = \hat{\mathbf{r}} \frac{\text{fg}}{2}(1 + C_2 - hS_2) \quad . \quad (35)$$

It follows that,

$$\overline{\overline{\phi_\cdot \mathbf{V}_\cdot}} = \hat{\mathbf{r}} \frac{\text{fg}}{2} \quad \text{and} \quad \{\phi_\cdot \mathbf{V}_\cdot\}_\cdot = \hat{\mathbf{r}} \frac{\text{fg}}{2}(C_2 - hS_2)$$

Combining Eq.(34) and (35),

$$\phi_a \mathbf{V} = \underbrace{\overline{\overline{\phi_a}} \overline{\overline{\mathbf{V}}}}_{\text{bulk}} + \underbrace{\overline{\overline{\phi_a}} \mathbf{V}_\cdot + \phi_\cdot \overline{\overline{\mathbf{V}}}}_{\text{periodic}} + \{\phi_\cdot \mathbf{V}_\cdot\}_\cdot \quad . \quad (36)$$

Comparing Eq.(33) and (36), the separated components of  $\phi_a \mathbf{V}$  are seen to be,

$$\overline{\overline{\phi_a \mathbf{V}}} = \overline{\overline{\phi_a}} \overline{\overline{\mathbf{V}}} + \overline{\overline{\phi_\cdot \mathbf{V}_\cdot}} \quad , \quad (\text{bulk})$$

and,

$$\{\phi_a \mathbf{V}\}_\cdot = \overline{\overline{\phi_a}} \mathbf{V}_\cdot + \phi_\cdot \overline{\overline{\mathbf{V}}} + \{\phi_\cdot \mathbf{V}_\cdot\}_\cdot \quad . \quad (\ell\text{-wave})$$

Using the same procedure, the separation equations for other properties such as the acceleration of the ether at a point can be found; but, even more useful is the separation of complete equations. For example, the ether conservation law of Eq.(30) can be expressed as,

$$\nabla \cdot \left( (\overline{\overline{\phi_a}} + \phi_\cdot)(\overline{\overline{\mathbf{V}}} + \mathbf{V}_\cdot) \right) = -\frac{\partial \overline{\overline{\phi_a}}}{\partial t} - \frac{\partial \phi_\cdot}{\partial t} \quad ,$$

expanded out, and separated. For convenience, the separation equations are listed in APPENDIX C.

## VIII VORTICITY AND ANGULAR PERSISTENCE

In Section III, the ether was described as a frictionless fluid that has no inertia or linear momentum, per se. There are situations, however, where it gives the appearance of having *angular* momentum. Wherever a steady state, closed *circulation* of ether occurs, since it is frictionless, the angular rotation will persist forever unless acted upon externally. This *angular persistence* gives the appearance of angular momentum, although it has no relationship to mass or inertia as commonly understood. A more complete discussion of this effect will appear later on, since it is closely related to difficulties with the conventional concept of magnetic energy.

## IX UNIVERSAL CONSTANTS

All of the equations developed here are written in Heaviside-Lorentz units so a table of conversion factors is included in APPENDIX B. The units for ether density (ether/cm<sup>3</sup>) have been called "descartes" here, because no name for them had been established in the past, and descartes seemed an appropriate name.

In the following, a number of universal constants appear, some familiar and some newly defined. The velocity of light with respect to the datum ether is the well known constant,  $c_0$ . If the ether density  $\phi_a$  is greater or less than  $\phi_d$ , in some large region, the velocity of light  $c$  will be greater or less than  $c_0$ . The datum density  $\phi_d$  is also a universal constant. Several others will be defined and discussed, later on, where they appear in the development. Table I gives the values of these constants (the basics are, aee, bee, phoe, dee). Since the accepted values of fundamental constants are regularly adjusted, as measurements gradually improve, the values here are not to be regarded as final; but they are accurate enough to allow proper exposition of the theory.

TABLE I

### UNIVERSAL CONSTANTS

Basic	Derived
$a = 7.954945 \times 10^{-24} \text{ cm}^2/\text{sec}$	$c_0 = 2.99792458 \times 10^{10} \text{ cm/sec}$
$b = 1.428438 \times 10^{26} \text{ sec/cm}^2$	$e = 1.7026924 \times 10^{-9} \text{ hlc}$
$\phi_d = 8.9875517 \times 10^{20} \text{ descartes}$	$h = 6.6260755 \times 10^{-27} \text{ erg-sec}$
$D = 2.7346139 \times 10^7 \text{ cm/sec}$	$G = 8.3850240 \times 10^{-7} \frac{\text{dyne-cm}^2}{\text{gm}^2}$

The important thing to notice about Table I is that the constants presented are divided into two sets, basic and derived. The basic constants appear in the fundamental field equations, whereas the derived constants only appear in the solutions of those equations. The only exception to this is  $c_0$ , which is a derived constant that is used instead of  $\phi_d$ , the basic quantity. The use of  $c_0$ , instead of  $\phi_d$ , in the field equations eliminates the requirement for a fifth basic constant to adjust for the units used.

## X THE FUNCTION OF $\ell$ - WAVES

The way in which  $\ell$ -waves contribute to the world's structure can be understood best by considering the process of pair production, i.e. the generation of an electron/positron pair using a high energy photon colliding with, say, a neutron. From the ether point of view, the pair of particles is produced by removing some ether from one region and depositing it in another, so that the slightly depleted region (electron) is separated from the slightly compressed region (positron). In this case, the fluid ether would ooze out of the positron and flow into the electron until nothing remained but the datum. In order for the electron and positron to be "stable" particles, something else must prevent this oozing. During pair production, an energyless, longitudinal *sustaining* wave is set up that goes out of the electron and into the positron to hold their bulk displacements of ether in place. These frictionless  $\ell$ -waves persist as long as the electron and positron remain separate particles.

---

### The electron as an example

The picture of the electron to be used here applies equally well to the positron, where some of the physical functions are reversed. The electron, *at rest*, is assumed to be a spherically symmetrical region where a small reduction of the central bulk ether density has been made, and which reduced density configuration is held in shape, and prevented from filling in, by an outgoing longitudinal wave. Figure 5 shows an electron greatly exaggerated in amplitude relative to  $\phi_d$ .

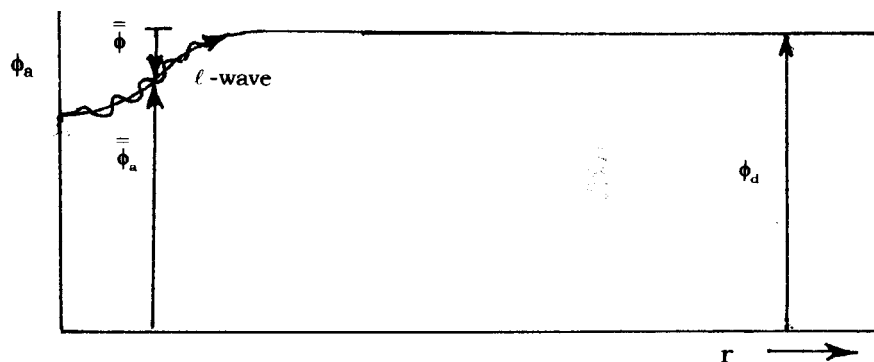


Figure 5. The electron ether density distribution.

---

The  $\ell$ -wave is a permanent part of each particle, and its first function is to stabilize and *sustain* the bulk distortion that constitutes the part of the particle that is directly measurable in the laboratory. A second function is to establish the particle's gravitic field. Third, the  $\ell$ -wave Doppler shift properties of a particle in motion determine many of what are conventionally called its quantum mechanical characteristics. Finally, many of the mysteries, such as the double-slit and Aharonov-Bohm experiments, can be explained by the  $\ell$ -waves. Therefore, *the  $\ell$ -wave is the fundamental ether property that most controls the phenomena that appear in experiments with particles and fields*; even though the bulk properties are the ones usually measured. For this reason, the  $\ell$ -wave equations are regarded as the basic equations of the ether; for once the fields  $\phi$  and  $\mathbf{V}$  are known, the bulk configurations  $\bar{\phi}$  and  $\bar{\mathbf{V}}$  can be found from them. Then, from the  $\bar{\phi}$  and  $\bar{\mathbf{V}}$  distributions come the physical definitions and visualizations of charge, energy, inertia, momentum, etc.

## XI THE $\ell$ -WAVE EQUATIONS

As mentioned in Section VII, there is no large experimental base to aid in discovering the basic  $\ell$ -wave equations. The number of experiments, past and present, on the *bulk* characteristics of particles and fields is so great as to be uncountable; yet, essentially all  $\ell$ -wave measurements made, to date, are indirect and are recognized for what they are by only a few dissident physicists. The consequence is that the  $\ell$ -wave equations presented here are the result of much circuitous relating of ostensibly unrelated facts, considerable guess work, and a remaining uncertainty. Until a solid groundwork of  $\ell$ -wave experiments is available, the formal description of the ether presented here must be used with care. Some part of it will undoubtedly be modified in the future. Nevertheless, the *picture* it has generated will probably endure.

The most desirable form of equation would be one that gives  $\mathbf{V}$  directly. Then the continuity equation could be used to get  $\phi$ . Because of the conditions described in the preceding paragraph, such an equation is not known at this time. What has been achieved is an equation for a scalar velocity potential  $\bar{\eta}$  from which  $\mathbf{V}$  can be found. Here, again, *the non-linearity of the ether requires the use of two separate  $\ell$ -wave equations; one for standing  $\ell$ -waves and one for traveling  $\ell$ -waves*. These equations are listed in APPENDIX A.

When using the *traveling*  $\ell$ -wave equation, the sign on the RHS is,

$$+ \text{ if } \bar{\phi} \cdot \bar{\mathbf{V}} \leq 0 \quad , \quad - \text{ if } \bar{\phi} \cdot \bar{\mathbf{V}} \geq 0 \quad (37)$$

and, for  $\ell$ -wave sources *at rest*,

$$\bar{\eta} = \bar{\mathbf{V}}^2 \quad . \quad (\ell \text{-wave sources at rest}) \quad (38)$$



If the  $\ell$ -wave sources are *moving*, the relationship between  $\mathbf{V}_\ell$  and  $\bar{\eta}$  must be modified. This will be discussed in a later section.

The angular frequency  $\omega$  functions as a *constant* while solving the equation for  $\mathbf{V}_\ell$ , and a separate conditional equation, to be discussed further on, is required to determine the value of  $\omega$ . The equation for  $\bar{\eta}$  involves both  $\mathbf{V}_\ell$  and  $\phi_\ell$ , so one other equation is needed to solve for them. This is the  $\ell$ -wave continuity equation. At the end of Section VII, the first step in separating the ether conservation Eq.(30) into its bulk and  $\ell$ -wave components was given. The  $\ell$ -wave component is listed at the end of APPENDIX C. Because  $\phi_a$  is of the order of  $\phi_d$ , which is immensely greater than  $\bar{\mathbf{V}}$ ,  $\phi_\ell$  and  $\mathbf{V}_\ell$  in any practical situation, the equation for the full  $\ell$ -wave conservation relationship can be approximated with extreme accuracy by,

$$\phi_d \nabla \cdot \mathbf{V}_\ell + \frac{\partial \phi_\ell}{\partial t} \cong 0 \quad (39)$$

The equation for  $\bar{\eta}$  and Eq.(39) allow  $\phi_\ell$  and  $\mathbf{V}_\ell$  to be found for traveling  $\ell$ -waves; but certain subtleties are involved, so that the examples should be consulted before attempting to solve these equations.

The *standing*  $\ell$ -wave equation is solved in essentially the same way.

### The electron as an example

Before the traveling  $\ell$ -wave  $\bar{\eta}$  equation in APPENDIX A and Eq.(39) can be solved for  $\mathbf{V}_\ell$  and  $\phi_\ell$ , the sign on the RHS of the  $\bar{\eta}$  equation must be determined. This is done as follows.

Since it is clear that, for an electron at rest, its fields are spherically symmetrical and drop off as some function of the radius  $r$ , measured from its center, a simple trial form for  $\mathbf{V}_\ell$  can be written,

$$\mathbf{V}_\ell = \hat{\mathbf{r}} \frac{a\psi}{r} C \quad , \quad \bar{\eta} = \bar{\mathbf{V}}^2 = \frac{a^2 \psi^2}{2r^2} \quad , \quad (40)$$

and  $\omega$  is as yet unspecified;  $a$  is the amplitude constant given in Table I; and  $\psi = \psi(r)$  is an *unknown*, monotonically increasing function to be found from the traveling wave  $\bar{\eta}$  equation in APPENDIX A.

From Eq.(40),

$$\nabla \cdot \mathbf{V}_\ell = \frac{a\psi}{r} \left( \left( \frac{1}{\psi} \frac{d\psi}{dr} + \frac{1}{r} \right) C + \frac{\omega}{c_0} S \right) \quad , \quad (41)$$

Now, combining Eqs.(39) and (41),

$$\frac{\partial \phi_\ell}{\partial t} = - \frac{\phi_d a\psi}{r} \left( \left( \frac{1}{\psi} \frac{d\psi}{dr} + \frac{1}{r} \right) C + \frac{\omega}{c_0} S \right) \quad ,$$

which can be integrated with respect to time, leading to,

$$\phi_{\cdot} = \frac{\phi_d a \psi}{c_0 r} \left( C - \frac{c_0}{\omega} \left( \frac{1}{\psi} \frac{d\psi}{dr} + \frac{1}{r} \right) S \right) . \quad (42)$$

The product of Eqs.(40) and (42) results in,

$$\phi_{\cdot} \mathbf{V}_{\cdot} = \hat{\mathbf{r}} \frac{\phi_d a^2 \psi^2}{c_0 r^2} \left( C^2 - \frac{c_0}{\omega} \left( \frac{1}{\psi} \frac{d\psi}{dr} + \frac{1}{r} \right) CS \right) , \quad (43)$$

which leads directly to the time average,

$$\overline{\overline{\phi_{\cdot} \mathbf{V}_{\cdot}}} = \hat{\mathbf{r}} \frac{\phi_d a^2 \psi^2}{2c_0 r^2} , \quad (44)$$

and its divergence,

$$\nabla \cdot \overline{\overline{\phi_{\cdot} \mathbf{V}_{\cdot}}} = \frac{\phi_d a^2}{2c_0 r^2} \frac{d\psi^2}{dr} . \quad (45)$$

Since  $\overline{\overline{\phi_{\cdot} \mathbf{V}_{\cdot}}} > 0$ , the RHS of the  $\overline{\overline{\eta}}$  traveling  $\ell$ -wave equation, in APPENDIX A, will have a *negative* sign. Note that this has been determined without actually solving for  $\mathbf{V}_{\cdot}$  and  $\phi_{\cdot}$ , since  $\psi$  is still unspecified.

The three equations necessary to solve for  $\ell$ -wave fields, then, are Eqs.(39), (40) and either the traveling or standing  $\ell$ -wave equation. All together, they are the main  $\ell$ -wave field equations, as they are now known. Until a larger program of  $\ell$ -wave experiments is carried out, they represent the only formal method for determining  $\mathbf{V}_{\cdot}$  and  $\phi_{\cdot}$  directly. Aside from certain auxiliary equations involved in the solutions for particles, they have within them the ability to describe everything related to the structure of matter.

### The electron as an example

Since an electron at rest is a “static” case, the  $\overline{\overline{\eta}}$  equation in APPENDIX A reduces to,

$$\nabla^2 \overline{\overline{\eta}} - \frac{1}{\overline{\overline{\eta}}} \left( \nabla \overline{\overline{\eta}} \right)^2 = - \frac{c_0 \omega}{\phi_d D} \nabla \cdot \overline{\overline{\phi_{\cdot} \mathbf{V}_{\cdot}}} . \quad (46)$$

This illustrates one of the subtleties of equations in which both bulk quantities and their time derivatives appear. In the full  $\overline{\overline{\eta}}$  equation, for example,  $\overline{\overline{\eta}}$  is a time averaged quantity; yet, in some situations, there can be time derivatives of  $\overline{\overline{\eta}}$ . *The double bar notation indicates only a time average over the high frequency  $\ell$ - wave cycles and not over the bulk time variations.* Only in a “static” case (where  $\overline{\overline{\phi}}$ ,  $\overline{\overline{\mathbf{V}}}$ ,  $\overline{\overline{\phi_a \mathbf{V}}}$  do not change with time) can the time derivatives in the full  $\overline{\overline{\eta}}$  equation, for example, be set equal to zero. This same dichotomy of bulk time

variations and  $\ell$ -wave time averages comes up in many places in the theory, so caution should be the guide.

When  $\bar{\eta}$  from Eq.(40) is substituted into Eq.(46) and the indicated differentiations are carried out, Eq.(46) is reduced to an equation, for the unknown function  $\psi(r)$  in  $\mathbf{V}_.$ , of the form,

$$\frac{d^2\psi}{dr^2} - \frac{1}{\psi} \left( \frac{d\psi}{dr} \right)^2 + \left( \frac{2}{r} + \frac{\omega}{D} \right) \frac{d\psi}{dr} - \frac{\psi}{r^2} = 0 \quad . \quad (47)$$

The simplest non-trivial solution of Eq.(47) is<sup>11</sup>,

$$\psi = \varepsilon^{-D/\omega r} \quad . \quad (48)$$

So, from Eq.(40),

$$\mathbf{V}_. = \hat{\mathbf{r}} \frac{\mathbf{a}}{r} \varepsilon^{-D/\omega r} \mathbf{C} \quad , \quad (49)$$

is the desired velocity  $\ell$ -wave **solution** of Eq.(46). The corresponding density wave **solution** is obtained by substituting Eq.(48) into Eq.(42), with the result,

$$\phi_. = \frac{\phi_d \mathbf{a}}{c_0 r} \varepsilon^{-D/\omega r} \left( \mathbf{C} - \frac{c_0}{\omega} \left( \frac{D}{\omega r^2} + \frac{1}{r} \right) \mathbf{S} \right) \quad . \quad (50)$$

The equation for  $\bar{\eta}$  and Eq.(39) are field *shape* determining equations; since, as stated before,  $\omega$  is a constant. The latter sets the *scale* of the solution, and is dependent on the compression properties of the ether, to be discussed next.

## XII THE COMPRESSION/OSCILLATION EQUATION

If ether is compressed, so that  $\phi_a$  exceeds  $\phi_d$  in some small region, and then is allowed to expand, the surrounding ether interacts with the expanding ether and an oscillation is set up. Since it is frictionless, the oscillation and the resulting  $\ell$ -waves continue unabated. The waves are attenuated with distance from the generating region, but the overall oscillation persists. This process is similar to a mass/spring system; but the ether is so non-linear that its compression/oscillation properties are quite different from familiar cases.

The mass/spring process is often described by an equation such as,

$$\frac{d^2\phi_.}{dt^2} + \mathcal{F}(\phi_.) = 0 \quad ,$$

where the non-linear function  $\mathcal{F}(\phi_.)$  includes the mass/spring

11. B.Liebowitz, Phys.Rev. **64**, 294 (1943). Liebowitz suggested a similar function in a different context.

characteristics. If  $\mathcal{F}(\phi.)$  is a known function, then the equation can be solved for a frequency/density relationship of the form,

$$\omega = G(\phi_{,m}) \quad , \quad (51)$$

where  $\phi_{,m}$  is the initial, maximum incremental density, and  $G(\phi_{,m})$  is generally an increasing, monotonic function.

The exact form of  $\mathcal{F}(\phi.)$  for the ether must be determined empirically, and is not known at this time. However, measured particle characteristics have been used to obtain much insight as to the form of the function  $G(\phi_{,m})$ . This will be discussed later.

### The electron as an example

In the case of the ether, the function  $G(\phi_{,m})$  appears to be a type of staircase function, with the electron as the lowest stable particle energy step. Its  $\ell$ -wave forms with the value  $\omega = 7.7634396 \times 10^{20}$  rad/sec.

Next to be discussed is the equation that connects the solutions  $\mathbf{V}_.$  and  $\phi_.$  found from the  $\ell$ -wave equations, to the bulk solutions for  $\bar{\bar{\phi}}$  and  $\bar{\bar{\mathbf{V}}}$ , which produce the directly measurable properties of matter.

## XIII THE BRIDGE EQUATION

The bulk properties of matter are found using the "bridge" equation, which gives, quantitatively, just how much ether distortion an  $\ell$ -wave can *sustain*. It takes its simplest form for static fields, as expressed by,

$$\nabla \bar{\bar{\phi}} = \mathbf{b} \bar{\bar{\phi}} \cdot \bar{\bar{\mathbf{V}}}. \quad ; \quad (\text{static}) \quad (52)$$

which says that, *if the phase between  $\phi_.$  and  $\mathbf{V}_.$  is 90 degrees, no gradient of the bulk density  $\bar{\bar{\phi}}$  can be supported. If  $\phi_.$  and  $\mathbf{V}_.$  have an in phase component, then the gradient of  $\bar{\bar{\phi}}$  depends linearly on their time average. Once the  $\ell$ -waves  $\phi_.$  and  $\mathbf{V}_.$  are known throughout a region,  $\bar{\bar{\phi}}$  can be determined everywhere in that region by integrating Eq.(52).*

The designation "static" field in Eq.(52) means that no bulk field quantity such as  $\bar{\bar{\phi}}$ ,  $\bar{\bar{\mathbf{V}}}$ ,  $\bar{\bar{\phi}}_a \bar{\bar{\mathbf{V}}}$ , etc. is changing with time. In cases where the bulk fields are time variable, the picture is complicated by the finite propagation time delay required to readjust the fields. So, in the general case, the bridge equation is written,

$$\nabla \bar{\bar{\phi}} + \frac{1}{c_0^2} \frac{\partial \bar{\bar{\phi}}_a \bar{\bar{\mathbf{V}}}}{\partial t} = \mathbf{b} \bar{\bar{\phi}} \cdot \bar{\bar{\mathbf{V}}}. \quad , \quad (\text{general}) \quad (53)$$

and is known as the "retarded" form (as in retarded potential).

---

### The electron as an example

If the electron is *at rest*, the static bridge Eq.(52) applies. Using Eq.(44), the gradient of the incremental bulk distortion can be written,

$$\nabla \bar{\phi} = \hat{\mathbf{r}} \frac{\partial \bar{\phi}}{\partial r} = \overline{\mathbf{b} \phi \cdot \mathbf{V}} = \hat{\mathbf{r}} \frac{\phi_d \mathbf{a}^2 \mathbf{b}}{2c_0 r^2} \varepsilon^{-2D/\omega r} \quad , \quad (54)$$

where the constants are those in Table I. Next,  $\bar{\phi}$  can be found directly by integrating Eq.(54) as follows (see APPENDIX D),

$$\bar{\phi} = \frac{\phi_d \mathbf{a}^2 \mathbf{b}}{2c_0} \int \frac{\varepsilon^{-2D/\omega r}}{r^2} dr + \phi_0 \quad ;$$

so,

$$\bar{\phi} = \frac{\phi_d \omega \mathbf{a}^2 \mathbf{b}}{4c_0 D} \varepsilon^{-2D/\omega r} + \phi_0 \quad .$$

To find the integration constant  $\phi_0$ , remember that as  $r \rightarrow \infty$ ,  $\bar{\phi} \rightarrow 0$ , which means that,

$$\phi_0 = -\frac{\phi_d \omega \mathbf{a}^2 \mathbf{b}}{4c_0 D} = -1.9233 \times 10^3 \quad \text{des} \quad . \quad (55)$$

Therefore, the final form of the bulk  $\bar{\phi}$  distribution for the electron is,

$$\bar{\phi} = \phi_0 (1 - \psi^2) = \phi_0 (1 - \varepsilon^{-2D/\omega r}) \quad . \quad (56)$$

Figure 6 is a plot of this very simple particle. It has only two features.

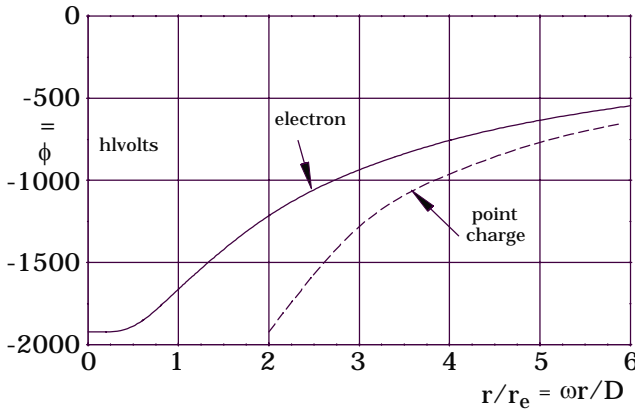


Figure 6. The bulk structure of the electron.

First, the electron is such a *minute* deformation. The greatest depletion of ether is at the center, and has the value  $\phi_0$ ; so that,

$$\frac{|\phi_0|}{\phi_d} = 2.1400 \times 10^{-18} \quad , \quad (57)$$

almost no depletion at all. Second, its inflection point at  $\omega r/D = 1$ , is the only *identifiable* radius. Fortunately, it is a good choice as the effective radius of the electron,

$$r_e = \frac{D}{\omega} = 3.522426 \times 10^{-14} \quad \text{cm} \quad . \quad (58)$$

Eq.(56) can now be written in the more intuitive and useful form,

$$\bar{\phi} = \phi_0 (1 - \varepsilon^{-2r_e/r}) \quad . \quad (59)$$


---

## XIV BULK EQUATIONS

Here again there are two sets of bulk equations, *microscopic* and *macroscopic*. Unfortunately, they are almost identical in appearance; but they have completely different physical meanings and are applied in quite different ways. To emphasize the disparity between them, *only the microscopic equations will be presented at this point. Discussion of the macroscopic bulk equations and their applications will be delayed until later.* Whether to use the microscopic or macroscopic form of the bulk equations is determined by the type of "charge" distribution to be analyzed. Most everyday electromagnetic problems involve the separation and recombination of groups of *whole* charged particles, such as electrons and other particles composing atomic nuclei. In all these cases, the "charge" is a number *assigned* to each whole particle, and the charge density distribution is described in terms of how many whole charged particles per cubic centimeter act at each point. *In these cases, the fundamental nature of "charge" is not considered, and the macroscopic equations are used.*

When the problem to be studied concerns the internal structure of particles, and an internal distribution of charge density that integrates throughout the particle to give the whole particle "charge" used in the macroscopic cases, then *the fundamental nature of "charge" is of concern, and the microscopic bulk equations are used.*

Even when analyzing a microscopic case, there are two ways to write some of the equations, because of the nature of bulk measurements. For example, in a field where the ether flow vector at each point is  $\overline{\overline{\phi_a \mathbf{V}}}$ , the bulk equations can be written in terms of  $\overline{\phi_a}$  and  $\overline{\overline{\phi_a \mathbf{V}}}$ . However,  $\overline{\phi}$  is the quantity found directly from the bridge equation, not  $\overline{\phi_a}$ ; and in the laboratory,  $\overline{\phi}$  is measured rather than  $\overline{\phi_a}$ ; so it is often more convenient to write the bulk equations in terms of  $\overline{\phi}$  and the flow vector  $\overline{\phi \mathbf{u}}$ , where  $\mathbf{u}$  is a velocity defined by the relationship,

$$\overline{\phi \mathbf{u}} = \overline{\overline{\phi_a \mathbf{V}}} \quad . \quad (60)$$

The significance of Eq.(60) is that the actual density  $\overline{\phi_a}$  at each point, moving at the actual ether velocity  $\overline{\mathbf{V}}$  defines a definite amount of ether actually flowing through any given small area, perpendicular to the flow at the point, as represented by the flow vector  $\overline{\overline{\phi_a \mathbf{V}}}$ ; so, if  $\overline{\phi}$  is used, instead of  $\overline{\phi_a}$ , there must be an apparent or effective velocity  $\mathbf{u}$  such that  $\overline{\phi \mathbf{u}}$  gives the *same net amount* of ether passing through the small area. Because  $\overline{\phi} \ll \overline{\phi_a}$  (due to the large value of  $\phi_d$ ),  $\mathbf{u} \gg \overline{\mathbf{V}}$ . In some rare

cases, the velocity  $\mathbf{u}$  can appear to be infinite; but, in those cases, reverting to  $\bar{\phi}_a$  and  $\bar{\phi}_a \bar{\mathbf{V}}$  eliminates any problem.

#### The bulk conservation equation

At the end of Section VII, the first step in separating the ether conservation Eq.(30) into its bulk and  $\ell$ -wave components was given. They are listed at the end of APPENDIX C. More compact forms of these separated equations are,

$$\nabla \cdot \bar{\phi}_a \bar{\mathbf{V}} + \frac{\partial \bar{\phi}_a}{\partial t} = 0 \quad , \quad (\text{bulk}) \quad (61)$$

and

$$\nabla \cdot \{\phi_a \mathbf{V}\} + \frac{\partial \phi_a}{\partial t} = 0 \quad . \quad (\ell\text{-wave}) \quad (62)$$

In Section XI, an extremely close approximation to the  $\ell$ -wave component was introduced in the form of Eq.(39). No such approximation is needed for the bulk Eq.(61), however, because the bulk equations are written directly in terms of  $\bar{\phi}_a$  and  $\bar{\phi}_a \bar{\mathbf{V}}$ . Thus, in the light of the discussion above regarding Eq.(60), the two forms of the bulk conservation law required are,

$$\nabla \cdot \bar{\phi}_a \bar{\mathbf{V}} + \frac{\partial \bar{\phi}_a}{\partial t} = 0 \quad \text{and} \quad \nabla \cdot (\bar{\phi} \mathbf{u}) + \frac{\partial \bar{\phi}}{\partial t} = 0 \quad . \quad (63)$$

These kinematic equations can be used interchangeably. The remainder of the bulk equations describe the ether's dynamics.

#### Bulk ether distortions

Having solved the  $\ell$ -wave equations and used the bridge to find  $\bar{\phi}$  everywhere, the  $\bar{\phi}$  field is a bulk distortion away from  $\phi_a$ ; but there are other ways to describe this distorted field. A good *visualization* of these is useful. Consider a "static"  $\bar{\phi}$  field held in place by its  $\ell$ -waves. Not only is the original field  $\bar{\phi}$ , itself, a distortion; but, for example, its gradient  $\nabla \bar{\phi}$  is a different, coexistent distortion field. The product  $\nabla \bar{\phi} \cdot \nabla \bar{\phi}$  is another different distortion field; as is any other function of  $\bar{\phi}$  such as  $\nabla^2 \bar{\phi}$ , for example. It becomes important to recognize these different, *coexisting* distortions, all *implicit* in the original  $\bar{\phi}$ , because in interactions between fields, each of these distortions accounts for a different effect in the interaction. A few distortions produce such unique and recognizable effects that they have been given special names. Each of these more important deformations will be discussed here in some detail.

*The principal thing to keep in mind is that there is nothing present in the field but the  $\bar{\phi}$  distortion distribution of ether.*

### Incremental bulk distortion

One of the most directly measurable properties of electric fields is the electric potential. In practical units it is given in volts, and is measured with the common voltmeter. The corresponding measurement in H-L units is the hlvolt. Physically, what is being measured here is the incremental ether density distortion  $\bar{\bar{\phi}}$ . When a potential of 1 hlvolt is *measured from the datum level*, the density  $\bar{\bar{\phi}}$  is 1 descartes. Thus, *the incremental bulk density is the physical definition of what has been named "electric potential"*. If this had been known at the time various electrical properties were being named, electric potential now probably would be called "ether density", and voltmeters would be called ether density difference meters. It is important to remember that the voltmeter does not measure the absolute ether density  $\bar{\bar{\phi}}_a$ , but either the incremental value  $\bar{\bar{\phi}}$  relative to the datum, or the difference in  $\bar{\bar{\phi}}$  between two regions.

### "Gradient squared" distortion

In 1837, Faraday first recognized the importance of the "gradient squared" distortion, when he defined the "electric energy density" in an electrostatic field as,

$$\varepsilon_e = \frac{1}{2}(\nabla\bar{\bar{\phi}}_a)^2 = \frac{1}{2}(\nabla\bar{\bar{\phi}})^2 \quad , \quad (\text{static}) \quad (64)$$

measured in ergs/cm<sup>3</sup>. From his point of view,  $\bar{\bar{\phi}}$  was the electric potential (hlvolts) in the field, but here it is clear *that the physical definition of "electric energy density" is the particular distortion in the ether described by Eq.(64)*, where  $\bar{\bar{\phi}}$  is measured in descartes (hlvolts).

If the fields are changing with time, the retardation due to the finite propagation velocity must be included, just as was done in the general bridge equation. Therefore, the general definition of electric energy density takes the (retarded) form,

$$\varepsilon_e = \frac{1}{2} \left( \left( \nabla\bar{\bar{\phi}}_a \right)^2 - \frac{1}{c_0^2} \left( \frac{\partial\bar{\bar{\phi}}_a}{\partial t} \right)^2 \right) \quad , \quad (\text{general}) \quad (65)$$

or,

$$\varepsilon_e = \frac{1}{2} \left( \left( \nabla\bar{\bar{\phi}} \right)^2 - \frac{1}{c_0^2} \left( \frac{\partial\bar{\bar{\phi}}}{\partial t} \right)^2 \right) \quad .$$

Here again, as in the case of the incremental bulk density  $\bar{\bar{\phi}}$ , the physical definition of electric energy density is a simple, physically visualizable property of the bulk ether density.



---

The electron as an example  
The Electron's *electric* energy

Since the space distribution of incremental density  $\bar{\phi}$  is now known, Eq.(64) can be employed to establish the electron's gradient squared distortion or electric energy density. Taking the gradient of  $\bar{\phi}$  in Eq.(59),

$$\nabla\bar{\phi} = -\hat{r} \frac{2\phi_0 r_e}{r^2} \varepsilon^{-2r_e/r} \quad . \quad (66)$$

When Eq.(66) is substituted into Eq.(64), the electric energy density is found to be,

$$\varepsilon_e = 2 \frac{\phi_0^2 r_e^2}{r^4} \varepsilon^{-4r_e/r} \quad , \quad \frac{\text{ergs}}{\text{cm}^3} \quad (67)$$

which is plotted in Figure 7. Apparently,  $\varepsilon_e$  is a smooth shell of

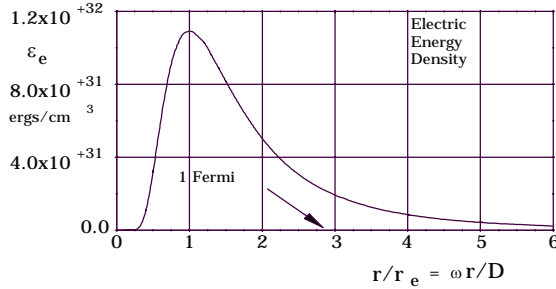


Figure 7. The electron's "gradient squared" distortion distribution.

distortion that peaks at  $r = r_e$ , which is one good reason for the choice of the  $\bar{\phi}$  inflection point as the electron's effective radius.

The total rest energy in the electron's field is found by integrating Eq.(67) over all space,

$$E_0 = \int_{\text{space}} \varepsilon_e d\text{vol} = 8\pi\phi_0^2 r_e^2 \int_0^\infty \frac{\varepsilon^{-4r_e/r}}{r^2} dr \quad ,$$

with the result,

$$E_0 = 2\pi\phi_0^2 r_e = 8.18711 \times 10^{-7} \quad . \quad \text{ergs} \quad (68)$$

The physical effects produced by this gradient squared distortion are numerous; so much so, that in the past some of the effects were attributed to "mass", a property thought related in some way to energy. Modern writers say that mass and energy are "equivalent" on the basis of the famous equation of Einstein ,et al,

$$m_0 = \frac{E_0}{c_0^2} \quad . \quad (69)$$

Here, the position is taken that they are *identical*, i.e. *one physical phenomenon, with two names, expressed in different units*. There is just one gradient squared distortion. It causes all the effects of electric energy and all the effects of mass, but the units identified with mass are  $c_0^2$  larger than those identified with energy.

---

"Surrounding function" distortion

The Laplacian  $\nabla^2\bar{\phi}$  of a scalar field  $\bar{\phi}$  is known to be the difference, at

each point in space, between the average of  $\bar{\phi}$  in a differential volume surrounding the point and the value of  $\bar{\phi}$  at the point. This is a simple visualization of the physical meaning of the "surrounding" function in any scalar field. *In the bulk incremental ether density field  $\bar{\phi}$ , the surrounding function distortion produces the unique effects attributed to "distributed charge density".* Formally, the definition of "distributed charge density" in a static field is,

$$\rho = -\nabla^2 \bar{\phi}_a = -\nabla^2 \bar{\phi} \quad , \quad (\text{static}) \quad (70)$$

measured in hlcoulombs/cm<sup>3</sup>. Lack of knowledge of the physical nature of charge resulted in the less convenient choice of sign in Eq.(70) by early investigators.

As before, the propagation delay time must be involved when the fields are changing with time, so the general expression for charge density is,

$$\rho = -\left( \nabla^2 \bar{\phi}_a - \frac{1}{c_0^2} \frac{\partial^2 \bar{\phi}_a}{\partial t^2} \right) \quad , \quad (\text{general}) \quad (71)$$

or,

$$\rho = -\left( \nabla^2 \bar{\phi} - \frac{1}{c_0^2} \frac{\partial^2 \bar{\phi}}{\partial t^2} \right) \quad .$$

Eqs.(70) and (71) look familiar, because when written with the RHS and LHS reversed, they have the same appearance as the well known Maxwell wave equation for the scalar potential. It is of utmost importance here to understand the *profound difference* between Maxwell's *macroscopic* equations and the *microscopic* Eqs.(70) and (71). In the macroscopic equations,  $\rho$  is the known function, being a count of *whole charged particle* density at each point. From this given source distribution, the potential function is found by solving the macroscopic equation. *The whole particles exert coulomb forces on each other.* Quite the opposite is true in the microscopic case described by Eqs.(70) and (71). There, the known field function  $\bar{\phi}$ , obtained from the  $\ell$ -waves and the bridge, is operated on to find the distribution of "surrounding" function distortion,  $\rho$ . *The elements of distributed charge  $\rho$  exert **no** force on each other.*

---

### The electron as an example

#### Electron charge

The coexistent charge density is found from the surrounding function distortion Eq.(70) by first taking the divergence of Eq.(66), leading to,

$$\rho = 4 \frac{\phi_0 r_e^2}{r^4} \varepsilon^{-2r_e/r} \quad , \quad \frac{hlc}{\text{cm}^3} \quad (72)$$

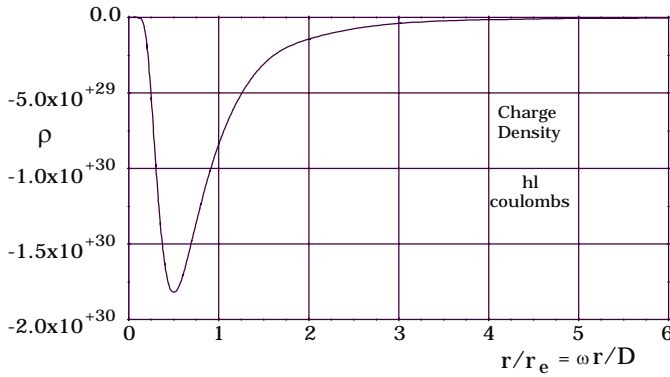


Figure 8. The electron's "surrounding " function distortion distribution.

which is plotted in Figure 8. Here, again,  $\rho$  is a smooth shell of distortion, but it peaks at  $r = r_e/2$ , half the radius of peak energy density. It should be noted that the electron's charge density,  $\rho$ , is negative because  $\phi_0$  is negative.

The total electron charge is calculated by integrating Eq.(72) over

all space,

$$q_e = \int_{\text{space}} \rho d\text{vol} = 16\pi\phi_0 r_e^2 \int_0^{\infty} \frac{\epsilon^{-2r_e/r}}{r^2} dr \quad ,$$

with the result,

$$q_e = 8\pi\phi_0 r_e = -\frac{2\pi\phi_d a^2 b}{c_0} = -1.702692 \times 10^{-9} = -e \quad , \quad (73)$$

Here, again,  $q_e$  is negative because  $\phi_0$  is negative.

Equations (59), (66), (72) and (73) apply equally well for the positron if the value of  $\phi_0$  in Eq.(55) is used without the negative sign. This is the result of an ingoing  $\ell$ -wave. However, Eqs.(44) and (45) change sign for the positron.

### The Bulk Ether Flow Equation

Some fields, eg. permanent magnets, solenoids and transformer coils, cannot be derived using the above bulk distortion equations. Other examples are the neutrinos and photons. Some of these, as well as the analysis of antenna radiation in the form of transverse waves, require what is called the ether flow equation, which takes the static form,

$$\rho \mathbf{u} = \nabla^2 \overline{\overline{\phi_a \mathbf{V}}} = \nabla^2 (\overline{\overline{\phi \mathbf{u}}}) \quad , \quad (\text{static}) \quad (74)$$

measured as hlcoulombs/cm<sup>2</sup>-sec. The form for time variable fields becomes,

$$\rho \mathbf{u} = - \left( \nabla^2 \overline{\overline{\phi_a \mathbf{V}}} - \frac{1}{c_0^2} \frac{\partial^2 \overline{\overline{\phi_a \mathbf{V}}}}{\partial t^2} \right) \quad ,$$

or,

$$\rho \mathbf{u} = - \left( \nabla^2 (\overline{\overline{\phi \mathbf{u}}}) - \frac{1}{c_0^2} \frac{\partial^2 (\overline{\overline{\phi \mathbf{u}}})}{\partial t^2} \right) \quad . \quad (\text{general}) \quad (75)$$

Here again, the equations have the same form as the *macroscopic* flow equations reversed; but in this case problems are sometimes solved the same way microscopically and macroscopically, even though the same profound difference exists in their physical interpretations.

Vortex flow

There is a whole class of flow problems where there are vortices present. In these cases, the incremental density has little effect, because all of the ether in  $\phi_d$  is circulating, so  $\bar{\phi}$  is effectively zero,  $\mathbf{u}$  is not defined, and the flow is handled using a reduced form of Eq.(75),

$$\nabla^2 \bar{\mathbf{V}} - \frac{1}{c_0^2} \frac{\partial^2 \bar{\mathbf{V}}}{\partial t^2} = 0 \quad . \quad (\text{vortex}) \quad (76)$$

The electron as an example

Electron spin and magnetic moment

In interaction processes between particles, a considerable amount of ether churning occurs; and when particles like the electron or positron are created from the splatter, they end up with a specific *angular momentum* or what is called *spin*. Since their charge density rotates with the ether, they have a *magnetic moment* as well. In Section VIII it was indicated that angular momentum in the ether is just the angular persistence of a circulation in a frictionless fluid. Thus, the first step in the determination of the spin angular momentum is to find the spin vortex velocity field. The vortex equation, Eq.(76), provides that information.

Calculation of the electron spin vortex is done by first ignoring the radial, outgoing  $\ell$ -waves that sustain the bulk gradient. The incremental bulk density  $\bar{\phi}$  also has little effect on the circulating flow. The simplest case is that where the electron is at rest and the circulation

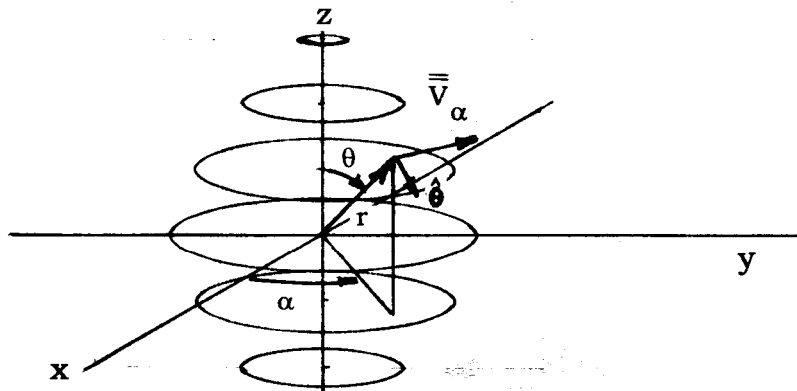


Figure 9. Spin flow.

is not changing with time. Eq.(76) then reduces to,

$$\nabla^2 \overline{\overline{\mathbf{V}}} = 0 \quad , \quad (77)$$

where,  $\overline{\overline{\mathbf{V}}}$  is the unchanging circulation about one specific axis through the electron's center (see Figure 9). In spherical coordinates  $(r, \theta, \alpha)$ ,

$$\overline{\overline{\mathbf{V}}} = \hat{\alpha} \overline{\overline{V_\alpha}} \quad ,$$

and Eq.(77) leads to,

$$\nabla^2 \overline{\overline{V_\alpha}} - \frac{\overline{\overline{V_\alpha}}}{r^2 \sin^2 \theta} = 0 \quad .$$

Considering the flow as separable into  $r$  and  $\theta$  dependent parts, let,

$$\overline{\overline{V_\alpha}} = \frac{\mathcal{R}(r)}{r^2} \mathcal{T}(\theta) \quad ,$$

and the separated equations can be solved in the usual way. The simplest solution free of non-physical attributes gives the spin velocity field  $\overline{\overline{V_\alpha}}$ . For obvious physical reasons, the solution has two regions, inner and outer, where  $\overline{\overline{V_\alpha}}$  of each matches at some radius  $\delta r_e$ . Thus,

$$\overline{\overline{V_\alpha}} = \begin{cases} K_s \frac{r}{(\delta r_e)^3} \sin \theta & , \quad \text{inside } \delta r_e \\ K_s \frac{1}{r^2} \sin \theta & , \quad \text{outside } \delta r_e \end{cases} \quad . \quad (78)$$

Customarily, angular momentum is found by integrating, over all space, the mass density at each radius times the velocity of that mass density; but considering what has been said about momentum and its meaning, i.e. particles have it but ether doesn't, it might be doubted that the same integration process would apply microscopically to the ether in electron spin. Nevertheless, it will be assumed here that the ether angular momentum can be made quantitative by the conventional approach, with minor modifications. In the light of Eq.(69), the spin is

$$\sigma = \kappa \int_0^\infty \int_0^\pi \int_0^{2\pi} \frac{\varepsilon_e}{c_0^2} \overline{\overline{V_\alpha}}(r \sin \theta) \, d\text{vol} \quad ,$$

and  $\varepsilon_e$  is the energy density of Eq.(67). Here,  $\kappa$  is a scaling constant that allows for the fact that the angular persistence of a frictionless fluid is not easily made quantitative, yet a relationship must be found that connects it to the momentum-like effects it produces in interactions with particles and fields. After the proper substitutions and integrations,

$$\sigma = \frac{\pi \kappa K_s \phi_0^2}{3c_0^2} \left[ 1 - \left( 1 + \frac{4}{\delta} \right) \varepsilon^{-4/\delta} + \frac{64}{\delta^3} T\left(\frac{\delta}{4}\right) \right] \quad , \quad (79)$$

where  $\delta$  establishes the break point of maximum  $\overline{\overline{V_\alpha}}$ , and  $T(x)$  is the Truncation integral (see APPENDIX D).

Following along the same lines, the spin magnetic moment is conventionally expressed as a vector,

$$\boldsymbol{\mu}_s = \frac{\kappa}{2c_0} \int_0^\infty \int_0^\pi \int_0^{2\pi} \mathbf{r} \times \rho \overline{\mathbf{V}} \, d\text{vol} \quad ;$$

but, because the charge density circulates always perpendicular to the radius vector  $\mathbf{r}$  (see Figure 9), the only components that do not cancel in the integration over all  $\theta$  and  $\alpha$  are the z components. Again, this is better described by writing the scalar spin magnetic dipole moment,

$$\mu_s = \frac{\kappa}{2c_0} \int_0^\infty \int_0^\pi \int_0^{2\pi} \rho \overline{V}_\alpha (r \sin \theta) \, d\text{vol} \quad ,$$

and  $\rho$  is the charge density of Eq.(72). With the proper substitutions and integrations,

$$\mu_s = \frac{4\pi\kappa K_s \phi_0}{3c_0} \left[ 1 - \left( 1 + \frac{2}{\delta} \right) \varepsilon^{-2/\delta} + \frac{8}{\delta^3} \Gamma\left(\frac{\delta}{2}\right) \right] \quad . \quad (80)$$

Taking the ratio  $\mu_s/\sigma$  with the help of Eqs.(71), (72) and (73),

$$\frac{\mu_s}{\sigma} = \pm \frac{e}{m_0 c_0} \frac{\left[ 1 - \left( 1 + \frac{2}{\delta} \right) \varepsilon^{-2/\delta} + \frac{8}{\delta^3} \Gamma\left(\frac{\delta}{2}\right) \right]}{\left[ 1 - \left( 1 + \frac{4}{\delta} \right) \varepsilon^{-4/\delta} + \frac{64}{\delta^3} \Gamma\left(\frac{\delta}{4}\right) \right]} \quad , \quad (81)$$

where the + is the positron and - the electron. It is well established that the value of  $\mu_s/\sigma$  given by Dirac's equation is  $e/m_0 c_0$ , and that the *measured* ratio is slightly larger, because the measurement must be made on an *ensemble* of particles. The actual, or *intrinsic*  $\mu_s/\sigma$  ratio of individual electron/positrons is given by Eq.(81); and for any  $\delta$  is slightly *smaller* than  $e/m_0 c_0$ . Since the effects of the brackets in Eq.(81) and the *measurements* are opposite, the value of  $\delta$  cannot yet be determined; but it seems that  $\delta < 0.06$ , and the peak  $\overline{V}_\alpha$  occurs at a radius less than  $2 \times 10^{-15}$  cm. Assuming that  $\delta < 0.06$ , then,

$$\sigma = \frac{\pi\kappa K_s \phi_0^2}{3c_0^2} \quad (82)$$

and

$$\mu_s = \frac{4\pi\kappa K_s \phi_0}{3c_0} \quad (83)$$

differ from the *intrinsic* values by less than  $10^{-13}$  parts. In the remainder of this work Eqs.(82), (83), (79), and (80) will all be referred to as *intrinsic*, unless otherwise specified.

*The constant  $K_s$  is not determined in this derivation*, because it is established during the particle production process. Its magnitude is specified by the complicated relationships set up by the input conditions

of the interaction. At the present time, this complicated interaction problem has not been solved. However, the value of  $\kappa K_s$  can be obtained by using the *experimental* value for  $\mu_s$ ,

$$\mu_s = 3.2875524 \times 10^{-20} \text{ ergs/hlG} \quad , \quad (84)$$

directly in Eq.(83), which yields,

$$\kappa K_s = 1.2233488 \times 10^{-13} \text{ erg-cm}^2/\text{des}^2\text{-sec} \quad . \quad (85)$$

Substituting this value for  $\kappa K_s$  in Eq.(82) produces a value for the electron's angular momentum,

$$\sigma = 5.2728633 \times 10^{-28} \text{ erg-sec} \quad . \quad (86)$$

L. O. Heflinger has pointed out that, since the outer field is equivalent to a magnetic dipole, combining Eqs.(78), (83) and (000),  $K_s$  can be eliminated and  $\kappa = 3\phi_d/\phi_0$ , or,

$$\kappa = 1.4018715 \times 10^{17} \quad .$$

If this value is used for  $\kappa$ , then,

$$K_s = 8.7265399 \times 10^{-31} \quad .$$

From Eq.(78), the maximum  $\overline{\overline{V}}_\alpha$  at  $\delta = 0.06$  ( $\theta = \pi/2$ ) is found to be

$$\overline{\overline{V}}_{\alpha\max} = 1.9537 \times 10^{-2} \text{ cm/sec} \quad .$$

## XV THE GRAVITIC FIELD

There are two classes of particles, the bulk layer type like the electron, and the high speed photons and neutrinos. Whereas the layerons do have gravitic fields, the c-ons appear not to. All layeron electric fields require *traveling*  $\ell$ -waves to sustain their bulk forms; but at the particle center, where the traveling  $\ell$ -wave starts, there is a region of pure compression/relaxation that also generates a radial *standing*  $\ell$ -wave. These radial waves constitute the particle's gravitic field.

---

### The Electron's Gravitic Field

From Eqs.(49), (50) and (58), the travelling  $\ell$ -waves are given by,

$$\mathbf{V}_{.t} = \hat{\mathbf{r}} \frac{\mathbf{a}}{r} \varepsilon^{-r_e/r} C \quad ,$$

and,

$$\phi_{.t} = \frac{\phi_d \mathbf{a}}{c_0 r} \varepsilon^{-r_e/r} \left( C - \frac{c_0}{\omega r} \left( 1 + \frac{r_e}{r} \right) S \right) \quad . \quad (87)$$

To understand how the electron's gravitic field is generated, it is helpful to look at the central region where  $r < 30r_e$ . This is facilitated by expanding the cosine, for example, as,

$$C = \cos \omega t \cos \frac{\omega r}{c_0} + \sin \omega t \sin \frac{\omega r}{c_0} \quad ,$$

which, in the region  $r < 30r_e$ , reduces to  $C \cong \cos \omega t$ . The sine becomes  $S \cong \sin \omega t$ . In the same region,

$$\frac{c_0}{\omega r} \left( 1 + \frac{r_e}{r} \right) \gg 1 \quad ,$$

so, the travelling  $\ell$ -waves in the central region of the electron are,

$$\mathbf{V}_t \cong \hat{\mathbf{r}} \frac{\mathbf{a}}{r} \varepsilon^{-r_e/r} \cos \omega t \quad ,$$

and,

$$\phi_t \cong -\frac{\phi_d \mathbf{a}}{\omega r^2} \varepsilon^{-r_e/r} \left( 1 + \frac{r_e}{r} \right) \sin \omega t \quad ,$$

(88)

In fact, they represent a pure compression/expansion oscillation, which, as a disturbance, also generates standing  $\ell$ -waves as well.

What the electron's standing  $\ell$ -wave looks like can be determined by solving the standing wave  $\bar{\eta}$  equation, listed in APPENDIX A, reduced to the static case,

$$\nabla^2 \bar{\eta}_s = 0 \quad ,$$

(89)

where  $\mathbf{V}_s$  and  $\bar{\eta}_s$  of the standing  $\ell$ -wave are related through Eq.(38),

$$\bar{\eta}_s = \overline{\mathbf{V}_s^2} \quad ,$$

In spherical coordinates  $(r, \theta, \alpha)$ , Eq.(89) can be written,

$$\frac{d^2 \bar{\eta}_s}{dr^2} + \frac{2}{r} \frac{d\bar{\eta}_s}{dr} = 0 \quad ,$$

which has a solution,

$$\bar{\eta}_s = K_h + \frac{K_f}{r} \quad .$$

Since all *incremental* fields approach zero as  $r \rightarrow \infty$ ,  $K_h = 0$ , and,

$$\bar{\eta}_s = \overline{\mathbf{V}_s^2} = \frac{K_f}{r} \quad .$$

(90)

The simplest standing  $\ell$ -wave solution, compatible with Eq.(88), that satisfies Eq.(90) is,

$$\mathbf{V}_s = \hat{\mathbf{r}} \sqrt{\frac{K_g}{r}} \cos \omega t \quad ,$$

(91)

where  $K_g = 2K_f$ .

Going back to the traveling  $\ell$ -wave of Eq.(88), the maximum amplitude of  $\mathbf{V}_t$  occurs at  $r = r_e$ . Here it will be assumed that the standing velocity wave  $\mathbf{V}_s$  matches  $\mathbf{V}_t$  at that radius, leading to,

$$K_g = \frac{a^2}{r_e \varepsilon^2} \quad ,$$

remembering that  $\varepsilon$  is the base of natural logarithms ( $\psi = \varepsilon^{-1}$  at  $r = r_e$ ).



Thus, in Eq.(91),

$$K_g = 2.43133 \times 10^{-34} \frac{\text{cm}^3}{\text{sec}^2} .$$

The standing wave field picture is completed by substituting Eq.(91) in Eq.(39) to find,

$$\phi_{.s} = -\frac{3\phi_d}{2\omega} \frac{\sqrt{K_g}}{r^{3/2}} \sin \omega t \quad . \quad r \geq r_e \quad (92)$$

Now it is possible to show that  $\mathbf{V}_{.s}$  and  $\phi_{.s}$  establish the electron's gravitic field, but first a brief summary of these standing waves' characteristics will be given that will prove helpful later on. Eqs.(91) and (92) indicate that these waves do not propagate; but, instead, the whole field quivers in and out in unison. Since,  $\overline{\phi_{.s} \mathbf{V}_{.s}} = 0$ , no contribution to the electron's bulk density field is made by these standing  $\ell$ -waves. Furthermore, for the electron at rest ( $\overline{\phi_a \mathbf{V}} = 0$ ), the third from last equation in APPENDIX C shows that  $\overline{\mathbf{V}_s} = 0$ . Considering the total velocity at each point as the sum of  $\mathbf{V}_t$  and  $\mathbf{V}_s$ , it is possible to show, with the help of the separated  $\overline{\mathbf{a}}$  equation in APPENDIX C, that the only significant contribution to the electron's acceleration field, at distances greater than  $100r_e$ , is,

$$\overline{\mathbf{a}_s} = \overline{\mathbf{V}_{.s} \cdot \nabla \mathbf{V}_{.s}} = -\hat{\mathbf{r}} \frac{K_g}{4r^2} . \quad (93)$$

All other contributions to the acceleration field are either much smaller than  $\overline{\mathbf{a}_s}$  or they change sign every  $4.853 \times 10^{-10}$  cm and will not have any effect on an object larger than  $10^{-9}$  cm across. Space will not permit including this straightforward but tedious demonstration.

All particles except photons and neutrinos have this standing wave field, and its importance appears when large numbers of particles are combined into sizable *neutral* objects. Under those conditions, the bulk fields are mostly confined inside the large object, and the sum of all the acceleration fields remains outside. Notice that  $\overline{\mathbf{a}_s}$  is directed radially *inward* for both negative and positive charged particles.

From Galilei's time onwards, it has been recognized that *the basic characteristic of a spherical gravitic field is that all objects at the same distance from its center accelerate towards its center at the same rate if unimpeded*. This is generally expressed in the form of Newton's law of gravitation,

$$\overline{\mathbf{a}} = -\hat{\mathbf{r}} \frac{GM}{4\pi r^2} , \quad (94)$$

where M is the mass of the source body, and G is the gravitational

constant. If, for the moment, it is assumed that *the natural state of any object is to move to oppose its time average acceleration with respect to the ether*, then any object in the field described by Eq.(93) will accelerate towards the center of the field. By comparing Eqs.(93) and (94), the constant G will be seen to have the value  $\pi K_g/M$ . Converting the electron's energy from Eq.(68) to mass units,

$$m_0 = 9.10939 \times 10^{-28} \text{ gm} \quad ,$$

and Newton's gravitation constant is found to be,

$$G = \frac{\pi K_g}{m_0} = 8.38503 \times 10^{-7} \frac{\text{cm}^3}{\text{g} - \text{sec}^2} \quad .$$

Here G differs from the usual value by a factor of  $4\pi$  used in Eq.(94) to express the idea that the  $4\pi r^2$  in all spherical fields has geometrical significance.

---

Gravitic fields are purely *standing* radial  $\ell$  - waves. In the *charged* layered particles, the gravitic field is overwhelmed by the electric field.; so the gravitic field plays no significant role. In large *neutral* bodies, however, eg. suns, planets and their satellites, all the charged particles are paired off, ie. their *traveling*  $\ell$  - waves go directly out of a negative particle into an associated positive particle and stay essentially *inside* the body. Thus, the only  $\ell$  - wave field outside the neutral body is the sum of all the radial standing  $\ell$  - waves from all the particles inside.

## XVI SUMMARY OF THE UNIFIED FIELD EQUATIONS

Eq.(76) is the last of the main equations constituting the unified field theory of the ether. For convenience, all of the key equations are summarized in APPENDIX A. The following sections will consist of solutions of these equations for much of the basic structure of matter observed in the world. They will not, however, delve into the physics of solids, liquids, gases or plasmas. Those areas, which develop logically and *statistically* from the more fundamental deterministic structures that will be derived here, are so voluminous as to prohibit inclusion. Moreover, the physics in those disciplines will be modified only slightly by the fundamental changes elaborated here. On the other hand, a number of, at present, mysterious phenomena will be examined on the basis of the ether theory.

## XVII THE DATUM

In Section III, it was said that a complete description of the ether has two parts, visualizable definitions of its physical characteristics and the formal equations that relate them. The latter are summarized in APPENDIX A, and most visualizations have been covered; but there are two important features that require further elaboration. These are basic

phenomena that can be visualized without considering the properties of particles. They are processes that occur, in the datum, before massive particles have been introduced. One was mentioned briefly in Section XII as the compression/oscillation condition that relates the ether's natural oscillation frequencies to its compression distortion. The other, called datum fluctuations, resembles the “chop” in the ocean of the datum ether. The present section concentrates on these two phenomena.

#### Datum fluctuations

Anyone who has seen a glassy lake mirror the scene about the shore understands the deterministic picture of the datum drawn in Section III. The absolute observer was defined as one who, in a region free of energy, sees the datum ether at rest, having zero velocity everywhere. In the case of the glassy lake, any activity in the water about the shore generally destroys the reflected image overall; because a gentle chop ripples across the surface. The same condition applies in the ether, where all the particles far away send out waves that produce a minute, random chop throughout space. *The effect is so small it can be ignored in most calculations of the type already discussed.* Nevertheless, these small datum fluctuations exert significant effects in situations where constructs are very close to being unstable. In some cases, datum fluctuations can push a construct “over the top” into instability. It is these fluctuations that introduce statistics into the deterministic picture.

#### The vacuum

Until very recently, modern physicists regarded the vacuum of space as a *void* in which particles and waves moved about. However, because of the considerable development of high energy particle physics, this void has been given more and more physical properties; until, now, it is clearly a physical entity.\*\* The present work is a study of its properties, and the use of “vacuum”, “quintessence” or any other term but “ether” to describe it is just an artifice.

Conventionally the fluctuations are viewed as more structured than the ether theory requires, with both the random chop and the forming of whole particles and their subsequent annihilation at each point, temporarily violating energy conservation. In the ether picture, there is distortion moving about in the form of the chop; but, although that distortion can pile up temporarily, at a point, to values as great as those of the particles, no actual particles are formed (with their bulk shapes and radial  $\ell$ -waves all properly deployed) in regions originally free of particles. This type of distortion does not require energy conservation violation.

The exact nature of the datum fluctuations is not yet known. They could be  $\ell$ -waves, t-waves or both. This lack of knowledge has little effect on the development of the deterministic part of the theory at this stage of development.

---

\*\*.*Physics Through the 1990s, Elementary Particle Physics*, (National Academy, Washington, D.C. 1986) p.71.

The compression/oscillation characteristic & particle mass

In Section XII, the compression/oscillation characteristic of the datum ether was said to be similar to that of a mass/spring system which obeys the frequency /density relationship of Eq.(51),

$$\omega = \mathcal{G}(\phi_{.m}) \quad . \quad (95)$$

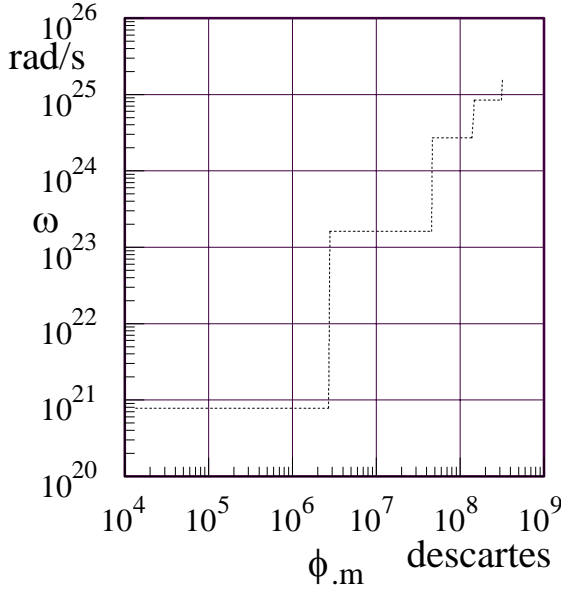


Figure 10 The ether's compression/oscillation characteristic.

No method of measuring this function directly is known at present, so all estimates of the form of  $\mathcal{G}(\phi_{.m})$  must be based on inferences from high energy particle physics and atomic data. In spite of the myriad of particle collision experiments and other related investigations, the present best guess as to the form of  $\mathcal{G}(\phi_{.m})$  is the very incomplete curve depicted in Figure 10. Only part of the lower three horizontal regions are known with any certainty, but even from this meager information, the predilection of the ether for certain preferred frequencies suggests the mechanism by which the particle masses are fixed.

In Figure 10, the lowest known particle frequency, that of the electron, is marked. It was this “preferred” frequency that was used in Section XII to fix the electron’s rest energy. It doesn’t require a great leap

TABLE II  
SELF-CONSISTENT PREFERRED FREQUENCIES

Level	$\omega_i$ (rad/sec)	$r_i$ (cm)
1	$7.76344 \times 10^{20}$	$3.52243 \times 10^{-14}$
2	$1.62973 \times 10^{23}$	$1.67796 \times 10^{-16}$
3	$2.69981 \times 10^{24}$	$1.01289 \times 10^{-17}$
4	$8.508 \times 10^{24}$	$3.214 \times 10^{-18}$
5	$1.580 \times 10^{25}$	$1.731 \times 10^{-18}$

of imagination to guess that other solutions of the  $\ell$ -wave equations will lead to more massive particles that correspond to higher preferred oscillation frequencies. Table II lists the known preferred ether frequencies, including levels 4 and 5 which are educated guesses.

### XVIII THE CONSTANT VELOCITY ELECTRON

The picture of the electron at rest has been completed. Table III lists the related properties found so far. However, the electron has many other interesting characteristics when it is in motion. These will be discussed in the following.

$\phi_d$	$8.9875517 \times 10^{20}$	descartes	Datum ether density
$\phi_0$	$-1.92333 \times 10^3$	descartes	Incremental density (r=0)
$r_e$	$3.522426 \times 10^{-14}$	cm	Effective radius
$q_e$	$-1.7026924 \times 10^{-9}$	hlc	Charge distortion
$E_0$	$8.18711 \times 10^{-7}$	ergs	Energy distortion
$m_0$	$9.10939 \times 10^{-28}$	gm	Mass
$\sigma$	$5.2728633 \times 10^{-28}$	erg-sec	Spin angular momentum (intrinsic)
$\mu_s$	$3.2875524 \times 10^{-20}$	erg/hlG	Spin magnetic moment (intrinsic)
$\omega_e$	$7.7634396 \times 10^{20}$	rad/sec	Electron $\ell$ - wave frequency
G	$8.38503 \times 10^{-7}$	$\text{cm}^3/\text{g} - \text{sec}^2$	Gravitational constant

An electron in motion exhibits several characteristics not evident when it is at rest. Some of these are velocity dependent and some result from acceleration. While the velocity dependent properties are amenable to formal analysis, most of the acceleration effects are mathematically intractable. Nevertheless, even in those cases, considerable insight evolves from the qualitative picture available. In the following constant velocity case, the concepts of kinetic energy, inertia and momentum will be derived, and the physical basis of the de Broglie frequency will be made clear.

The analysis begins with the derivation of the  $\bar{\eta}$ -waves as a solution of the traveling wave  $\bar{\eta}$  equation in APPENDIX A. It is well known that a moving point source of waves produces wave fronts that are spherical, but with centers strung out along the axis of motion, so the sustaining wave is set up in cylindrical coordinates ( $x, R, \alpha$ , electron velocity  $\mathbf{u}$  in the  $x$  direction). The solution will be presented here with no proof other than it satisfies the equation by direct substitution.

The solution for  $\bar{\eta}$  is,

$$\bar{\eta} = \gamma \frac{a^2 \psi^{*2}}{2r^{*2}} \quad ,$$

and the compatible  $\mathbf{V}$ . and  $\phi$ . are,

$$\mathbf{V}_{.x} = \frac{a\psi^* \mathbf{x}^*}{r^{*2}} \mathbf{C} \quad , \quad \mathbf{V}_{.R} = \gamma \frac{a\psi^* R}{r^{*2}} \mathbf{C} \quad , \quad (96)$$

$$\phi_{.} = \pm \frac{\phi_d a \psi^*}{c_0 r^*} \left( \mathbf{C} \mp \gamma \frac{c_0}{\omega_e \mathcal{R}} \left( 1 + \frac{R}{\psi^*} \frac{\partial \psi^*}{\partial R} + \frac{\mathbf{x}^*}{\gamma \psi^*} \frac{\partial \psi^*}{\partial \mathbf{x}} \right) \mathbf{S} \right) \quad .$$

With some nomenclature borrowed from the theory of sound<sup>12</sup>,

$$\mathbf{C} = \cos \frac{\omega_e}{\gamma} \left( t \mp \frac{\mathcal{R}}{c_0} \right) \quad , \quad \mathbf{S} = \sin \frac{\omega_e}{\gamma} \left( t \mp \frac{\mathcal{R}}{c_0} \right) \quad , \quad \psi^* = \varepsilon^{-r_e/r^*} \quad ,$$

and, (97)

$$\mathbf{x}^* = \gamma(\mathbf{x} - \mathbf{u}t) \quad , \quad r^* = \sqrt{\mathbf{x}^{*2} + R^2} \quad , \quad \mathcal{R} = \gamma(r^* \pm \beta x^*) \quad , \quad \beta = \frac{\mathbf{u}}{c_0} \quad .$$

Here, the value of  $\omega_e$  is that found for the electron at rest. The upper sign results in the outgoing waves of the electron, whereas the lower sign represents the incoming waves of the positron. *In the following, only the upper signs, applying to the electron, will be retained.* Because the source is in motion, the relationship between  $\bar{\eta}$  and  $\mathbf{V}$ . becomes,

$$\bar{\eta} = \gamma \frac{r^{*2}}{\mathbf{x}^{*2} + \gamma^2 R^2} \bar{\mathbf{V}}^2 \quad .$$

In visualizing the moving particle, it is possible to use a slightly simpler form, in *which the ether density pattern of the constant velocity electron is frozen* at one instant of time, say  $t = 0$ . Then  $\bar{\phi}$  becomes,

$$\bar{\phi} = -\gamma \frac{e}{8\pi r_e} \left( 1 - \varepsilon^{-2r_e/r'} \right) \quad , \quad (98)$$

where,

$$r' = \left( \gamma^2 \mathbf{x}^2 + R^2 \right)^{\frac{1}{2}} = r \left( 1 + \zeta \cos^2 \theta \right)^{\frac{1}{2}} \quad , \quad (99)$$

and  $\zeta = \gamma^2 - 1$  .

---

12. E.U.Condon, H.Odishaw, Handbook of Physics, p.3-117, McGraw-Hill, N.Y. (1958).

The first question of interest is: When the moving charge density is integrated over all space, what is the total charge of the moving electron? Has it changed? From the surrounding function distortion equation in APPENDIX A, the moving charge density distribution function can be obtained with the small change,

$$\rho = - \left( \nabla^2 \bar{\phi} - \frac{\mathbf{u}^2}{c_0^2} \frac{\partial^2 \bar{\phi}}{\partial \mathbf{x}^2} \right) ,$$

which, upon substitution of  $\bar{\phi}$  from Eq.(98), results in,

$$\rho = - \gamma \frac{e \mathbf{r}_e}{2\pi r'^4} \varepsilon^{-2r_e/r'} .$$

Just as in the static case, the total charge is found from,

$$q_e = - \int_{\text{space}} \frac{\gamma e \mathbf{r}_e \varepsilon^{-\frac{2r_e}{r\sqrt{1+\zeta \cos 2\theta}}}}{2\pi r'^4 (1 + \zeta \cos^2 \theta)^2} d\text{vol} ,$$

where  $r'$  has been replaced by its spherical polar coordinate form as taken from Eq.(99). This simplifies the integration, which yields,

$$q_e = - e .$$

From what is known about moving charged particles, this result was expected.

To observe the same process applied to the energy density distribution, the gradient squared distortion energy equation, in APPENDIX A, can be used. With  $\bar{\phi}$  from Eq.(98), the energy density of the constant velocity electron is,

$$\varepsilon_e = \frac{\gamma^2 e^2}{32\pi^2 r'^4} \varepsilon^{-4r_e/r'} ,$$

and the total moving energy of the particle is,

$$E = \int_{\text{space}} \frac{\gamma^2 e^2 \varepsilon^{-\frac{4r_e}{r\sqrt{1+\zeta \cos 2\theta}}}}{32\pi^2 r'^4 (1 + \zeta \cos^2 \theta)^2} d\text{vol} .$$

The result of the integration is,

$$E = \gamma E_0 , \tag{100}$$

where  $E_0$  is the electron/positron rest energy in Table III.

The energy relationship of Eq.(100) is well known, and is usually ascribed to so called special relativity. Clearly, no relativistic approach was used in the preceding derivation. All of the physics involved only one observer, and the result is directly attributable to properties of the ether and the structure of the electron/positron fabricated from it. Implicit in the preceding development is the resolution of the infamous 4/3 problem. Its key resides in the proper understanding of and definition of energy and energy density. Rohrlich discussed the problem in detail from the present day accepted viewpoint and described earlier attempts

to resolve it<sup>13</sup>. Those earlier investigators managed a mathematical solution that gave the correct form of Eq.(100). Rohrlich, himself, used a similar approach; i.e. forcing Lorentz invariance and coming up with correction terms for the static definitions of energy and momentum. Although Rohrlich's results are formally the same as Butler's<sup>14</sup>, the latter took the correct approach based upon redefining energy density, allowing a much more intuitive interpretation of the mathematical forms. He was prevented from obtaining the correct physical interpretation by using  $\mathbf{E}$  and  $\mathbf{H}$  to define energy density rather than  $\mathbf{A}$  and  $\phi$ .

To see exactly what happens when an electron is brought up to some velocity  $\mathbf{u}$ , first consider the particle *at rest*. The contour surfaces of constant  $\bar{\phi}$  are spheres, as represented in Figure 11a. Corresponding surfaces of constant  $\bar{\phi}$  for a moving e/p are the oblate spheroids appearing in Figure 11b. In present day texts, it is almost always overlooked that *the potential  $\bar{\phi}$  does not contract longitudinally to the motion but expands laterally*, which is why the surrounding function or charge density of the particle changes. It is also why the  $(\nabla\bar{\phi})^2/2$  distortion of the moving particle, integrated over all space, increases. Note that for each different constant velocity  $\mathbf{u}$ , a specific lateral exten-

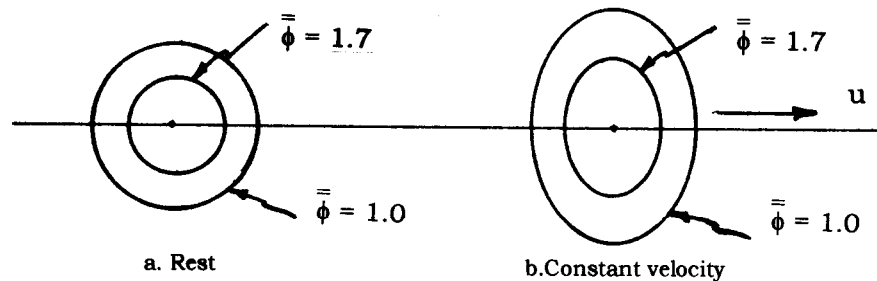


Figure 11 Lateral expansion of the moving electron/positron, (e/p).

sion and shape is required. So, a specific amount of charge distortion is identified with each velocity, as is a specific amount of energy distortion.

#### Particle interaction

The exact details of interaction of, say, two electrons, will be deferred till later; but here it is possible to form a useful mental picture. An electron will be acted upon to bring it from rest up to some velocity  $\mathbf{u}$ . However, there are no sticks or stones to move it. There is only ether, and specifically, only ether in the form of another particle. So, as illustrated in Figure 12, the sequence starts with one energized electron moving at velocity  $\mathbf{u}_1 = i\mathbf{2}$  approaching another electron which is at rest. It must be emphasized that the contours shown are not edges or surfaces

13. F.Rohrlich, Classical Charged Particles, Addison-Wesley Publ. Co., Reading, MA (1965).

14. J.W.Butler, Amer. J. Phys. **36**, 936 (1968); **37**, 1258 (1969).



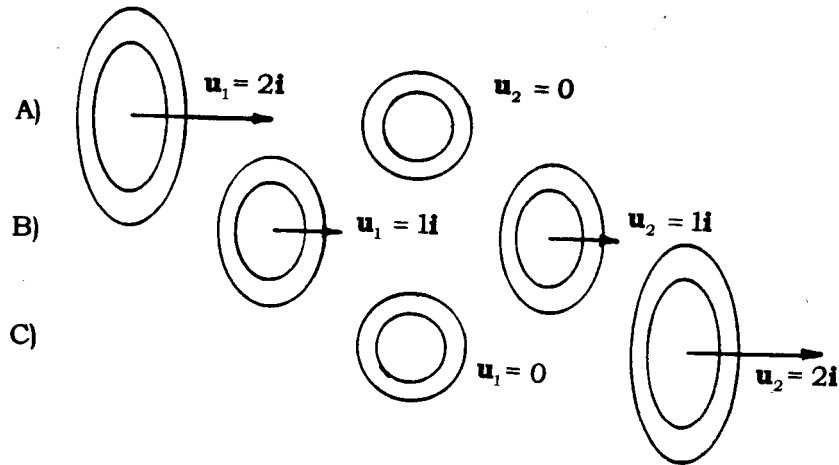


Figure 12 Energy exchange between two electrons.

in any real sense; they are equipotential or equidensity levels of the ether. There are an infinite number of these imaginary surfaces increasing in size from the electron center to the far reaches of space. Clearly, certain liberties are taken in the simplified picture of Figure 12. Nevertheless, electron number one is originally carrying excess deformation energy (over its rest value) and number two is at rest. Later, the excess in 1 has caused 2 to move away, at the same time resulting in a transfer of distortion from 1 to 2. Number 1 cannot run slower unless distortion is removed from its field and the latter is allowed to change shape to exactly match the reduced velocity. Number 2 cannot take on the transferred distortion unless it moves and changes shape to exactly match the condition of its moving at its new velocity. As the process of transfer continues, the first electron finally gives up all of the excess distortion and comes to rest. Number 2, meanwhile, has taken on all of the original distortion and is now moving at the velocity originally exhibited by 1. The shape of 2 is now also exactly the same as the original shape of 1. *In this example, radiation has been neglected.*

Delving further into the operation of an e/p, Eq.(100) can be written as,

$$E = \frac{E_0}{\sqrt{1 - \frac{u^2}{c_0^2}}} = E_0 \left( 1 + \frac{1}{2} \frac{u^2}{c_0^2} + \dots \right) .$$

For small velocities, all higher order terms of the series are negligible; and, making use of Eq.(69), the excess energy of the particle due to its constant velocity is,

$$E_k \cong \frac{1}{2} \frac{E_0}{c_0^2} u^2 = \frac{1}{2} m_0 u^2 .$$

This is called the *kinetic energy* of the moving particle. At higher

velocities, the exact form is found by subtracting  $E_0$  from  $E$  of Eq.(100), so that,

$$E_k = E - E_0 = E_0(\gamma - 1) \quad .$$

This brings the discussion to the following point. The electron is a small depletion of ether prevented from sagging by a sustaining wave running away from its geometrical center. There is no rock in the middle, there are no objects in the field. It has two kinds of deformation that are significant in determining its charge and energy. When it moves, it changes shape in a very precise way, increasing its distortion content. The excess distortion, called its kinetic energy, is determined by its shape and velocity. Eq.(98) represents the total energy of the moving electron/positron. Contrary to conventional belief, the electron's magnetic field carries no energy. The full implication of this will be discussed in detail later.

### Inertia and Momentum

The quantitative discussion of momentum, etc., will be presented later on. All that is needed here is a brief statement about the physical nature of momentum and inertia. In connection with Figure 12, the interaction of two electrons was described. Before the #1 electron had approached close enough to #2 to have a significant effect on it, their condition could be described as follows. Number 2, being at rest, was a solution of the field equations, and assuming the boundary conditions did not change, it would sit permanently at the same location forever. Number 1, being in motion at constant velocity, was also a solution of the field equations, and assuming the boundary conditions did not change, it would continue along a straight line at constant velocity forever. These are not mathematical statements, but physical. In both cases, the boundary conditions are  $\bar{\phi} \cong 0$ ,  $\bar{\phi}_a \cong \phi_d$  far out. For the electron at rest, the reduced  $\bar{\phi}_a$  near the center has spherical contours, held up by spherical wave fronts, all matched up from  $r = 0$  to  $r \rightarrow \infty$ . For the charge in motion, the reduced  $\bar{\phi}_a$  is oblate in its contours, all moving in a single direction, while curved wave fronts leave the geometrical center along paths all exactly proportioned so that just the right amount of  $\bar{\phi}_a$  arrives at each point in the field to maintain the shape and overall velocity distribution  $\bar{V}$ , etc. Otherwise, the "particle" would cease to exist. Only when #1 approached close enough to #2 to lower the ether density from  $\phi_d$  to some  $\bar{\phi}_a$ , on the side of approach to #1, would both see the boundary conditions change and then adjust their representative flow pattern solutions of the field equations. *This is the physical meaning of inertia.* Only when the boundary conditions change will a solution of the field equations be modified. Inertia is obviously not a property of the ether

itself, but of the solutions to the field equations; i.e. *inertia is a property of particles, not ether.*

Momentum,  $\mathbf{p} = m\mathbf{u}$ , can be understood physically by realizing that it is a combination of the effect of inertia and the fact that *it takes time to bring about the changes in velocity* of a particle such as the electron. First the boundary conditions must change, usually by bringing another field into the outermost regions of the electron's field. As the electron moves away from or towards the changing region, the excess deformation energy must be carried throughout the electron's field by the modified sustaining waves, which are propagating at the speed of light. Only when the shifted deformation moves in a very prescribed manner and causes the shape of the electron density  $\bar{\phi}$  to maintain the proper configuration to match the overall instantaneous velocity and motion of the electron field can the electron-external field combination remain as a valid solution of the field equations. Thus, *time* is involved. *It is this time delay that begets the concept of momentum.* Later on, the formal connection between the time variation of the particle deformation and the change in the external boundary conditions will be worked out. Clearly momentum is not a property of the ether but of solutions of the field equations; i.e., *momentum is a property of particles, not ether.*

Numerical examples reviewing momentum and energy calculations will be presented later, but the equations most often used for this are given here in TableIV. These equations are always called relativistic in modern texts, but no relativistic condition has entered into their derivation. They come directly from a single observer's solution of the field equations for a moving electron/positron.

TABLE IV

ENERGY AND MOMENTUM FORMULAS

$E = E_0 + E_k$	$E^2 = (pc_0)^2 + E_0^2$	$\gamma = 1 + \frac{E_k}{E_0}$
$p = mu = \frac{E}{c_0} \sqrt{1 - \frac{1}{\gamma^2}}$	$u = c_0 \sqrt{1 - \frac{1}{\gamma^2}}$	$u = \frac{pc_0^2}{E}$
	$p = \frac{E_k}{c_0} \sqrt{1 + 2 \frac{E_0}{E_k}}$	

### Electron radiation

Propagating energy in the form of radiation is normally detected at long distance from a changing configuration of charges. Some of the most puzzling phenomena in conventional physics originate at the interface of the emitting charge and the freely propagating radiation. That is the inevitable result of the lack of knowledge about the charge's internal structure.

The standard approach to this problem is to first solve Maxwell's equations for the fields radiated from *point* charges moving in explicit ways. Using this to define the net radiated energy leaving a charge, that energy is associated with the acceleration of the charge. This whole approach is basically unsound. As it turns out, many situations exist where electrons accelerate but do not radiate. Certainly the most conspicuous case is that of atoms in their ground state, where electrons orbiting and accelerating towards the nucleus do not radiate. So strong is the belief that Maxwell's equations determine the presence or absence of radiation, that the belief in atomic orbits has been relinquished. Too bad, since they are there. The simple fact is that Maxwell's equations are necessary but not sufficient to indicate whether charges radiate. The full field equations must be solved to see whether the total field has a free or radiated part.

From the ether viewpoint, particles engage in motions that can result in variations in the deformation, which, although conserved, moves about. Some part of the total deformation is bound in the particles, i.e. is an intrinsic part which, if it were not there, would mean the particle identity was lost. As a particle speeds up, this bound deformation increases; and, conversely, when it slows down, decreases. When increasing, the source of the acquired deformation unloads distortion energy by first shifting it into the form of an interaction deformation shared between them, after which it is absorbed by the speeded up particle. Radiation occurs during the shifting process. In situations where the speed change is too rapid or the direction changes sharply, i.e. high acceleration occurs, it happens that interaction energy out in the field cannot move in just the right way to keep up with the particle. In such cases, the renegade deformation cannot be reclaimed by either the particle or the external field and it escapes. That lost deformation is the radiation.

What is needed is a simple intuitive way to decide when radiation will occur. The ether provides this. When no bound ether element is changing shape, no radiation can occur. When bound ether elements are changing shape, radiation occurs, with greater radiation resulting from more violent changing. The full import of this concept will gradually appear as more complicated structures, such as atoms and macroscopic field problems, are studied.

## Turning

One aspect of the electron's characteristics that has no counterpart in contemporary physics is the result of its shape change with motion. By expanding laterally, the electron has an established axis in the direction of its motion; and, in certain situations, that axis could shift direction. In other words, the electron shape could turn. It might then reasonably be expected, based on the previous discussion, that whether or not its incremental ether elements turned, as its path deviated from a straight line, could have a profound effect on its physical operation. At this point, it cannot be emphasized enough that *this turning is not the least like the spin* examined earlier; and often, when turning is discussed, the spin will be ignored, because the frictionless, massless nature of the ether allows them both to operate without interfering with each other.

Once the electron/positron has a new *shape*, due to its motion, the *relative* motion of that shape and the ether that composes the particle represents one of the most significant and controlling properties of that particle, fundamental to important aspects of e/p radiation. Figure 13 illustrates two alternative modes of path deviation; one of e/p radiation with no ether turning, and the other with full ether turning and no radiation. The dots on the equi-density contours identify particular ether elements in the  $\bar{\phi}$  field of an electron. In the full turning case these elements move with a flow pattern that corresponds to rigid body rotation. In the non-turning case, the flow pattern is more complex, with particular elements in the density pattern approaching one another (2 and 4) and other elements receding from each other (1 and 3). This corresponds to the fact that in the non-ether turning or partial ether turning particle, the  $\bar{\phi}$  field around each point is deforming, or changing shape; whereas, in the full ether turning particle the  $\bar{\phi}$  field around each numbered point is not deforming, or changing shape. Thus, in the former case, radiation will take place; whereas, in the latter, it will not. Here, again, the full significance of this phenomenon will gradually appear as more complicated processes are discussed.

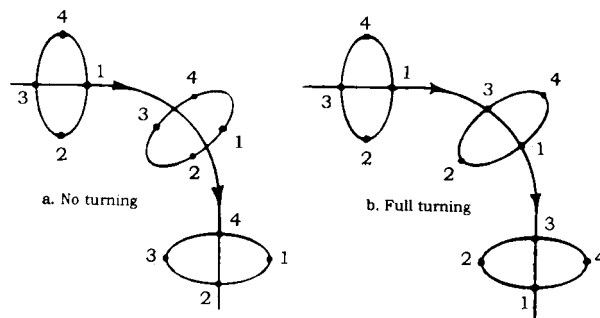


Figure 13 Path deviation with and without turning.

### The de Broglie frequency

There is another property of the electron that results from its  $\ell$ -wave. Except for the behavior of atoms, none of the observations of the related phenomena had been made before 1924 when de Broglie first proposed "matter waves" and the current explanations by quantum mechanical approaches are both inaccurate and non-intuitive.

Figure 14 illustrates the condition of a constant velocity electron as described earlier. The first half of the figure indicates the outgoing  $\ell$ -waves, whereas the second part is a plot of their wave-fronts at any particular time, say  $t = 0$ . From Eqs.(96) and (97), those fronts are spe-

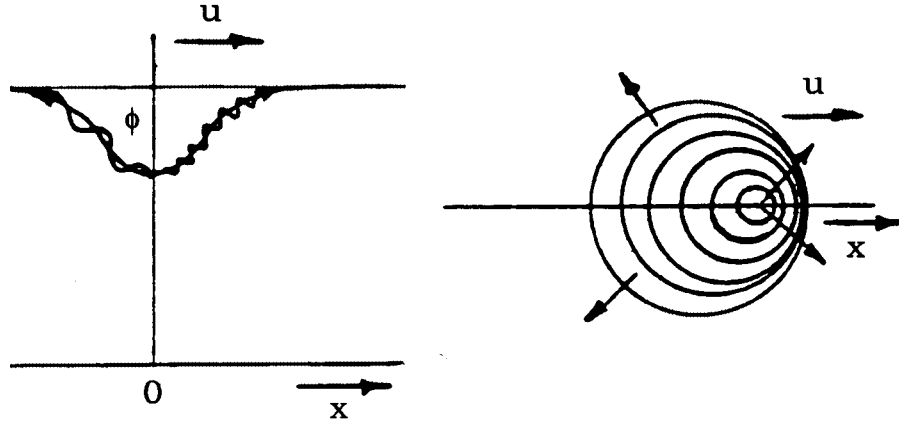


Figure 14 A constant velocity electron.

cified by the phase angle,

$$\delta = \frac{2\pi v_e \mathcal{R}}{\gamma c_0} \quad ; \quad (101)$$

and  $\mathcal{R}$  can be found along the  $x$  axis, where,

$$\mathcal{R} = \begin{cases} \frac{x}{1-\beta} & , \quad x > 0 \\ \frac{|x|}{1+\beta} & , \quad x < 0 \end{cases} \quad . \quad (102)$$

Substituting these values into the phase  $\delta$ , the frequency along the  $x$  axis is found to be changed to,

$$\begin{aligned} v_f &= \frac{v_e / \gamma}{1-\beta} \quad , \quad x > 0 \\ v_b &= \frac{v_e / \gamma}{1+\beta} \quad , \quad x < 0 \end{aligned} \quad . \quad (103)$$

This change is exactly equivalent to the ordinary doppler shift of a source or sink of sound; and, the electron's being a source of the  $\ell$ -waves, the front edge frequency is increased and the back is decreased, which is the opposite of the positron (sink).

For a free electron, the only effect of these changes is the adjusted shape described before. However, when interacting with another particle, the effect produced on the outcome is related to the *difference* between the front and back frequencies. For this reason, the difference frequency assumes a significance of major importance. Combining the frequencies of Eqs.(103), the difference frequency is,

$$\nu_d = \nu_f - \nu_b = \frac{\nu_e}{\gamma} \left( \frac{1}{1-\beta} - \frac{1}{1+\beta} \right) ,$$

which can be manipulated into the form,

$$\nu_d = 2\gamma\beta\nu_e . \quad (104)$$

To bring the derivation more in line with the conventional approach, the momentum (see Table IV) and Eq.(104) can be used to write,

$$pc_0 = \gamma m_0 u c_0 = \frac{m_0 c_0^2}{\nu_e} \frac{\nu_d}{2} , \quad (105)$$

which shows that the momentum and the difference frequency vary linearly because,

$$h = \frac{m_0 c_0^2}{\nu_e} \quad (106)$$

is a constant. When  $\nu_e$ ,  $m_0$  and  $c_0$  from Table III are substituted into Eq.(106), the value of the constant  $h$  is found to be,

$$h = 6.6260759 \times 10^{-27} , \quad \text{erg-sec} \quad (107)$$

the well known Planck's constant. With this in mind, Eq.(105) can be written as the de Broglie difference frequency<sup>15</sup>,

$$\nu_d = 2c_0 \frac{p}{h} . \quad (108)$$

The customary way of writing this expression is,

$$\lambda = \frac{h}{p} , \quad \text{WRONG} \quad (109)$$

and this relationship is called a "quantum mechanical" equation; but it is simply another way of writing Eq.(108) which comes from the doppler shift of the electron's  $\ell$ -wave. Physically there is a difference *frequency*. However, the Eq.(109) is probably better not used, because there is no difference wave, so the wavelength  $\lambda$  is nothing more than the inverse of Eq.(108) expressed in different units. The proper way to invert Eq.(108) is to write,

$$\Lambda_d = \frac{2c_0}{\nu_d} = \frac{h}{p} . \quad (110)$$

---

15. Although the author has chosen to call  $\nu_d$  the de Broglie frequency, it should not be confused with the conventional  $\nu_{db} = E/h$ , a fictitious frequency of a fictitious wave that is thought to travel along with the moving particle; not as a single wave (which leads to very unphysical velocities), but as a wave packet composed of many waves. The electron's radial  $\ell$  – waves, however, are just as real as t-waves.

$\Lambda_d$  is **not** the wave length of a mysterious wave that travels along curved paths. It is determined by real  $\ell$  – waves that propagate *radially* from the electron's center. It has nothing to do, directly, with the wavelength of any wave. Instead, *in this constant velocity case*, it is simply *the distance the electron travels during  $2/\beta$  cycles of the difference frequency*.

## XVIV THE LAYERED PARTICLES

### Introduction

For the last 100 years, particle physics has been successful primarily on the experimental side. The rare theoretical success has been the classification scheme called the "Standard Model", and the prediction of the existence of *one* particle. An extensive mathematical literature, e.g. string theory, N dimensions, etc., has done little to advance the knowledge of particle structure or predict particle masses.

The normal mutual support of theory and lab work has failed here, because QM is *non-visualizable* and suppresses *cause and effect*. This has guided experimentalists to the "bigger machine" approach; but particles are very flexible, and at some collision energy level they just come apart and new particles are formed. So, the limit has perhaps been reached in "bigger is better".

The ultimate goal is to change the present approach to particle structure by avoiding the difficulties of a dogged adherence to the use of successive layers of *point particles* to describe matter. The following is a small step in applying Main-Line physics to find a more flexible particle classification system and to point the way to a simpler, visualizable analytical picture.

### Particle categories

Here, the *conventional* categories of particles (e.g. leptons, baryons, etc.) will be abandoned. A new set, based on simple intuitive ether properties will be adopted. Particles are ether configurations that can act as relatively concentrated units for some significant time. If the structure cannot change without some outside influence, the particle is stable. If it *must* redistribute itself into a new form (i.e. "convert"), it is unstable. In the simplest organization of particle categories, no distinction between stable and unstable particles is made; and stability is just another property. However, as discussed later, stability is a complex problem. Based on the available information, there are only two different classes of fundamental particles:

1. Layered particles (layerons) - electric
2. c particles (c-ons) - magnetic

The *c particles*, photons and neutrinos, travel at the speed of light in free space, *and are quite different in structure from all the other particles*.



Neutrinos allow conservation of spin angular momentum in particle interactions. Just how they carry electric energy away from interactions is not yet understood. Photons carry energy away from charged particles, generally orbiting. Some details of the c-on particles' makeup will be presented later on.

The *layered* particles are composed of spherically symmetrical ether density distributions, very much like the electron, supported by  $\ell$ -waves and stacked in various arrangements of potential  $\bar{\phi}$  (see Figure 15). Examples of 1, 2 and 3 layered particles are the positron, pion and proton respectively. In the following, the layerons will be discussed

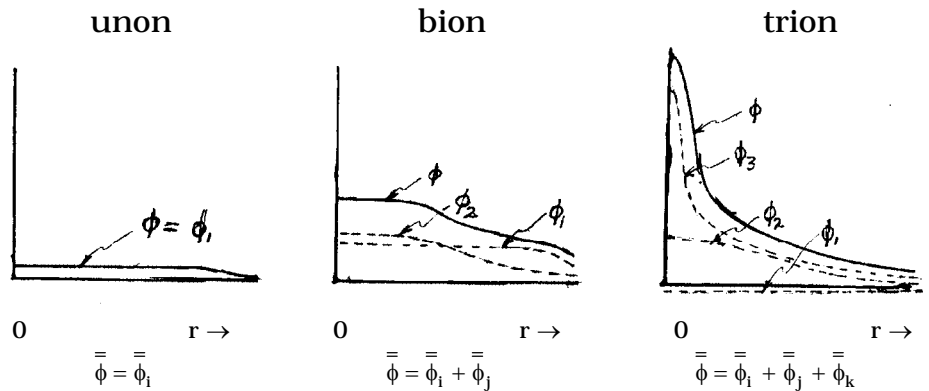


Figure 15 Layered particles.

in detail. The separation of layerons and c-ons helps to emphasize that layerons are bulk distortions with purely *electric* energy (see Sec. XVIII).

A proper analysis of the layerons begins with the unons, for which the theory is much advanced. The subsequent description of the bions and trions is far from complete, and leans heavily on the unon analysis. Nevertheless, the *visualization* is carried to the point where, even without the final rigorous answers to many important questions, the overall picture is almost totally understandable and only awaits the formal filling out of the many specific cases.

### Particle measurements

Many of the particle types studied by physicists are man-made, and only a very few are involved in the structure of the world (e, p, n). Table V lists the most important low energy particles and shows their decay products, which help to visualize how the particles are constructed. Numerous other vacuum disturbances, called *resonances*, have some particle-like behavior, but here they are not considered to be particles.

In spite of the fact that most of the data used to describe particle characteristics at present are obtained by high energy collisions of beams and targets, and that this information is indispensable, it is not of paramount importance here where the goals are somewhat different.

Instead, the discussion will lean toward particle decay, because only the electron and the proton (and the neutron when part of a nucleus) are stable. All other particles decay in a relatively short time after formation. The only difference between the bombardment and decay conversion processes is in the complexity of the initial conditions. Particle *conversion* involves only *one* pseudo-stable or unstable particle that redistributes its distortion to a lower energy configuration.

TABLE V  
PARTICLE CONVERSION PRODUCTS

		<u>Products</u>	<u>Percent</u>
<u>Unons</u>			
	$e^+ \rightarrow$	stable	
	$\mu^- \rightarrow$	$e^- \bar{\nu}_e \nu_\mu$	100
	$\tau^- \rightarrow$	$\mu^- \bar{\nu}_\mu \nu_\tau$	18
		$e^- \bar{\nu}_e \nu_\tau$	17
		bions, c-ons	65
<u>Bions</u>			
	$\pi^0$	$\gamma\gamma$	98.8
		$\gamma e^+ e^-$	1.2
	$\pi^-$	$\mu^- \bar{\nu}_\mu$	100
	$\eta$	$\gamma\gamma$	39.3
		$3\pi^0$	32.1
		$\pi^+ \pi^- \pi^0$	23.2
		$\pi^+ \pi^- \gamma$	4.8
	$K^+$	$\mu^+ \nu_\mu$	63.5
		$\pi^+ \pi^0$	21.2
		bions, unons	15.3
	All others yield mixes of bions, trions and c-ons		
<u>Trions</u>			
	$p \rightarrow$	stable	
	$n \rightarrow$	$p e^- \bar{\nu}_e$	100
	$\Lambda^0 \rightarrow$	$p \pi^-$	63.9
		$n \pi^0$	35.8
	$\Sigma^+ \rightarrow$	$p \pi^0$	51.6
		$n \pi^+$	48.3
	$\Sigma^0 \rightarrow$	$\Lambda \gamma$	100
	$\Sigma^- \rightarrow$	$n \pi^-$	100
	All others yield mixes of bions, trions and c-ons		

In particle *decay*, energy distortion, uninfluenced by any outside presence other than the datum fluctuation, will always redistribute in a downhill direction, i.e. produce only constituents of energies smaller

than the original (all adding up to the original energy, of course). This means that any of the particles to be examined will convert to one or more of those listed in Table V at lower rest energies only. These are not the only conversions the listed particles undergo, but those omitted, which may be very numerous in type, are found only a small fraction of the time, less than a few percent, and often as little as, say,  $10^{-6}$  percent.

### Unons

The most common single layer particle is the electron/positron, which was previously discussed in detail. Referring back, the e/p is a single dip (bump) of ether density  $\bar{\phi}$ , held in place by its  $\ell$ -waves, and of a form,

$$\bar{\phi} = \phi_0(1 - \psi^2) \quad , \quad (111)$$

where  $\psi = \varepsilon^{-r_i/r}$  is the intrinsic  $\ell$ -wave shape function, and  $r_i$  is the inflection radius. This single layer of potential yields single layers of energy and charge density, which indicates that the e/p is a unon with total rest energy and charge,

$$E_0 = 2\pi\phi_0^2 r_i \quad \text{and} \quad q = 8\pi\phi_0 r_i \quad . \quad (112)$$

*It is important to recognize that the solution of Eq.(47) for the  $\ell$ -wave shape function was in no way specific to the electron. Only when the particular frequency  $\omega_e$  was used, in Eq.(55), did the central density  $\phi_0$  of the bulk distribution  $\bar{\phi}$  identify the particle as the electron. The implication was that, during the formation process (e.g. pair production), the ether was distorted enough to start the oscillating  $\ell$ -wave with a peak density of at least  $\phi_{.m} = 1.3457 \times 10^4$  des. Then, in accordance with the  $\omega/\phi_{.m}$  characteristic of Figure 10, the  $\ell$ -wave oscillation continued at  $\omega_e = 7.7634 \times 10^{20}$  rad/sec. This suggests that, if the initial distortion had been much greater, unons of higher frequencies corresponding to the steps in Figure 10 would have been found, *and they have been*.*

The previous electron analysis applies to all the unons, if  $\omega$  is properly chosen, so Eq.(88) for the traveling  $\phi_{.}$  wave in the particle's central region can be used to find  $\phi_{.m}$  for the various unons. The density oscillates, so the *peak* amplitude at every radius is reached each time  $\sin\omega t = \pm 1$ , reducing Eq.(88) to,

$$\phi_{.p} = \frac{\phi_d a}{\omega r^2} \varepsilon^{-r_i/r} \left( 1 + \frac{r_i}{r} \right) \quad , \quad r < 30r_i \quad (113)$$

where  $r_i$  designates the *effective* radius (inflection point of the bulk density distribution) of each unon as determined by its  $\omega$ . Eq.(58)

establishes  $r_i$  as,

$$r_i = \frac{D}{\omega} \quad , \quad (114)$$

Combining Eqs.(113) and (114), it can be seen that the maximum  $\ell$ -wave density  $\phi_{.m}$  occurs at the radius  $r_p = C_m D / \omega$ , where  $C_m = (\sqrt{3} - 1) / 2$ .

Thus,

$$\phi_{.m} = \frac{\phi_d a}{\varepsilon^{\frac{1}{C_m}} C_m^2 D^2} \left( \frac{1}{C_m} + 1 \right) \omega \quad ,$$

or,

$$\omega = K_\omega \phi_{.m} \quad , \quad (115)$$

where,

$$K_\omega = 5.769032 \times 10^{16} \quad . \quad (116)$$

The difference between Eqs.(115) and (95), is that  $\omega = \mathcal{G}(\phi_{.m})$  describes the compression/oscillation property of the ether itself, whereas  $\omega = K_\omega \phi_{.m}$  describes a property of particle structure, a *solution* of the

$\ell$ -wave equation. *Both conditions must be satisfied.* Eq.(115) can be plotted over the  $\mathcal{G}(\phi_{.m})$  curve of Figure 10, and a union is found at each intersection with a frequency plateau. Figure 16 shows this plot.

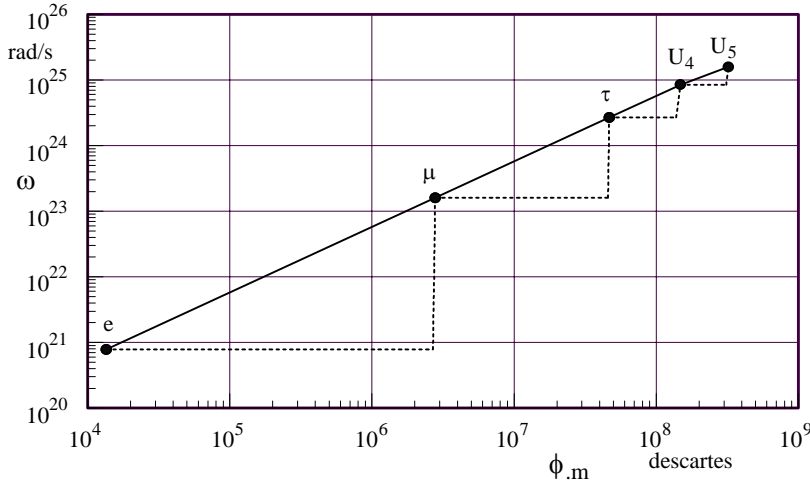


Figure 16 The unon family.

The electron is a stable particle, but the  $\mu$  has a mean life of only  $2.1970 \times 10^{-6}$  sec. It is still possible, however, that all unons are *basically* stable. In fact, since they are described by the same set of equations as the electron, it is likely. If they are basically stable, then it is only the datum fluctuations, triggering them into “conversion” into lower energy particles, that gives the appearance of instability. The amount of distortion compressed into their small volumes then establishes their mean lifetimes. The next higher energy unon is the  $\tau$ ,

which has a shorter mean life of  $2.910 \times 10^{-13}$  sec. No other unons have been observed, but properties of the multi-layer particles suggest that the higher frequencies of Figure 16 make 4th and 5th unons possible.

#### Measurement of the Unon Family $\omega$ 's

At this point, something more should be said about the compression/oscillation curve, and the roundabout method for measuring it. Farther on, a completely classical derivation of the hydrogen atom will be presented that uses only Newton's laws and some properties of the extended electron that were described earlier. That derivation can be used to find the equation for the frequencies in the hydrogen spectrum in the form,

$$v = \frac{e^4}{8m_0^2 c_0^6} v_e^3 \left( \frac{1}{n_f^2} - \frac{1}{n_i^2} \right) ; \quad (117)$$

or in the more usual form of the inverse wavelength,

$$\bar{v} = \frac{1}{\lambda} = R_H \left( \frac{1}{n_f^2} - \frac{1}{n_i^2} \right) , \quad (118)$$

where,

$$R_H = \frac{e^4}{8m_0^2 c_0^7} v_e^3 , \quad (119)$$

and  $n_f$  and  $n_i$  are the final and initial orbit numbers of the radiating electron respectively. The *measured* values of  $\bar{v}$  from the many transitions, including microwaves from free hydrogen in outer space, provide a value for  $R_H$ , the Rydberg constant, *one of the most accurately measured constants known*. It is found to be,

$$R_H = 1.0973731572 \times 10^5 \text{ cm}^{-1} . \quad (120)$$

If this value is used in Eq.(119), along with the measured values of  $m_e$ ,  $e$  and  $c_0$ , then  $v_e$  is,

$$v_e = \sqrt[3]{\frac{8m_0^2 c_0^7}{e^4} R_H} = 1.2355898 \times 10^{20} \text{ cyc/sec} , \quad (121)$$

or  $\omega_e = 7.7634396 \times 10^{20}$ . *This is essentially a measured value for  $\omega_e$ .*

The same procedure can be used to find  $\omega_\mu$  and it is found to be very close to the value used in the present work. Because the measurement of  $\ell$ -wave frequency just described is difficult for higher energy unons with very short lifetimes, a more practical shortcut is used here. The unon  $\omega$ 's are calculated from their measured bulk rest energies by combining Eqs.(55), (114) and (112) to give,

$$E_0 = \frac{\pi \phi_d^2 a^4 b^2}{8c_0^2 D} \omega . \quad (122)$$

The expression can be simplified by using the derived constant of Eq.(106), leading to,

$$E_0 = h\nu \quad , \quad (123)$$

where,

$$h = \frac{\pi^2 \phi_d^2 a^4 b^2}{4c_0^2 D} = 6.6260755 \times 10^{-27} \text{ erg-s} \quad . \quad (124)$$

Eq.(122) is represented in Figure 17, showing the bulk energies of the extended unon family of particles as a function of their frequencies.

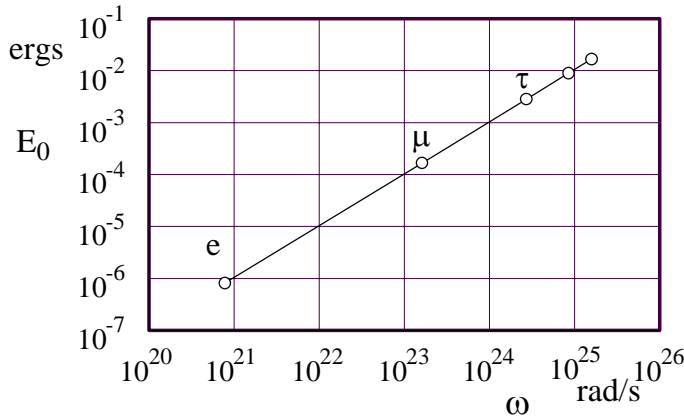


Figure 17 The unon family.

Unfortunately, determinations of  $\omega$  by this method require the fore knowledge of each unon's existence, and the measurement of its rest energy or mass. As mentioned earlier, there is no known method for measuring the  $\mathcal{G}(\phi_m)$  curve directly, so the two top steps shown in Figures 16 and 17 are just guesswork inspired by

some inferred ideas based on multi-layer particle structure. Even if unons  $U_4$  and  $U_5$  can be formed, their tremendous compaction would lead to such extremely short mean lives that their observation might be out of the question.

#### The energy compaction relationship

Eliminating  $\phi_0$  between the rest energy  $E_0$  and charge  $q$  found in Eqs.(112) above,

$$E_0 r_i = \frac{q^2}{32\pi} \quad , \quad \text{erg-cm} \quad (125)$$

a relationship called the *energy compaction equation*. It indicates that the more energetic unons have smaller radii. For  $q = e^\mp$ ,  $E_0 r_i = 2.8838 \times 10^{-20}$  erg-cm.

#### Unon size and stability

The unons of interest will be limited to the series of whole charged particles, i.e.  $e$ ,  $\mu$ ,  $\tau$ , ..., that can exist alone and be observed for some finite time. Using the compaction relationship, and the *measured* values of  $E_0$  for each of the unons, the calculated values for  $r_i$  and  $\phi_0$  are listed in Table VI with each particle's observed mean life.

TABLE VI  
UNONS, THE "PREFERRED" ETHER STATES

E <sub>0</sub> (ergs)	r <sub>i</sub> (cm)	φ <sub>0</sub> (hvolts)	mean life (s)
e 8.1871 × 10 <sup>-7</sup>	r <sub>1</sub> = 3.5224 × 10 <sup>-14</sup>	1.9233 × 10 <sup>3</sup>	Stable
μ 1.6929 × 10 <sup>-4</sup>	r <sub>2</sub> = 1.7035 × 10 <sup>-16</sup>	3.9768 × 10 <sup>5</sup>	2.1970 × 10 <sup>-6</sup>
τ 2.8472 × 10 <sup>-3</sup>	r <sub>3</sub> = 1.0129 × 10 <sup>-17</sup>	6.6886 × 10 <sup>6</sup>	2.9100 × 10 <sup>-13</sup>

The interesting features of Table VI are that, first, although each of these unons has the same charge  $e^\mp$  the more energetic particles have larger center potentials; and, their energy being packed into a smaller volume correlates with their being less stable. Second, it appears that the unon sequence is a set of *preferred* states that can exist as "pseudo-stable" particles *because of a fundamental property of the ether*.

Preferred Ether States

The  $\mu$  and  $\tau$  are often called "big electrons", because, like the electron, they have only the same two simple characteristics, their center potentials and their inflection radii. In the later discussion of multi-layer particles, it becomes clear that the multiple layers are similar to these three unons. In fact, *the radii of the layers in multi-layer particles are essentially the same as those listed in Table VI*. In one way this is surprising, but why it is true can be understood better from the following.

The Layer Radius/Frequency Equation

An important relationship between the inflection sphere radius of a unon and the unon's  $\ell$  - wave frequency is obtained by eliminating  $E_0$  from Eqs.(123) and (125), with the result,

$$\omega_i r_i = \frac{q^2}{16h} = D \quad , \quad (126)$$

where  $D = e^2/16h = 2.7346139 \times 10^7$  rad-cm/s. Eq.(126) takes the surprise out of the concept of preferred ether states, for although it is difficult to imagine how preferred *radii* could be a basic condition in the ether, it is comfortable to think of preferred ether *frequencies* as basic. So, assuming that Figure 16 indicates that the ether has preferred *frequency* states, Eq.(126) shows that this establishes preferred radii.

Figure 16 indicates two possible unons,  $U_4$  and  $U_5$ , *that have not yet been observed*. In analyzing the more massive, composite particles, it is

clear that there are at least two more preferred states, 4 and 5; but their great instability may make their existence possible only inside the composite particles and not observable as unons of higher order. The values shown are *educated guesses*. Table VII lists the important "rest" characteristics of the three known unons.

TABLE VII  
UNONS

Electron e	Muon $\mu$	Tau $\tau$
$\tau_e = \text{Stable}$	$\tau_\mu = 2.1970 \times 10^{-6} \text{s}$	$\tau_\tau = 2.910 \times 10^{-13}$
$E_{0e} = 0.51100 \text{ MeV}$	$E_{0\mu} = 105.66 \text{ MeV}$	$E_{0\tau} = 1,777.1 \text{ MeV}$
$r_e = 3.5224 \times 10^{-14} \text{ cm}$	$r_\mu = 1.7036 \times 10^{-16}$	$r_\tau = 1.0129 \times 10^{-17}$
$q_e = 1.7027 \times 10^{-9} \text{ hIC}$	$q_\mu = q_e = e$	$q_\tau = q_e = e$
$\phi_{0e} = 1923.3 \text{ hIV}$	$\phi_{0\mu} = 3.9768 \times 10^5$	$\phi_{0\tau} = 6.6886 \times 10^6$
$\sigma = \frac{h}{4\pi} = 5.2729 \times 10^{-28} \text{ erg-s for all } \rightarrow$		
$\mu_e = 3.2910 \times 10^{-20} \frac{\text{erg}}{\text{hIG}}$	$\mu_\mu = 1.5920 \times 10^{-22}$	$\mu_\tau = 9.4258 \times 10^{-24}$
$m_e = 9.1094 \times 10^{-28} \text{ g}$	$m_\mu = 1.8835 \times 10^{-25}$	$m_\tau = 3.1679 \times 10^{-24}$
$\omega_e = 7.7634 \times 10^{20} \frac{\text{rad}}{\text{sec}}$	$\omega_\mu = 1.6052 \times 10^{23}$	$\omega_\tau = 2.6998 \times 10^{24}$

### Elementary particles and quarks

From the foregoing it can be said that the unons are truly *elementary particles*. Each one stands alone with its own set of properties. From the 1960's on, it has been understood that the more elaborate particles are constructed of objects, now called quarks, that sometimes behave in a manner similar to particles but have fractional charges  $\pm e/3$  and  $\pm 2e/3$ . They are thought to be "point" charges like the conventional electron model. *Little is known about the spatial arrangement of these objects inside a composite particle.*

In interactions between quarks and external projectile particles, the *quarks behave as if they were independent entities, but no individual quark has ever been observed outside its housing particle.* This suggests that the composite particles might be made up of very flexible constructs similar to the finite unons described earlier, but having fractional charges, two components for the mesons and three for the baryons. In that case, although the components might freely move for short



distances, if one of the components were forced out of a composite particle, *because of its fractional charge, it would not qualify as one of the preferred unon solutions listed in Table VII nor as an elementary particle*, and so would decay; as would the remaining debris from the original particle. If this is a correct description of composite particles, then all of the properties of the Standard Model are preserved and yet a greater flexibility results.

The classification scheme described in the following includes all *whole charge* particles, but not photons and neutrinos. Using the Standard Model as a guide, the two "point" quarks that make up mesons and the three "point" quarks that make up baryons are replaced with the finite solutions of Eq.(111). *To avoid confusing the properties of the "point" quarks with these finite constructs, the term quark will not be used to describe the multiple particle components.*

## XX MULTI-LAYER PARTICLES

At this point the overall particle problem expands intolerably, and a logical, stepwise process of solving it demands an almost endless chain of decisions between possible alternative choices of methods and visualizations. The writer has made certain specific choices, and has carried the process as far as time and resources permit. Although most of the key structure is presented here, there are still volumes of calculations and measurements to be made in verifying and filling out of the structure as developed. Since the same can be said for the conventional "Standard Model", in its present state, the two approaches should be evaluated on the basis of their simplicity and their ability to complete the picture.

### The Multi-layer Classification System

Whereas the quarks have specific charges assigned, *the present scheme first indicates only the number of components a particle has.*

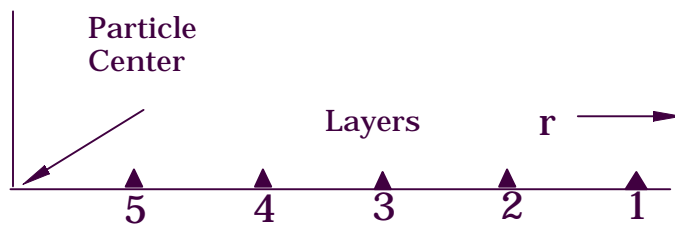


Figure 18 The preferred ether layer radii.

The basis for the nomenclature system is represented in Figure 18. The numbered markers represent the relative radii of layers, which are not equally spaced, indicating only the stacking order. The unons, bions and trions

are designated by  $U_i$ ,  $B_{ij}$  and  $T_{ijk}$  respectively, *where the i, j and k indicate the layers, and read from the outermost layer inwards.* The possibility that "quadrons" also exist can be accommodated by writing

$Q_{ijkl}$ , etc. In all these cases, *the Eq.(111) constructs take on only the preferred radii listed in Table II*, so the subscripts indicate the size and shape of the components.

In this system, the correspondence of the  $U_i$  designation to the unon family is,  $U_1 \rightarrow e$ ,  $U_2 \rightarrow \mu$  and  $U_3 \rightarrow \tau$ , etc., each successive particle having a single potential structure with a higher frequency, a smaller radius and a greater energy (see Fig. 15). The total charge of each is  $\pm e$ .

When considering the multi-layer particles, several new characteristics appear. For example, *the individual layers do not have different frequencies, each multi-layer particle has just one basic frequency  $\omega$ , and a single  $\ell$ -wave establishes all the layers*. The frequency  $\omega$  is not one of the "preferred" layer frequencies. Instead, the single  $\ell$ -wave of a multi-layer particle acts like a driver that *rings* the two or three "preferred" layers constituting that particular particle. As an example, the proton will be shown to have the structure  $T_{123}$ ; i.e. a potential component  $\phi_1$  with inflection radius  $r_1$ , a higher potential component  $\phi_2$  with smaller inflection radius  $r_2$ , and a very high potential component  $\phi_3$  with a still smaller inflection radius  $r_3$  (see Figure 15). On the other hand, there could be another trion  $T_{245}$ , with components  $\phi_2$ ,  $\phi_4$  and  $\phi_5$ , and inflection radii  $r_2$ ,  $r_4$  and  $r_5$ . Only those "preferred" *radii* given in Table II and the possible  $r_4$  and  $r_5$ , still to be determined accurately, ever appear in the *components* of multi-layer particles; but, each multi-layer particle has just one  $\ell$ -wave frequency  $\omega$ . It is an empirically determined fact that each whole charge particle has a rest energy  $E_0$  given by Eq.(122),

$$E_0 = \frac{\pi\phi_d^2 a^4 b^2}{8c_0^2 D} \omega = \hbar\omega \quad . \quad (127)$$

It is convenient to set up the next step in the classification system on the basis of the smoothed out charge density shell  $\rho$  rather than the potential  $\phi$  or the energy density shell  $\epsilon_e$ , *since the total integrated charge of any shell is constant, even when the particle is in motion*. The conventional "Standard Model" adopts a very rigid classification scheme that *combines* the layers and charges in a way that is too inflexible. The increased flexibility of the new system comes from the fact that after the structure of the particle has been established in the subscripts, the *charges of each component have yet to be specified*. Now it appears that *all independent, observable particles have total charges that are integral multiples of  $e$* . Because of this empirically determined fact the *total* particle charge distortion is  $\pm Ne$ , where  $N$  is an integer; so, at least in the two layer particles with charge  $e$ , *some of the layers must have fractional charge*. The fractional charges are found to be  $\pm e/3$  or  $\pm 2e/3$ .

In the new system, *the charge sign and magnitude are indicated, separately from the layers, by superscripts.* For example, the proton is identified as the trion  $T_{123}^{-++}$  where the superscripts indicate that the fractional charges of the components are  $-e/3, +2e/3, +2e/3$ . Thus,  $B_{ij}^{\alpha\beta}$  ( $i \leq j$ ) and  $T_{ijk}^{\alpha\beta\gamma}$  ( $i < j < k$ ) represent the complete description of the multi-layer particle categories (except for the spins), where  $\alpha, \beta, \gamma$  are given values of  $\overset{+}{1}, \overset{-}{1}, \overset{+}{2}, \overset{-}{2}, \overset{+}{3},$  or  $\overset{-}{3}$  for the six possible charge choices. Here,  $\overset{+}{1}$  indicates a charge of  $+e/3$ ,  $\overset{-}{2}$  a charge of  $-2e/3$  and  $\overset{+}{3}$  a charge of  $+e$ .

### Bion Configurations

Bions are classified into three groups:

1. Concentric layer bions,
2. Eccentric layer, inside orbiters, }  $B_{ij} \quad i < j$
3. Outside orbiters  $B_{ii}$

Group 1 bions have two shells, one inside the other, with a common center. They have a net charge of  $e^\pm$ , whereas the orbiters have two layers of equal and opposite charge that give a net charge of zero. Group 2 bions have two shells, one inside the other, with centers displaced and both orbiting a common center. Group 3 bions form a "system" like positronium, with two separated, equal fractional charge shells, orbiting a common center. Observed *concentric* bions are tentatively identified as  $\pi^\pm, D^\pm, D_s^\pm,$  and  $B^\pm$ . *Inside orbiter* bions are probably  $K^0, D^0, B^0$  and  $B_s^0$  and *outside orbiter* bions are most likely  $\pi^0, \eta, \eta', \eta_c$  and  $\Upsilon$ . The latter ( $B_{ii}$ ) decay like Positronium and, similarly, produce two photons. *This two photon radiation is their hallmark.*

All the bions are possibly stable, in a fundamental sense (if it were not for the datum fluctuations), but *all bions convert to lower energy forms shortly after their formation.* Because the bions decay rapidly, their correct analysis must address the transient case, which has many mathematical difficulties. Therefore, the measured bion energies are always slightly smaller than the values calculated from the "concentric, static" approximation.

$B_{ij}$  bions decay mostly into unons and neutrinos. Figure 19 diagrams the first six forms of the  $B_{ij}$  bion hierarchy. For each of these  $B_{ij}$  designations, there are *several* possible combinations of charge. For complete generality the charges  $\overset{+}{3}$  and  $\overset{-}{3}$  were included earlier; but in the following, to relate to the present view of quarks, the  $\overset{+}{3}$  and  $\overset{-}{3}$  classes

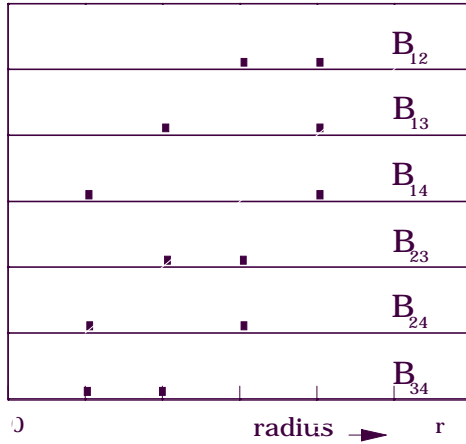


Figure 19 The  $B_{ii}$  bion hierarchy

will not be developed. As an example, consider the lowest order bion category  $B_{12}^{\alpha\beta}$ . Each of the two layers could have one of four different charge distortions, so the total possible types of  $B_{12}$  bions is 16. However, this number is reduced considerably because the total particle charge must be zero or an integral multiple of  $\pm e$ . Therefore, the total combinations that could possibly represent real particles is reduced to:

$$\begin{aligned}
 & B_{12}^{+-}, B_{12}^{++}, B_{12}^{+-}, B_{12}^{+-}, \\
 & B_{12}^{-+}, B_{12}^{--}, B_{12}^{--}, B_{12}^{-+}.
 \end{aligned}$$

Now, since the second row represents four particles that are exactly like those in the first row, except that their charges are opposite, the second row particles are called the “anti-particles” of those in the first row. Thus, the  $B_{12}$  category describes only four different, possible particles (and their anti-particles). Subsequent analysis, using the  $\ell$ -wave equation, can help to decide which, if any, is a real particle and to identify one or all with those observed possible particles (and their anti-particles):

$$B_{ij}^{+-}, B_{ij}^{++}, B_{ij}^{+-}, B_{ij}^{+-}. \tag{128}$$

The first and last of these are inside orbiters, the second and third are concentric bions.

Unlike the unons, which have the “stable” electron at the base of their energy ladder, bions are short lived, and even the lowest energy  $B_{ij}$  bion is triggered to convert. No more need be said about  $B_{ij}$  bions until later, when solutions of the  $\ell$ -wave equation reduces their possible number.

In the most general case of the outside orbiter category, each  $B_{ii}^{\alpha\beta}$  yields only three possible types of bions (they are their own anti-particles):

$$B_{ii}^{+-}, B_{ii}^{+-}, B_{ii}^{+-}. \tag{129}$$

The last,  $B_{ii}^{33+-}$ , is positronium, which is not considered a fundamental particle.

### Trion Configurations

The trions come in combinations of *concentric* shells, or *eccentric inside orbiters*. Although work is in progress, the only accurately calculable concentric trion at this time is the stable proton. The great majority of trions appear to be *inside* orbiters, none of which has been finally identified yet due to mathematical intractability. The success of the proton analysis demands that the much more difficult problem of the

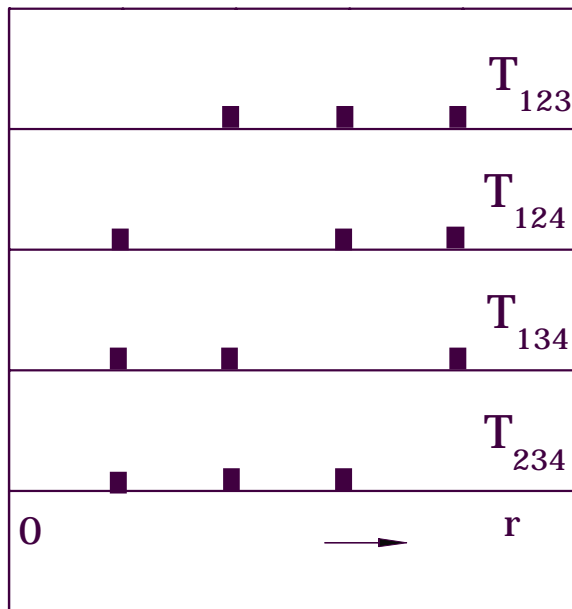


Figure 20 Concentric trions.

*orbiter* trions be pursued, particularly that of the neutron.

The same procedure that established the possible bions is applicable to the trions as well. However, in the basic trion hierarchy, there might not be outside orbiters. Thus, for now, the *basic* trion configurations *given here* involve only concentric cases of  $T_{ijk}^{\alpha\beta\gamma}$  where  $i < j < k$ . The result is that the first few  $T_{ijk}$

appear as in Figure 20. Each category has 3 layers, and each layer can have one of 4 possible charges, so every category has 64 *possible*

particles. Here, again, the requirement for  $\pm Ne$  ( $N=0,1,2,\dots$ ) total particle charge reduces the number of possibles to one out of eight, or 8 (plus their anti-particles). Subsequent analysis can reduce this number.

Of particular interest in this class is the proton, since it is the only “stable” trion known. As before, with the unons and bions, all of these concentric trions might be *basically* stable but susceptible to triggering into energy conversions by the datum fluctuations, which accounts for their short mean lifetimes. The proton, however, is stable, and the lowest sustainable trion form, just as the electron, at the bottom of the unon energy ladder, is stable.

The charge assignments for the 8 tentative trions of each set are:

$$\begin{array}{cccc} \bar{\bar{\bar{1}}\bar{\bar{1}}\bar{\bar{1}}} & \bar{\bar{\bar{1}}\bar{\bar{1}}\bar{2}} & \bar{\bar{\bar{1}}\bar{2}\bar{1}} & \bar{\bar{\bar{1}}\bar{2}\bar{2}} \\ (111) & (112) & (121) & (122) \\ \\ \bar{2}\bar{1}\bar{1} & \bar{2}\bar{1}\bar{2} & \bar{2}\bar{2}\bar{1} & \bar{2}\bar{2}\bar{2} \\ (211) & (212) & (221) & (222) \end{array}$$

## Multi-layer Particle Analysis

Analysis of *concentric* multi-layer particles runs parallel to the derivation for the electron in Sections X - XVI, and pages 58 - 63. Figure 21 lists the principal steps involved. Although the multi-layer equations are more elaborate, the outline in Figure 22 shows that roughly the same steps are necessary to determine the concentric *layered* particle's characteristics. In the following, these steps are elaborated upon and the method is applied to *concentric* bions and trions.

**UNON ANALYSIS**

1. Assume a simple trial potential.  

$$\bar{\phi} = \phi_0(1 - \psi_i^2)$$
2. Find a correct  $\ell$  - wave shape function.  

$$\psi_i = \varepsilon^{-r_i/r}$$
3. Solve for the correct charge density.  

$$\rho = -\nabla^2 \bar{\phi} = 4 \frac{\phi_0 r_i^2}{r^4} \varepsilon^{-2r_i/r}$$

Figure 21. Unon analysis outline.

**MULTI-LAYER ANALYSIS**

1. Assume a trial potential.  

$$\bar{\phi} = \phi_0(1 - \psi^2) = \phi_{01}(1 - \psi_1^2) + \phi_{02}(1 - \psi_2^2) + \phi_{03}(1 - \psi_3^2) + \dots$$
2. Find each layer's new  $\ell$  - wave shape function.  

$$\psi_i = \varepsilon^{-\frac{r_e}{r}} \left[ 1 + K_i E_2\left(\frac{r}{r_e}\right) \right]$$

( $r_e$  is the *effective* radius of the whole particle)
3. Find the  $K_i$  for each layer.  

$$K_i = \left( \frac{r_i}{r_e} - 1 \right) \varepsilon^{r_i/r_e} = \left( \frac{\omega}{\omega_i} - 1 \right) \varepsilon^{\omega/\omega_i}$$
4. Solve for the correct layer charge densities.  

$$\rho_i = -\nabla^2 \bar{\phi}_i = \frac{q_i r_e}{2\pi} \left( 1 + K_i \varepsilon^{-r/r_e} \right) \frac{\psi_i^2}{r^4}$$

Figure 22. Multi-layer analysis outline.

Earlier it was said that *all* unons had charge distortion  $\pm e$ . When *multi-layer* particles are observed, at least two types are found to have a total charge of  $\pm 2e$ . Although a few multi-layer particles form with  $N = 2$ , most have the same *total charge*  $\pm e$  found in the unons.

### Multi-layer Trial Potential

Although later the proton will be used as an example, it is straightforward to generalize the process for any *concentric* particle. The principal idea is that, as discussed in Sections III, IV and XIV, *the only physical presence in a particle layer is its potential*  $\bar{\phi}_i$ ; so, in the multi-layer particle, *the only physical presence is the **sum** of the potentials*  $\bar{\phi}_i$  of the particle's layers (see Figure 15),

$$\bar{\phi} = \bar{\phi}_1 + \bar{\phi}_2 + \bar{\phi}_3 + \dots \quad , \quad (130)$$

Paralleling the unon derivation, the same simple form of *trial solution* of Maxwell's scalar equation is taken as,

$$\bar{\phi} = \phi_0(1 - \psi^2) \quad , \quad (131)$$

where  $\psi$  is the *multi-layer* shape function. In terms of the individual layer potentials, this becomes,

$$\bar{\phi} = \phi_{01}(1 - \psi_1^2) + \phi_{02}(1 - \psi_2^2) + \phi_{03}(1 - \psi_3^2) + \dots \quad , \quad (132)$$

which reduces to,

$$\bar{\phi} = \phi_0 - (\phi_{01}\psi_1^2 + \phi_{02}\psi_2^2 + \dots) \quad , \quad (133)$$

where,

$$\phi_0 = \phi_{01} + \phi_{02} + \phi_{03} + \dots \quad . \quad (134)$$

The  $\phi_{0i}$ 's can each be positive or negative.

### Multi-layer Shape Function

*All layerons have a single ingoing or outgoing  $\ell$ -wave with a single characteristic frequency  $\omega$ .* The thing that distinguishes the *multi-layer* particles is that they have a *composite* shape function. In summarizing the results of the classification system and the multi-particle analysis, to this point, a conflict arises in the following way. Looking back to Eq.(127), *that relationship between the particle's rest energy and frequency appears to hold for all concentric layerons*, and it is an essential part of the so called "quantum" properties of matter. Furthermore, tests which included pionic atoms (electron replaced by a  $\pi^-$  bion) have been repeated with more massive bions. All such tests indicate that the orbit selection implied by the de Broglie frequency, to be discussed later, applies in general. Thus, *all these phenomena require that any particle have one, single  $\ell$ -wave frequency.*

On the other hand, the preceding analysis shows that if the same shape function  $\psi = \varepsilon^{-r_i/r}$  used for the unons were used for each of the layers, *multiple frequencies would be required, one for each layer.* The resolution lies in the use of a more general, layer  $\ell$ -wave shape function.

### The New Layer Shape Function

The most interesting aspect of multi-layer particles is that *the layers are essentially independent*, though an indispensable part of the whole particle; i.e. *the shape functions,  $\psi_i$ , of the individual layers must satisfy the  $\ell$ -wave equation independently*. Analysis available in footnote reference 1 (2009) reveals that the  $\psi_i$  must satisfy the equation,

$$\frac{d^2\psi_i}{dr^2} - \frac{1}{\psi_i} \left( \frac{d\psi_i}{dr} \right)^2 + \left( \frac{2}{r} + \frac{\omega}{D} \right) \frac{d\psi_i}{dr} - \frac{\psi_i}{r^2} = 0 \quad . \quad (130)$$

*This equation, which applies to the individual layers, is identical to Eq.(47) which gave the unon's shape function. In the previous unon cases, for simplicity, a very limited solution of Eq.(130) was used that applies only to unons. At this point, it is necessary to use a more general solution.*

The new  $\ell$ -wave shape function for each layer takes the form,

$$\psi_i = \varepsilon^{-\frac{r_e}{r} \left[ 1 + K_i E_2\left(\frac{r}{r_e}\right) \right]} \quad , \quad (131)$$

where  $E_2(r/r_e)$  is the exponential integral of the second kind<sup>16</sup>,  $r_e$  the effective radius of the whole multi-layer particle and  $K_i$  an, as yet, unspecified constant. Figure 23 depicts the family of  $\psi_i$  curves with  $K_i$  as the parameter. The  $K_i = 0$  curve applies to the unons, and gives the simple structure discussed earlier. However, *in multi-layer particles, each layer has a different value of  $K_i$  ; and the radii of the layers are specified*

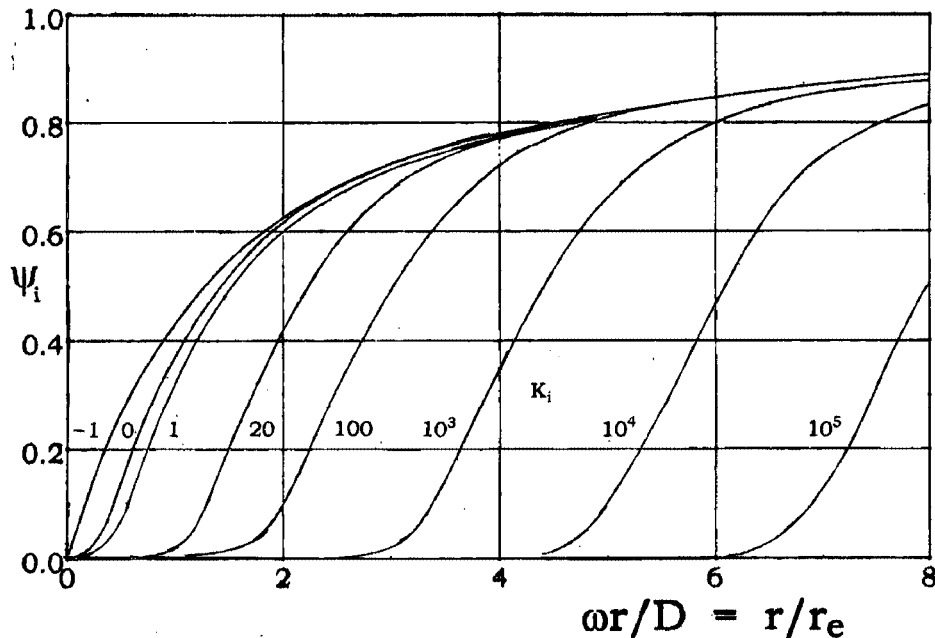


Figure 23. Layer shape function curves as a function of  $K_i$ .

16. Handbook of Mathematical Functions, National Bureau of Standards, AMS 55, p228.



by both the particle frequency  $\omega$ , which is common to all layers in any one particle, and the values of the parameter  $K_i$ , which sets the inflection radius of each potential layer. The *shapes* of the  $\psi_i$  are determined primarily by the factor  $\varepsilon^{-r_e/r} = \varepsilon^{-D/\omega r}$ , just as before, but *the purpose of the  $K_i$  is to allow each layer to adjust itself, relative to the total particle frequency  $\omega$ , so that the layer frequencies  $\omega_i$ , given by Eq.(126), match the "preferred" layer frequencies.*

Two forms of the derivative of  $\psi_i$  are required in the following,

$$\frac{d\psi_i}{dr} = \frac{D}{\omega r^2} \left( 1 + K_i \varepsilon^{-\frac{\omega r}{D}} \right) \psi_i \quad , \quad (132)$$

and,

$$\frac{d\psi_i^2}{dr} = \frac{2D}{\omega r^2} \left( 1 + K_i \varepsilon^{-\frac{\omega r}{D}} \right) \psi_i^2 \quad . \quad (133)$$

### Multi-layer Particle Charge Density

The charge density of a *concentric* multi-layer particle is,

$$\rho = \frac{q}{4\pi r^2} \left( \frac{\phi_{01}}{\phi_0} \frac{d\psi_1^2}{dr} + \frac{\phi_{02}}{\phi_0} \frac{d\psi_2^2}{dr} + \frac{\phi_{03}}{\phi_0} \frac{d\psi_3^2}{dr} + \dots \right) \quad , \quad (134)$$

which can be integrated over all space from  $r = 0$  to  $r \rightarrow \infty$ , with the result,

$$q = q_1 + q_2 + q_3 + \dots \quad , \quad (135)$$

where,

$$q_i = \mp \frac{\phi_{0i}}{\phi_0} q \quad . \quad (136)$$

From Eqs.(134) and (133), the charge density of each layer is,

$$\rho_i = \frac{q_i D}{2\pi\omega} \left( 1 + K_i \varepsilon^{-\frac{\omega r}{D}} \right) \frac{\psi_i^2}{r^4} \quad . \quad (137)$$

For larger  $K_i$ , the charge shells move out to larger radii and their peak values are lowered. Nevertheless, when Eq.(137) for the layer charge density is integrated over all space, the *layer charges  $q_i$  are found to be independent of  $K_i$* . It is this fortunate circumstance that permits using the layer charges in the classification scheme. Thus,  *$K_i$  is a parameter that can be varied after specifying the charge structure to be examined;* and, although it changes the radii of the charge shells as well as the energy shells, its major effect is on the magnitudes of the layer energies.

### The Multi-layer Bulk Density Equation

The *single*  $\ell$ -wave that rings a multi-layer particle is written as,

$$\mathbf{V}_\pm = \hat{\mathbf{r}}\sqrt{N} \frac{\mathbf{a}}{r} \psi C^\mp \quad , \quad C^\mp = \cos \omega \left( t \mp \frac{r}{c_0} \right) \quad , \quad (138)$$

(upper sign outgoing, lower sign in going) where  $N$  is an integer that determines the particle's *total charge*  $\mp Ne$ , and  $\psi$  is the multi-layer shape function. From Eq.(138) and the  $\ell$ -wave continuity equation,

$$\phi_\pm = \pm \sqrt{N} \frac{\phi_d \mathbf{a} \psi}{c_0 r} \left( C^\mp \mp \frac{c_0}{\omega} \left( \frac{1}{\psi} \frac{d\psi}{dr} + \frac{1}{r} \right) S^\mp \right) \quad . \quad (139)$$

Combining Eqs.(138) and (139) gives,

$$\overline{\phi \cdot \mathbf{V}_\pm} = \pm N \frac{\phi_d \mathbf{a}^2 \psi^2}{2c_0 r^2} \quad \text{and} \quad \nabla \cdot \overline{\phi \cdot \mathbf{V}_\pm} = \pm N \frac{\phi_d \mathbf{a}^2}{2c_0 r^2} \frac{d\psi^2}{dr} \quad . \quad (140)$$

From Eqs.(54) and (70),

$$\rho = -b \nabla \cdot \overline{\phi \cdot \mathbf{V}_\pm} = \mp N \frac{\phi_d \mathbf{a}^2 b}{2c_0 r^2} \frac{d\psi^2}{dr} \quad , \quad (141)$$

which can be integrated over all space from  $r = 0$  to  $r \rightarrow \infty$ , with the result,

$$\mathbf{q} = \mp 2\pi N \frac{\phi_d \mathbf{a}^2 b}{c_0} = \mp Ne \quad . \quad (142)$$

Starting with the bridge equation and Eq.(140),

$$\nabla \bar{\phi} = b \overline{\phi \cdot \mathbf{V}_\pm} = \pm \hat{\mathbf{r}} N \frac{\phi_d \mathbf{a}^2 b}{2c_0 r^2} \psi^2 \quad , \quad (143)$$

and,

$$\frac{d\bar{\phi}}{dr} = \pm N \frac{\phi_d \mathbf{a}^2 b}{2c_0 r^2} \psi^2 \quad . \quad (144)$$

Integration produces the bulk density distribution,

$$\bar{\phi} = \bar{\phi}_1 + \bar{\phi}_2 + \bar{\phi}_3 + \dots \quad , \quad (145)$$

where,

$$\bar{\phi}_i = S_i - \frac{q_i}{4\pi} \int_0^r \frac{\psi_i^2}{r^2} dr \quad , \quad (146)$$

and  $S_i$  is a constant of integration. When  $r = 0$ ,  $\bar{\phi}_i = \phi_{0i} = S_i$ ; so,

$$\bar{\phi}_i = \phi_{0i} - \frac{q_i \omega}{4\pi D} I_i(r) \quad \text{and} \quad I_i(r) = \frac{D}{\omega} \int_0^r \frac{\psi_i^2}{r^2} dr \quad . \quad (147)$$

As  $r \rightarrow \infty$ ,  $I_i(r) \rightarrow I_i(\infty)$  and  $\bar{\phi}_i \rightarrow 0$ . The  $\ell$ -wave analysis leading to Eq.(114) determines the effective radius of a whole multi-layer particle to be,

$$r_e = D/\omega \quad . \quad (148)$$

### Determination of $K_i$

It was stated earlier that each potential layer is associated with a  $K_i$  that determines the inflection radius of that layer. Starting with the gradient of the layer potential in Eq.(146), differentiating it with respect to  $r$ , setting the differential to zero and solving for  $K_i$  leads to,

$$K_i = \left( \frac{\omega r_i}{D} - 1 \right) \varepsilon^{\omega r_i / D} \quad , \quad (149)$$

where  $r_i$  is the inflection and maximum energy density radius of the layer. One way to look at Eq.(149) is to recognize that with Eq.(147) it can be written in the form,

$$K_i = \left( \frac{r_i}{r_e} - 1 \right) \varepsilon^{r_i / r_e} \quad . \quad (150)$$

If  $K_i$  of a layer is a very large number, that layer is far out from the main energy of the particle. If  $K_i$  is near zero the layer is close to the effective radius  $r_e$ . For  $-1 < K_i < 0$ , the layer is smaller than  $r_e$ . An even more useful way to think about Eq.(149) results from combining Eqs.(144), (150) and (147) in the form,

$$K_i = \left( \frac{\omega}{\omega_i} - 1 \right) \varepsilon^{\omega / \omega_i} \quad , \quad (151)$$

where the  $\omega_i$  are the "preferred" frequencies listed in Table VIII. Eq.(151) is the most convenient for determining the multi-layer particle structure.

TABLE VIII  
"PREFERRED" FREQUENCIES

Layer	$\omega_i$ (rad/sec)	$r_i$ (cm)
1	$7.76344 \times 10^{20}$	$3.52243 \times 10^{-14}$
2	$1.60523 \times 10^{23}$	$1.70356 \times 10^{-16}$
3	$2.69981 \times 10^{24}$	$1.01289 \times 10^{-17}$
4	$8.508 \times 10^{24}$	$3.214 \times 10^{-18}$
5	$1.580 \times 10^{25}$	$1.731 \times 10^{-18}$

### Multi-layer Particle Energy

Starting with the incremental ether density of Eq.(145), the gradient at each point in space is,

$$\nabla\bar{\phi} = \nabla\bar{\phi}_1 + \nabla\bar{\phi}_2 + \nabla\bar{\phi}_3 + \dots \quad ;$$

and, from Eq.(64), the total electric energy density of a *concentric* layeron is found to be,

$$\begin{aligned} \varepsilon_e = \frac{1}{2}(\nabla\bar{\phi})^2 &= \frac{1}{2}(\nabla\bar{\phi}_1)^2 + \frac{1}{2}(\nabla\bar{\phi}_2)^2 + \dots \\ &+ \nabla\bar{\phi}_1 \cdot \nabla\bar{\phi}_2 + \nabla\bar{\phi}_1 \cdot \nabla\bar{\phi}_3 + \dots \\ &+ \nabla\bar{\phi}_2 \cdot \nabla\bar{\phi}_3 + \nabla\bar{\phi}_2 \cdot \nabla\bar{\phi}_4 + \dots \\ &+ \dots \end{aligned} \quad . \quad (152)$$

Integrating Eq.(152) over all space gives the total energy of the particle in the form,

$$\begin{aligned} E_0 &= E_1 + E_2 + E_3 + \dots \\ &+ E_{12} + E_{13} + E_{14} + \dots \\ &+ E_{23} + E_{24} + E_{25} + \dots \\ &+ \dots \end{aligned} \quad , \quad (153)$$

where the  $E_i$  are the layer “self” energies and the  $E_{ij}$  are the “interaction” energy deformations, between the layers, stored in the ether during the particle formation process.

The energies,  $E_i$ , of the individual layers are found by first differentiating Eq.(146) to obtain,

$$\frac{d\bar{\phi}_i}{dr} = -\frac{q_i}{4\pi} \frac{\psi_i^2}{r^2} \quad , \quad (154)$$

and then writing the energy density as,

$$\varepsilon_{ei} = \frac{1}{2}(\nabla\bar{\phi}_i)^2 = \frac{q_i^2}{32\pi^2} \frac{\psi_i^4}{r^4} \quad . \quad (155)$$

When Eq.(155) is integrated over all space, the *layer* self energy is found to be,

$$E_i = \frac{q_i^2}{8\pi r_e} J_i(\infty) \quad , \quad J_i(r) = r_e \int_0^r \frac{\psi_i^4}{r^2} dr \quad (156)$$

The interaction energies,  $E_{ij}$ , can be written,

$$E_{ij} = \frac{q_i q_j}{4\pi r_e} J_{ij}(\infty) \quad , \quad J_{ij}(r) = r_e \int_0^r \frac{\psi_i^2 \psi_j^2}{r^2} dr \quad (157)$$

In the more complicated cases, involving orbiters, in addition to the self and interaction energies, the orbiting layers are deformed and include their extra orbital kinetic energies which must be added in to give the total particle energy.

## Multi-layer Particle Calculations

In the preceding analysis, certain integrals that depend upon  $\psi_i$  were derived. No closed form solution for any of these is known to the writer. Instead, they must be evaluated by numerical integration. The integrals, including several left out of this reduced version, are designated as,  $I_i(\infty)$ ,  $J_i(\infty)$ ,  $J_{ij}(\infty)$ ,  $L_i(\infty)$  and  $M_i(\infty)$ , and they have been used in both graphical and tabular form. The most fundamental application of the analysis starts by *choosing a particular layer/charge configuration to see what kind of particle it represents*. The analysis **predicts** its frequency  $\omega$ , its rest energy  $E_0$ , and beyond that its physical structure, charge distribution, magnetic moment etc. These are then used to determine whether or not such a particle has been observed. In every case, the basic "existence" test is that Eqs.(127) and (153) are satisfied simultaneously. Several techniques were used to evaluate the integrals, including computer integration with Q Basic, and graphics. When solving problems it is convenient to have the program in Basic provide, *during the calculation*, the values of all the integrals for a given  $K_i$ . In some cases, a table that permanently provides sets of the integrated values for several frequencies over a selected range is more useful.

Tables of  $I_i(\infty)$ ,  $J_i(\infty)$ ,  $J_{ij}(\infty)$ ,  $L_i(\infty)$  and  $M_i(\infty)$  are presented in Appendix I of PHYSICS2001Rev. In the following the argument,  $\infty$ , will not be indicated, and these integrals will just be designated by  $I_i$ ,  $J_i$ , etc. The tabulated values are nowhere near as accurate as particle physicists generally take their work, but the purpose here is to illustrate the techniques rather than to supply final particle characteristics. In making up the tables, certain approximations were used in the extreme ranges. Generally, these have a very small effect on total particle structure.

In doing the integrals for the interaction constants  $J_{ij}$ , it is easy to show that substitution of,

$$K_{ij} = \frac{1}{2}(K_i + K_j) \quad , \quad (158)$$

allows using the  $J_i$  integral calculations for the  $J_{ij}$ , thus eliminating the need for a considerable amount of computation. In that case, an effective  $\omega_{ij}$  can be defined so that,

$$K_{ij} = \left( \frac{\omega}{\omega_{ij}} - 1 \right) \varepsilon^{\omega/\omega_{ij}} \quad . \quad (159)$$

### The Concentric Particle Existence Criterion

As mentioned above, the existence criterion is based upon the two energy Eqs.(127) and (153). In terms of the derived integrals, Eq.(153) becomes,

$$E_0 = \frac{1}{8\pi r_e} \left[ q_1^2 J_1 + q_2^2 J_2 + \dots + 2q_1 q_2 J_{12} + 2q_1 q_3 J_{13} + \dots \right. \\ \left. + 2q_2 q_3 J_{23} + \dots \right. \\ \left. + 2q_3 q_4 J_{34} + \dots \right] \quad , \quad (160)$$

and Eq.(127) is,

$$E_0 = h\nu = \hbar\omega \quad . \quad (161)$$

Eqs.(156) and(157) indicate that the  $J_i$  values depend upon  $\omega$  through  $\psi_i$  (see Figure 23), so *there are 2 independent equations for  $E_0$  as a function of  $\omega$ .*

Considerable ease in the calculations derives from a slight change of variable. By defining a quantity,

$$J = \frac{8\pi D}{e^2 \omega} E_0 = \left[ \frac{q_1^2}{e^2} J_1 + \frac{q_2^2}{e^2} J_2 + \dots + 2 \frac{q_1 q_2}{e^2} J_{12} + 2 \frac{q_1 q_3}{e^2} J_{13} + \dots + 2 \frac{q_2 q_3}{e^2} J_{23} + \dots \right] \quad , \quad (162)$$

Eq.(161) becomes,

$$J = \frac{4hD}{e^2} = 0.25 \quad . \quad (163)$$

For a given layer/charge configuration, Eqs.(162) and (163) can be plotted as functions of  $\omega$ , as illustrated in Figure 24; and the ***predicted*** particle frequency  $\omega$  is found at their intersection. The particle's rest energy  $E_0$  follows from Eq.(161).

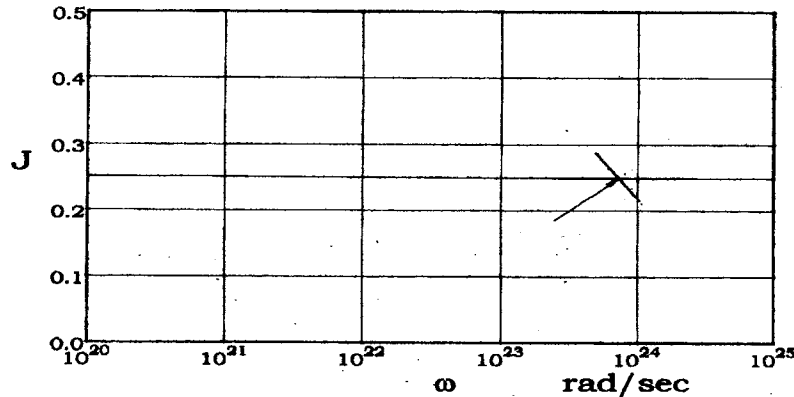


Figure24. Eqs.(162) and (163) solved for  $\omega$ .

No measured data taken from a particle being investigated are used in this calculation. The only *measured* data involved in setting up the system are the unon frequencies and radii of Table VIII required to establish the "preferred" vacuum frequencies. The only integrals involved in the existence criterion are the  $J_i$  's and the  $J_{ij}$  's.

Predicted Concentric Particles

It is now possible to plot the various concentric bion and trion predictions along the  $J = 0.25$  line of Figure 24.

Concentric Bions

The existence criterion for bion layer/charge forms is,

$$J = \frac{q_i^2}{e^2} J_i + \frac{q_j^2}{e^2} J_j + 2 \frac{q_i q_j}{e^2} J_{ij} = 0.25$$

A typical example is the  $B_{23}^{++}$ , which leads to,

$$J = \frac{1}{9} J_2 + \frac{4}{9} J_3 + \frac{4}{9} J_{23}$$

The graphical solution is done with a programmable hand calculator to add the three terms. The analysis has been used to plot the intersecting curves for all concentric bions up to, and including, the fifth layer. Figure 25 shows the result. In trying to assess which observed particles might correspond to these solutions, it must be remembered that all bions are "unstable", i.e., they convert into lower energy particles. Later on, in calculating the proton properties, the fact that it is a truly stable particle that does not convert in its free state allows the intersection values and the observed  $E_0, \omega$  to be essentially exact. This is not true for the concentric bions, so the results require some interpretation. For example, their mean life is about  $10^{-8}$  to  $10^{-12}$  seconds. If, as has been suggested earlier, they are basically stable, but are triggered by the datum fluctuations, the mean lives should be dependent on both the

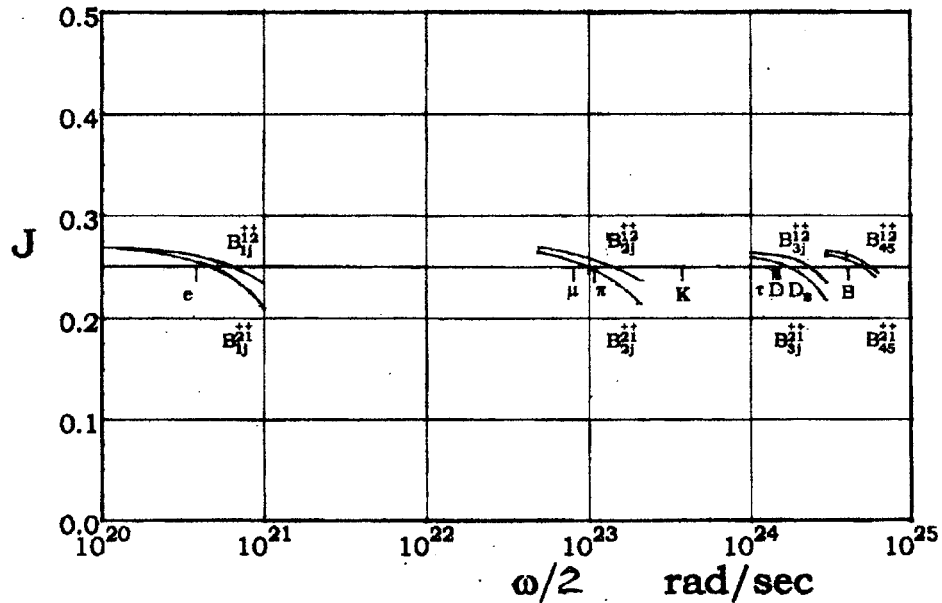


Figure 25. The concentric bion solutions.

fluctuations themselves and the energy of the particles' layers. However, no solutions of the time dependent  $\ell$ -wave equations have been carried out. Furthermore, the cutoff frequency for the datum fluctuation spectrum is not known. Thus a certain amount of guesswork is involved in the following, and *the observed particles should not be expected to exactly match the intersection points*. Notice that Figure 25 is plotted versus  $\omega \setminus 2$ .

### Concentric Trions

The existence criterion for trion layer/charge forms is,

$$J = \frac{q_i^2}{e^2} J_i + \frac{q_j^2}{e^2} J_j + \frac{q_k^2}{e^2} J_k + 2 \frac{q_i q_j}{e^2} J_{ij} + 2 \frac{q_i q_k}{e^2} J_{ik} + 2 \frac{q_j q_k}{e^2} J_{jk} = 0.25 \quad .$$

A typical example is the  $T_{123}^{122}$ , which leads to,

$$J = \frac{1}{9} J_1 + \frac{4}{9} J_2 + \frac{4}{9} J_3 - \frac{4}{9} J_{12} - \frac{4}{9} J_{13} + \frac{8}{9} J_{23} \quad .$$

From the tables, the above sum is found for each  $\omega$ , and plotted in Figure 26. The crossover point is at  $\omega = 1.40 \times 10^{24}$  rad/s . The accurate non-graphical, program value is  $\omega = 1.4051 \times 10^{24}$  . Thus, the  $\omega$  predicted

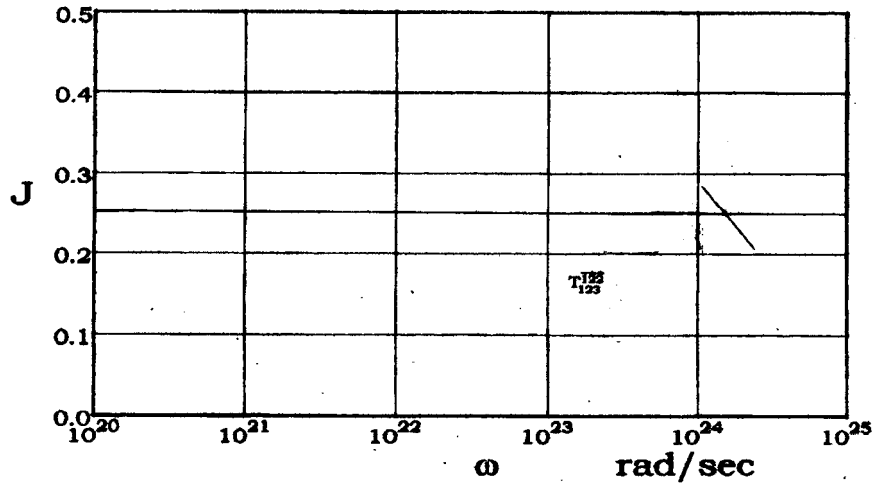


Figure 26. Predicted  $T_{123}^{122}$  Frequency.

for the  $T_{123}^{122}$  is just 1.43% lower than the *measured* proton frequency,

$$\omega = 1.42548 \times 10^{24}, \text{ so the } T_{123}^{122} \text{ is tentatively identified as the proton.}$$

When the existence criterion is applied to the remaining trion layer/charge forms depicted in Figure 20, the total energy of Eq.(153) is almost always too low to cross over the  $J = 0.25$  level. This indicates that most other trions are orbiters requiring the added orbital kinetic energy to make up the total.



### The Self Consistent Adjustment

The close agreement between the predicted and measured proton frequencies encourages confidence in the method, and invites effort to find the source of the error. Since the system, to this point, just uses three given numbers (the  $e$ ,  $\mu$  and  $\tau$  frequencies) to determine a fourth (the  $p$  frequency), if properly set up, it should be *self-consistent* and without error. One of the many possible sources of error could be the specification of the unon preferred frequencies. Of the four particles, the  $e$  and  $p$  are *stable* (the only stable particles known), and their rest energies can be measured with great accuracy. On the other hand, the  $\mu$  and  $\tau$  are very short-lived and their frequencies quickly shift lower during their decay, making their rest energies difficult to measure accurately. *With a small adjustment of the preferred frequencies of layers two and three the system becomes self-consistent.*

The reality is that *both might need correcting*, but a simple calculation indicates that to correct the 1.4% error, the second layer  $\omega_2$  need only change a comparable amount, whereas the third layer  $\omega_3$ , because of its location, must change about 40%. It is unreasonable to suppose that the *measured*  $\tau$  energy is anywhere near that low, so only the second layer  $\omega_2$  will be adjusted. The *corrected* preferred frequencies are listed in Table IX. *Future concentric bion and orbiter trion work might show both need changing.* The corrected  $\omega_2$  is increased by 2.5%, which has only a small effect on the bion predictions expressed in Figure 25.

TABLE IX  
SELF-CONSISTENT PREFERRED FREQUENCIES

Layer	$\omega_i$ (rad/sec)	$r_i$ (cm)
1	$7.76344 \times 10^{20}$	$3.52243 \times 10^{-14}$
2	$1.62973 \times 10^{23}$	$1.67796 \times 10^{-16}$
3	$2.69981 \times 10^{24}$	$1.01289 \times 10^{-17}$
4	$8.508 \times 10^{24}$	$3.214 \times 10^{-18}$
5	$1.580 \times 10^{25}$	$1.731 \times 10^{-18}$

### Self Consistent Proton Structure

The overall analysis of proton structure can now be presented in *self-consistent* form. It follows a procedure somewhat different from the one used in the *prediction* calculation. Once the prediction shows that the layer/charge combination indicates a particular observed particle, as

many characteristics of that particle are tested as possible.

The *measured*  $E_0$  for the proton is 938.27203 MeV or  $1.5032818 \times 10^{-3}$  ergs. To satisfy Eq.(161), it must have a frequency  $\omega = 1.4254856 \times 10^{24}$  rad/sec. If it is to be a real particle, at that frequency it must also satisfy Eq.(153) for the three layers 1,2,3, so that,

$$E_0 = E_1 + E_2 + E_3 + E_{12} + E_{13} + E_{23} \quad . \quad (164)$$

With  $\omega_i$ 's from Table IX:

$$\frac{\omega}{\omega_1} = 1.8361527 \times 10^3 \quad , \quad \frac{\omega}{\omega_2} = 8.7467592 \quad , \quad \frac{\omega}{\omega_3} = 0.52801199$$

Invoking Eq.(151):

$$\begin{aligned} K_1 &= \text{out of range} \quad , \quad K_{12} = \text{out of range} \\ K_2 &= 4.8729207 \times 10^4 \quad , \quad K_{13} = \text{out of range} \\ K_3 &= -0.80028312 \quad , \quad K_{23} = 2.4364203 \times 10^4 \end{aligned}$$

Using the accurate, non-graphical program:

$$\begin{aligned} J_1 &= 5.44617 \times 10^{-4} \quad , \quad J_{12} = J_{13} = 5.4482266 \times 10^{-4} \\ J_2 &= 0.09611 \quad , \quad J_{23} = 0.10153 \\ J_3 &= 0.26428 \end{aligned}$$

Eq.(148) gives  $r_e = 1.9183736 \times 10^{-17}$ , so the energies of Eqs.(156) and (157) are:

$$\begin{aligned} E_1 &= 3.63871 \times 10^{-7} \quad , \quad E_{12} = E_{13} = -1.45604 \times 10^{-6} \\ E_2 &= 2.56853 \times 10^{-4} \quad , \quad E_{23} = 5.42677 \times 10^{-4} \\ E_3 &= 7.06299 \times 10^{-4} \end{aligned} \quad (165)$$

Then, Eq.(164) leads to  $E_0 = 1.50328 \times 10^{-3}$  ergs, to the accuracy limit of the more accurate program.

#### Proton Structure and Dark Matter

This is a good place to point out a significant difference between the ether theory and the quantum mechanical standard model. Recently a quantum mechanical model of the proton produced the result that most of the proton mass is **not** found in the quarks, but in the space between them. This has led to more speculation about "dark matter". From Eq.(165), it is clear that most of the proton's mass (energy) is concentrated in the layers (quarks), and the remainder is the normal interaction energy always found in the space between layers. The introduction of an idea like "dark matter" is just another example like the introduction of "color" in the standard model. One problem that arose in the quark model was the three parallel quark spins in a particle such as the  $\Delta^{++}$ , which was assigned *three identical u quarks*, a clear violation of

the Pauli exclusion principle. To resolve this problem, **the property of quark color was adopted.** *The exclusion principle is a manifestation of the single solution principle, i.e. no two identical solutions of the field equations can exist in the same place at the same time.* Referring back to Figure 15, three *concentric layers* with parallel spin clearly do not represent identical solutions of the field equations, so **no need for color arises**, resulting in a great simplification, no "color". Many other examples similar to this are given throughout PHYSICS 2001Rev.

### Orbiters

Analysis of the orbiters, is considerably more difficult; particularly that of the *inside* orbiters, since they have *overlapping* shells on which is superimposed a dynamic orbiting motion. *The proper analysis would involve solving for the full field, transient case.* It is clear that to do this for all the possible ground state configurations and then identify the observed particles accordingly is a task that could take many man-years.

## XXI THE ATOM

### Introduction

A firm belief that no deterministic description of the atom's interior is possible can be considered the basis of "Modern" physics. Why? Take the hydrogen atom. An electron, with 98 percent of its energy/mass and 99 percent of its charge concentrated inside a sphere of radius  $200r_e$ , approaches a proton that is essentially the same size as the electron. If the electron is captured, the innermost stable orbit it can occupy is a circle of radius  $1.5024 \times 10^5 r_e$ . Thus, the distance between the two particles is greater than 750 times the sphere of significant influence of either one (earth to moon distance is only 60 times the radius of the earth). If the electron is not captured, it sails past the proton on an hyperbolic orbit, and no serious change in the electron or proton occurs. In the circular and elliptic orbits of capture, the great distance between the particles and the relatively slow motion of the electron argue that just as little change takes place. So, since these particles exhibit inertia, momentum and all other common properties of ordinary matter, it should be clear that *no obstacle to their executing planetary type orbiting motion exists in any general way*, and Newton's laws must apply.

Earlier, the electron's properties were presented because it was lack of knowledge of the electron and the related particle behavior that diverted physics away from the deterministic form needed to finish the picture. It is not impossible to describe what is going on inside atoms. It can be done using only Maxwell's potential equations and Newton's laws. The following presents a planetary type description, of electrons orbiting nuclei, that shows how close Bohr and Sommerfeld came to the correct picture. They were unable to see the extended nature of the orbiting electrons, and did not realize that the electron, in turning as it orbited, contributed to the total angular momentum. Thus, they failed to

match the orbital angular momentum to the value predicted by Newton's laws. *The standard QM analysis of the atom makes the same error*, and, since Shroedinger's equation *cannot* give the correct answer unless the exactly correct mechanical picture is used to enter the energy of the system, QM carries some of the errors along. Using the extended electron described earlier, this will be corrected.

The turning of the orbiting electrons in the ground state ensures that no radiation takes place and that the ground state is stable. Quantization of the orbits is established by the electron's real, doppler shifted longitudinal wave difference frequency. Here, the structure and operation of the deterministic atom will be described using only ordinary Newtonian mechanics.

### The Hydrogen Atom

The simplest atom consists of a single electron orbiting around a single proton. Quantum mechanics gives a proper evaluation of certain aspects of mechanical systems *when the correct description of the mechanics is known*. In the case of the hydrogen atom, past lack of knowledge of the *electron* has caused QM to be used erroneously. The radiated frequencies and total angular momenta predicted are correct; but, because a minute electron angular momentum (due to its extension) has been omitted, the orbital periods and *orbital* angular momenta usually given are incorrect. If the "turning" angular momentum is added to the QM analysis, the latter also gives the same results for the *ensemble* that are found here.

### Orbit Analysis

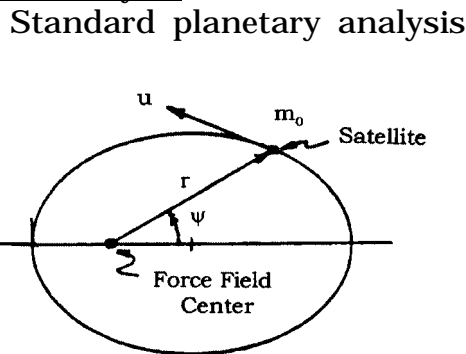


Figure 27 A planar orbit

Standard planetary analysis begins by considering the motion of a satellite of mass  $m_0$  moving in a central field (see Figure 27), e.g. the Moon orbiting a fixed Earth. To keep the discussion simple, *even in the atomic case, mass variations will be ignored* ( $\gamma = 1$ ). This will have no important effect on either the picture or the principles presented. The satellite's energy is defined as  $E = T + V$ .  $V = -k/4\pi r$  is its potential energy, and

its kinetic energy is (HL units),

$$T = \frac{1}{2m_0} \left( p_r^2 + \frac{p^2}{\eta^2 r^2} \right) , \quad (166)$$

where  $p_r$  is its radial momentum and  $p$  its *total* angular momentum. To be defined later,  $\eta$  is unity in the ordinary planetary case. In the simplified Moon-Earth system, the orbital angular momentum is,

$$\boxed{p_\psi = m_0 r^2 \dot{\psi}} , \quad (167)$$

and this is usually entered for  $p$  in Eq. (166). However, *the Moon always presents the same face to the Earth*, rotating one turn about its own axis for each complete orbit. In the atom, the electron *must* turn that way in all possible orbits (see Section XVIII, Turning ), with a turning angular momentum (not the spin),

$$p_t = K_t p_\psi \quad . \quad (168)$$

Thus, for a close parallel to the atomic case the planetary example must be visualized with the total angular momentum written as,

$$p = p_\psi + p_t = (1 + K_t) p_\psi \quad . \quad (169)$$

Next, Newton's second law is used to write the radial force equation,

$$F_r = m_0 (\ddot{r} - r(1 + K_t)\dot{\psi}^2) \quad ,$$

and the angular momentum equation,

$$\frac{dp}{dt} = 0 \quad , \quad p = k_\psi \quad . \quad (\text{constant})$$

In the general case, for  $E < 0$  and attractive force  $F_r = -k/4\pi r^2$ , a rather long and convoluted derivation<sup>17</sup> leads to closed elliptical orbits ( $K_t = 0$ ) or almost elliptical orbits (precessing,  $K_t < 0$ ; recessing,  $K_t > 0$ ), given by,

$$r = \frac{a(1 - \varepsilon^2)}{1 + \varepsilon \cos(\eta\psi)} \quad , \quad \eta = \sqrt{1 + K_t} \quad (170)$$

with the parameters (HL units),

$$E = -\frac{k}{8\pi a} \quad \text{Constant energy } E \text{ for each possible orbit.}$$

$$p = k_\psi = \eta \sqrt{\frac{m_0 k}{4\pi} (1 - \varepsilon^2) a} \quad \text{Constant total angular momentum for each possible orbit.}$$

$$a = \frac{r_{\min} + r_{\max}}{2} \quad \text{Similar to the semi-major axis of the elliptical case.}$$

$$b = \sqrt{r_{\min} r_{\max}} \quad \text{Corresponds to the semi-minor axis.}$$

$$\varepsilon = \sqrt{1 - \left(\frac{b}{a}\right)^2} \quad \text{Orbit eccentricity parameter.}$$

In terms of these parameters, the radial momentum is given as a function of  $r$  by,

$$p_r = \sqrt{2m_0 E + \frac{2m_0 k}{4\pi r} - \frac{k_\psi^2}{\eta^2 r^2}} \quad . \quad (171)$$

---

17. A.Ruark and H.Urey, Atoms, Molecules and Quanta, Vol. 1, p. 133, Dover Publications, N.Y.(1964).  
B.Shore and D.Menzel, Principles of Atomic Spectra, p. 45, J.Wiley and sons, N.Y.(1968).

Without the *turning* constraint,  $K_t = 0$  and  $\eta = 1$ , reducing these equations to the usual textbook elliptical case. All of this is well known, along with the fact that *any choice of semi-major axis  $a$  and eccentricity  $\varepsilon$  in the astronomical case (with  $k = Gm_0M$ ) will produce a physically realizable orbit* as long as the satellite is far enough away from the force field central mass. Because the energy  $E$  is not a function of the eccentricity, any specific choice of  $a$  applies to a whole family of pseudo-ellipses and their corresponding total angular momenta  $p$ , the largest of which matches the circular orbit with radius  $a$  and  $\varepsilon = 0$  (see Figure 31).

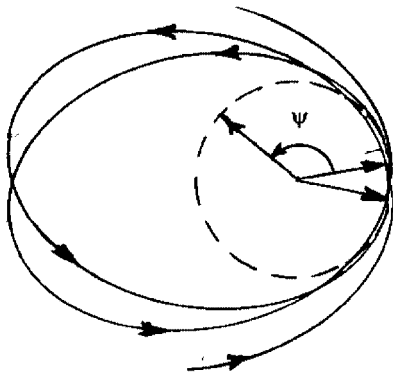


Figure 28

The  $r_{\min}$  period is less than  $\psi = 2\pi$ .

To apply the preceding equations to the hydrogen atom, it is only necessary to set  $k = e^2$  and supply a rationale for choosing semi-major axis  $a$ ,  $\varepsilon$  and  $K_t$ . However, it is at this point that the atomic case begins to differ significantly from the astronomical. For example, in the purely elliptical case, the period of the orbit represents one complete circuit of the ellipse repeated over and over again. In the atomic case, the orbits are not closed but *recess*, as shown in Figure 28. Here, the cycle is considered to go from one  $r_{\min}$

to the next  $r_{\min}$ , *which shifts orientation* in the cases where  $K_t \neq 0$ . Because of this shift, each pseudo-ellipse cycle is completed when  $\psi$  has swept out only  $2\pi/\eta$  radians.

From the time of Bohr and Sommerfeld, it has been clear that atoms exist in stable or pseudo-stable states; and only when an electron shifts from one orbit to another does radiation occur. Because this was never tied to a cause and effect explanation, but only to the mysterious "quantum", the de Broglie "wave" and "h", the orbits and the visualization were ultimately lost. *Here, the cause and effect chain is traced directly to the properties of the electron and its  $\ell$ -waves*, and the method for finding the semi-major axis values of  $a$  that give the observed selected orbits is presented.

### The de Broglie Difference Frequency and Planck's Constant

At the end of Section XVIII, it was demonstrated, using only Newton's laws, that Planck's constant  $h$  is a *derived* constant that relates the electron's momentum to the Doppler difference frequency of its front and back longitudinal waves. The following shows the way the difference frequency and the derived constant  $h$  enter the *orbit* analysis.

Refer back to Section XVIII. There it was shown that when an electron moves along a path at velocity  $u$ , its radially outward moving  $\ell$ -waves are Doppler shifted, resulting in a difference frequency

between the front and back waves of,

$$v_d = 2\gamma\beta v_e \quad , \quad (172)$$

where,  $\beta = u/c_0$  and  $v_e$  is the electron's intrinsic  $\ell$ -wave *rest* frequency ( $1.2355898 \times 10^{20}$  cyc/s, as determined by the Rydberg constant). Eq.(172) and the *linear* momentum  $p_L$  were used to write,

$$p_L c_0 = \gamma m_0 u c_0 = h \frac{v_d}{2} \quad ,$$

where  $h$  is the *derived* Planck's constant,

$$h = \frac{m_0 c_0^2}{v_e} = 6.6260755 \times 10^{-27} \quad . \quad (173)$$

However, *for the atomic orbit*, the derivation of Section XVIII must be modified, as follows, to account for the separation of the *orbital* and *turning* angular momenta.

Using Eq.(167), the electron's orbital *linear* momentum is,

$$p_L = \frac{P_\psi}{a} = \gamma m_0 u \quad . \quad (174)$$

Combining Eqs.(172) and (174),

$$p_L c_0 = h \frac{v_d}{2} \quad , \quad (175)$$

where again  $h$  is the *derived* constant of Eq.(173). Eq.(175), when transposed, gives the de Broglie difference frequency<sup>18</sup>,

$$v_d = 2c_0 \frac{p_L}{h} \quad .$$

However, it is the *total* angular momentum,

$$p = p_\psi + p_t = \eta^2 p_\psi \quad ,$$

that sets the electron's velocity and the difference frequency. Defining the *total* linear momentum, including the "turning", as,

$$p_{Lt} = \frac{p}{a} = \eta^2 p_L = \eta^2 \gamma m_0 u \quad ,$$

Eq.(175) becomes,

$$p_{Lt} c_0 = \eta^2 \frac{h v_d}{2} \quad . \quad (176)$$

As discussed in Section XVIII, *although there is a difference frequency, there is no difference wave*. For an atomic orbit, the proper inversion of Eq.(176) is,

$$\Lambda_d = \frac{2c_0}{\eta^2 v_d} = \frac{h}{p_{Lt}} \quad . \quad (177)$$

where  $\Lambda_d$  is **not** the wave length of a mysterious wave that travels along

---

18. Although the author has chosen to call  $v_d$  the de Broglie frequency, it should not be confused with  $v_{db} = E/h$ , a fictitious frequency of a fictitious wave.

curved paths. It is determined by real, longitudinal waves that emanate and propagate *radially* from the electron's center.  $\Lambda_d$  has nothing to do directly with the wavelength of any wave. Instead it is simply *the distance the electron travels during  $2/\eta^2\beta$  cycles of the difference frequency  $\nu_d$* .

### The Steady-State Orbiting Electron Field

To better understand the nature of  $\Lambda_d$  in the atom, the total field of an orbiting electron will be visualized. One of the most significant effects of the electron Doppler *difference* frequency occurs when the electron moves periodically in a closed path in a central electrostatic field. In that situation the conditions for the *total* field solution are quite different from those of the free electron. In the *circular* orbit case, for example, only when the effective circumference of the orbit,  $L = 2\pi a / \eta$ , is related to the *difference* frequency by,

$$\nu_d = n \frac{2}{\eta^2} \frac{c_0}{L} \quad , \quad (178)$$

where  $a$  is the orbit radius, and  $n = 1, 2, 3, \dots$ , can a steady state field solution exist. This can be explained as follows.

An attempt will be made to visualize the overall field surrounding the orbiting electron near the orbit and at great distances from the center. It will be shown that *Eq.(178) is the criterion necessary to maintain the combined solution in steady state*.

In the hydrogen ground state, because  $u/c_0$  is small, the electron's  $\ell$ -waves drawn to scale cannot show the minute but significant effects taking place along the orbit. By *artificially exaggerating the velocity  $u$* , the effect in space is seen to be a shifting of the positions of maximum and minimum bunching of the  $\ell$ -waves, as illustrated in Figure 29. Full turning of the electron's field is implicit.

The same exaggerated orbit velocity and, in addition, *artificially reduced wave propagation velocity* allows a plot of the *outer* regions of the field. Figure 30 shows every 2,348<sup>th</sup> wave front, and the bunching and extending of those fronts can be seen to spiral outward so that the spacing between successive bunching or extending is,

$$D = c_0 T_{orb} \quad . \quad (179)$$

By turning the figure in the direction of the electron's motion, the outward motion of the spirals can be seen as a good representation of the total field equation solution for the hydrogen ground state. To be a steady state solution, *the spiral must occupy exactly*

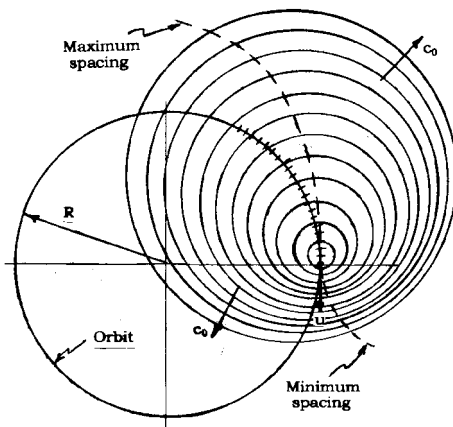


Figure 29.  
Orbiting electron  $\ell$ -waves



the same position relative to the orbit, as the electron returns to the same orbit position, taking into account the orbit recession. There is no problem in the outer field, as long as the correct phasing occurs along the orbit.

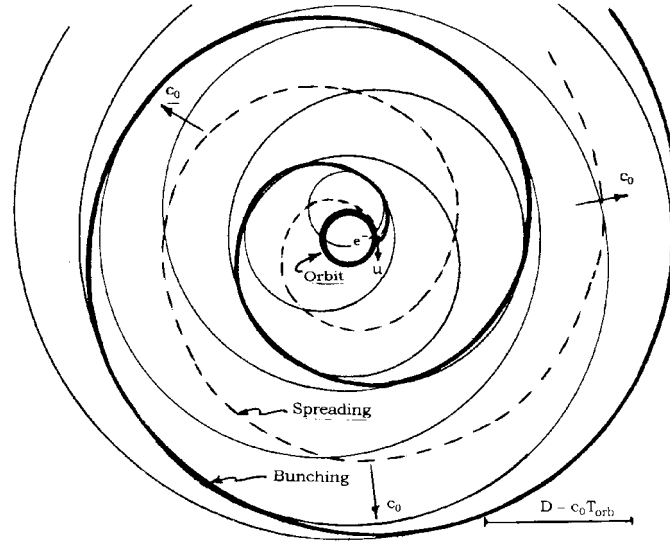


Figure 30

Outer field diverging waves, exaggerated ground state orbit.

In Figures 29 and 30, the two spirals (bunching and spreading) can be seen to approach the orbit tangentially and to join at the electron center. As the electron orbits, the same picture is repeated at each point. Again this can be seen by simply rotating the plots to simulate the electron's motion. Clearly, depending upon the velocity  $u$  and the *effective* orbit circumference  $L$ , the phase position of the wave fronts at the electron center may or may not be exactly the same as the electron completes its round trip and returns to the recessed starting point. But, if those phases are not identical, then the outer field will be *changing* and the total field equation solution will *not* be steady state.

To find the criterion for a return to the same phase condition, think of a point on the orbit just as the electron is passing. First, a series of front waves, moving in the direction of the electron's motion, cause an oscillation at the point of frequency  $\nu_f$ . Then a series of back waves, leaving in a direction opposite to the electron's motion, cause an oscillation at the point of frequency  $\nu_b$ . *The same phenomenon occurs at each point of the orbit circumference*, differing only in the time when the electron passes. Only if the number of front wave cycles  $N_f = \eta^2 \nu_f L / 2c_0$ , in the distance equal to the *effective* circumference  $L$ , and the number of back wave cycles  $N_b = \eta^2 \nu_b L / 2c_0$ , in that same distance, are both

*integers* can the phases and electron oscillation match at each point. Thus *the condition for a steady-state field in this circular orbit* is that the difference between  $N_f$  and  $N_b$  is also an integer,

$$n = N_f - N_b = \eta^2(v_f - v_b) \frac{L}{2c_0} = \eta^2 v_d \frac{L}{2c_0} \quad , \quad (189)$$

which is just Eq.(187) rearranged.

Thus, those *circular* paths specified by Eqs.(187) or (189) are stable, and the elliptical orbits with the same semi-major axis  $a$  are pseudo-stable. The profound effect this has on atomic structure was first pointed out by L. de Broglie, through Eq.(109), although he was inspired by a shrewd guess based on symmetry rather than an understanding of the electron's structure. Unfortunately, the de Broglie wavelength has been emphasized, and a mysterious wave of a much different frequency than the actual frequencies,  $v_f$  and  $v_b$ , directly involved has been used to describe "matter waves" of quantum mechanics. The preceding picture gives a much more realistic description of the phenomena in three dimensions.

#### The Semi-Major Axis $a$

It is fortunate that the solution for the orbital energy  $E$  is degenerate for all of the non-circular paths that have the same semi-major axis  $a$ , because in all those paths the difference frequency and electron velocity *vary*, and those cases are not truly steady-state. The criterion for finding the allowed  $a$  values can be obtained from the *circular* orbit.

Earlier it was shown that Newton's laws were adequate in the astronomical problem. They provided the orbit solution of Eq.(170), which includes the parameter equation for the *circular* orbit case ( $\varepsilon = 0$ ),

$$p = k_\psi = \eta \sqrt{\frac{m_0 k}{4\pi}} a \quad . \quad (190)$$

In the astronomical solution, no further restriction is placed on either the constant total angular momentum  $p$  or the orbit radius  $a$ . The arbitrary choice of either one determines the other through Eq.(190). It is at this point the atomic case deviates most, for the choices of  $p$  and  $a$  are not arbitrary in the atom, *since the electron itself imposes another condition on  $p$* . Consequently,  $p$  is determined and  $a$  follows directly from Eq.(190). Thus,  $p$  and  $a$  are fixed and not arbitrary.

The criterion for finding the allowed total angular momentum and semi-axis  $a$  results from the combination of Eqs.(177) and (187),

$$L = \frac{2\pi a}{\eta} = n\Lambda_d \quad . \quad n = 1, 2, 3, \dots \quad (191)$$

Here,  $n$  is the familiar principal "quantum number", *obtained using only Maxwell's equations and Newton's laws*. Only those orbits specified by Eq.(191) are stable or pseudo-stable.

Now, to find the alternative equation for  $p$ , combine Eqs.(177) and (191) to read,

$$p = ap_{Lt} = \frac{\eta nh}{2\pi} \quad . \quad (192)$$

Equating Eqs.(190) and (192) yields,

$$a = \frac{n^2 h^2}{\pi m_0 e^2} \quad . \quad n = 1, 2, 3, \dots \quad (193)$$

These values of  $a$ , used with the energy parameter in the list following Eq.(170), specify all the allowable total angular momenta, orbit energies and sizes. They do not establish the *shapes* of the elliptical orbits. That is taken up next.

### Orbit Shape and Eccentricity

The selection rule for *circular* orbits can be rewritten, with the help of Eq.(192) above, in the form,

$$p_{Lt} L = nh \quad , \quad n = 1, 2, 3, \dots \quad (194)$$

where  $L$  is the length of path and  $p_{Lt}$  is the *total* linear momentum of the electron along the path. If the orbit is *elliptical* the electron's distortion with changing velocity precludes that orbit's stability. Nevertheless, the rate of radiation is not that great, so a kind of pseudo-stability exists. If the radiation is neglected for the moment, it is clear that the steady state field about the orbit is not the simple cyclic spiral discussed above. However, even when the path is elliptical, it is possible to visualize the outer field spiraling outward in non-circular form, always matching the electron's difference frequency as it speeds up and slows down along the path of the orbit. If the match at each point is instantaneously correct, then the proper pseudo-steady state criterion suggested by Eq.(194) is,

$$\int_{r_{min1}}^{r_{min2}} \mathbf{p}_{Lt} \cdot d\mathbf{s} = nh \quad , \quad n = 1, 2, 3, \dots \quad (195)$$

where  $\mathbf{p}_{Lt}$  is the total linear momentum of the electron,

$$\mathbf{p}_{Lt} = m_0 \dot{r} \hat{\mathbf{r}} + m_0 (1 + K_t) r \dot{\psi} \hat{\psi} = p_r \hat{\mathbf{r}} + \frac{p}{r} \hat{\psi} \quad ,$$

and  $d\mathbf{s}$  is the differential displacement of the electron along the elliptical path. The integration is carried out over the unclosed section of the ellipse corresponding to the cycle or repetition period from  $r_{min}$  to  $r_{min}$  and angle of  $2\pi/\eta$ . In terms of the components, Eq.(195) becomes,

$$\int_{r_{min1}}^{r_{min2}} \mathbf{p}_{Lt} \cdot d\mathbf{s} = \int p_r dr + \int p d\psi = nh \quad . \quad (196)$$

The components integrated give,

$$\int p d\psi = p \int_0^{2\pi/\eta} d\psi = \frac{2\pi}{\eta} p \quad , \quad (197)$$

and,

$$\int p_r dr = \int_0^{2\pi/\eta} \frac{p\varepsilon^2 \sin^2(\eta\psi)}{(1 + \varepsilon \cos(\eta\psi))^2} d\psi \quad . \quad (198)$$

To complete the analysis, it is necessary to ask which orbits are circular and which are elliptical. It can be seen from Eq.(193), that the smallest orbit is specified by  $n = 1$ , and succeeding values of  $n$  give larger and larger paths; but their *shapes* are not indicated by  $n$ . In fact, it is easy to visualize a set of orbits for which  $n$  would be the same, i.e. the total number of difference frequency beats would be the same around the loop, and yet the shape of the paths could be quite different because of the *changing* de Broglie difference frequency. Some clarification comes from a consideration of Eq.(196), in which, for the same  $n$ , the two components of momentum could make different contributions. For example, if the orbit was circular,  $p_r$  would be zero and the total momentum contribution would be the angular momentum  $p$ . In an orbit of non-circular shape, the radial momentum would not be zero, and the angular momentum ( $p = \text{constant}$ ) would be smaller. This would give an elliptical type path with a semi-*minor* axis less than  $a$ .

Once the allowed orbit sizes have been found through Eqs.(193) and (196), the shapes of the various orbits, due to differences in the de Broglie frequency, can be found from the components of Eq.(196). It should be emphasized that *it is the whole three dimensional field that must be orbit compatible*. In other words, not only is the total momentum along the orbit path matched to the circumference, but all components of the field must also repeat starting with the new  $r_{\min}$ . This can only happen if the components obey integer relationships such as,

$$\int p d\psi = p \int_0^{2\pi/\eta} d\psi = n_\psi h \quad , \quad \int p_r dr = n_r h \quad . \quad (199)$$

Finally, from Eqs.(170), (196) and (199),

$$n = n_r + n_\psi \quad , \quad (200)$$

and,

$$\sqrt{1 - \varepsilon^2} = \frac{n_\psi}{n} = \frac{\text{min or axis}}{\text{major axis}} \quad ; \quad (201)$$

where the axes here are loosely equivalent to those of an ellipse. Figure 31 sketches the first few allowed orbits. In order to determine them, it was necessary to specify  $K_t$ , which is not a universal constant, but a *different constant for each distinct orbit*. In making the sketches in Figure 31,  $K_t$  was assumed to be,

$$K_t = \frac{1}{n_\psi} \quad ; \quad (202)$$

but the reasons for the choice will only be discussed later on. Ultimately,  $K_t$  should come as a result of solutions of the total field equations. At present, it is only agreement with experiment that confirms the choice of Eq.(202).

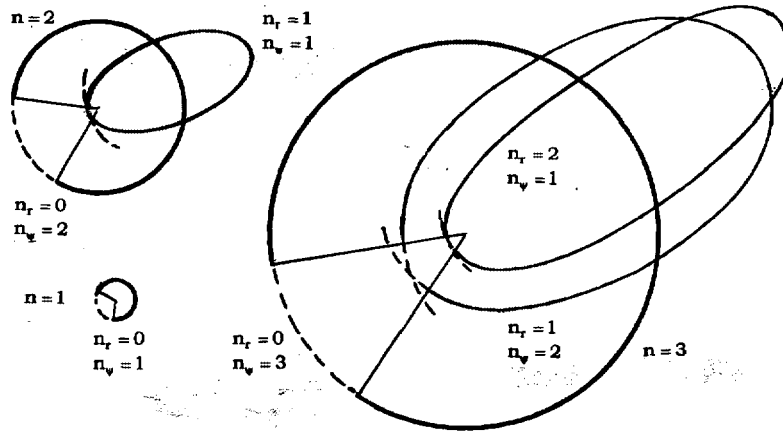


Figure 31. Recessing atomic orbits.

### Odds and Ends

Before concluding the specific discussion of hydrogen, a few salient points as well as the values and ranges of the various  $n_i$  are in order. Just as in the Bohr atom, the principal quantum number can range from 1 to  $\infty$ . *Since strong physical reasons have been given to show that circular orbits are basically the most stable*, the lowest value of  $n_r$  is zero, or conversely, the maximum value of  $n_v$  is  $n$ . On the other hand, the often published *orbits corresponding to linear oscillation of the electron through the nucleus have not been shown* in Figure 31, since it is clear that a large amount of energy is needed to force an electron to approach very close to a proton, and experiments have shown that the proton breaks up and other particles (s quarks) are formed. Also, if the linear orbit were allowed, the electron's rate of radiation would be extreme, and the lifetime of that burst of radiation would be so short as to not qualify this case as even pseudo-stable. In fact, that radiation would present a broad spectrum rather than a line. The upshot of these arguments is that the quantum number ranges are,

$$n = 1, 2, 3, \dots, \infty ; \quad n_v = 1, \dots, n ; \quad n_r = 0, \dots, (n-1) . \quad (203)$$

Another important item is the omission of the electron's mass variability from the derivation. A proper derivation must include it. Whereas the turning momentum causes the orbit to *recess* a considerable amount, the mass variation has the opposite effect, causing a minute precession. Nevertheless, the effect of the mass variation enters into the energy in a different way and so leads to a measurable

effect. Finally, a word should be said in connection with the "Correspondence Principle" used by Bohr, et al. Here *there is no need for it*. In the early days, because the Thomson atom, with its *linearly* oscillating electrons provided discrete radiation to be identified with the observed spectral lines, the model makers were looking for a match between the mechanical oscillation frequencies and the radiation. In the real atoms, the spectral lines are radiation emitted during a transition of the electron from one orbit to another. In a typical shift down from one orbit to the next, the electron starts in orbit 1 where the persistent buffeting of the zero point fluctuations and its own speed changes perturb the electron's motion. Gradually, the motion reaches a deviation that prevents recovery of the exact orbit and a slow spiral inwards commences. Soon, the de Broglie match is badly broken and the electron shape oscillates with velocity to produce faster inward spiraling and greater radiation per cycle. Finally, as it approaches closer to the inner orbit, the radiation lessens, the spiraling is slower, although the new velocity is greater, and the electron slowly settles into orbit 2. It would be surprising if the radiation had the frequency of one of these two orbits. Rather it should be a line of some width, centered perhaps close to the average frequency between the two. In fact, the original Bohr model predicts just such a thing. The presently corrected analysis does so as well. Table X lists the parameters of the first five circular orbits of hydrogen. The *radii* are essentially those predicted by Bohr, *but the angular velocities of the electron in orbit are found from the Eqs.(193), (169) and (167)*. The average  $\omega_{mn}$  are calculated and the *measured* values are also given. These latter are the lowest terms of the Lyman, Balmer, Paschen and Brackett series respectively. It is clear that the calculated *average*  $\omega_{mn}$  is always less than 8% different from that measured in the line spectrum. Except for the innermost transition, the measured frequency is always higher than the calculated average, which suggests

TABLE X  
THE HYDROGEN ATOM

n	R (cm)	$\omega_n = \dot{\psi}$ (sec <sup>-1</sup> )	$\omega_{mn} = \frac{\omega_m + \omega_n}{2}$ (sec <sup>-1</sup> )	$\omega_{mn}$ (measured) (sec <sup>-1</sup> )
1	$5.2918 \times 10^{-9}$	$2.9232 \times 10^{16}$	$1.6726 \times 10^{16}$	$1.5495 \times 10^{16}$
2	$2.1178 \times 10^{-8}$	$4.2193 \times 10^{15}$	$2.7727 \times 10^{15}$	$2.8702 \times 10^{15}$
3	$4.7651 \times 10^{-8}$	$1.3260 \times 10^{15}$	$9.5188 \times 10^{14}$	$1.0046 \times 10^{15}$
4	$8.4714 \times 10^{-8}$	$5.7776 \times 10^{14}$	$4.3983 \times 10^{14}$	$4.6496 \times 10^{14}$
5	$1.3237 \times 10^{-7}$	$3.0191 \times 10^{14}$		

that the electron spends more time or oscillates more vigorously nearer the inner orbit. None of these details pose a problem to the intuition; so the operation of the hydrogen atom is "classical" right down to its innermost orbit (even by the Bohr Theory), making the "correspondence" principle unnecessary.

It is important to realize that *none of the orbiting rates given in Table X match those given by the standard solution of Shroedinger's equation.* For example, the value  $2.9232 \times 10^{16}$  rad/s for the ground state orbit represents the actual, Newtonian orbiting rate found from Eq.(167). In QM, the total angular momentum  $p$  is called the *orbital* angular momentum, and the existence of the electron's angular momentum is not recognized although it is unconsciously included. If the proper mechanical format for the energy, separating the orbital and electron angular momenta, is used as the energy in Schroedinger's equation; then, also taking into consideration the present discussion of the linear orbit vs. the circular, the QM result agrees with Table X.

The details of the last few paragraphs should not obscure the fact that the numbers in Table X, for example, are not in any way final. They were obtained from the foregoing equations, ignoring such subtleties as the reduced mass resulting from proton motion. Correct procedure would also consider the turning energy of the proton. Table X overlooks this detail in the calculation of  $\psi$  and  $\omega_{mn}$  (average).

### Orbital Angular Momentum

The main difference between the preceding development and the Bohr-Sommerfeld atom is in the interpretation of the angular momentum and its effect on the type of orbits, etc. The *orbital* angular momentum is taken here to be  $p_\psi$  of Eq.(167) which corresponds to the usual mechanical planetary concept of orbital momentum. In the B-S model, there was no other angular momentum. In the present case, however, there is included the separated angular momentum of the electron's *turning*. According to Eqs.(168) and (202), the added turning angular momentum is,

$$p_t = \frac{1}{n_\psi} p_\psi \quad . \quad (204)$$

The total angular momentum is then,

$$p = p_\psi \left( 1 + \frac{1}{n_\psi} \right) \quad . \quad (205)$$

By uniting Eqs.(197), (199) and (205),

$$p_\psi = \frac{1}{\eta} \frac{n_\psi h}{2\pi} = \frac{n_\psi}{\sqrt{1 + \frac{1}{n_\psi}}} \frac{h}{2\pi} \quad ; \quad (206)$$

so that when Eqs.(205) and (206) are combined, the total angular momentum is seen to be,

$$p = \sqrt{n_\psi(n_\psi + 1)} \frac{h}{2\pi} , \quad (207)$$

a very familiar form. Since its first appearance in the early days of wave-mechanics, it has entered into every situation where angular momentum is present; and has remained disturbing to student and thinking physicist alike, with its forced acceptance, unexplained, take it or leave it. It is now clear that it represents the inevitable form taken when orbital and *turning* angular momenta are combined. Now, since electrons and all other fundamental particles in which distortion energy binds a  $\bar{\phi}$  distribution, when moving along curved paths in electric fields, have *full turning*, the form of the angular momentum will always be that of Eq.(207). It corresponds to the orbital kinetic energy plus the turning energy,

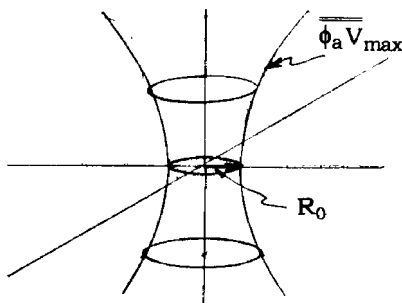
$$T_{\text{total ang. mom.}} = T_\psi + T_t = T_\psi \left( 1 + \frac{1}{n_\psi} \right) . \quad (208)$$

It was this condition that led to the choice of  $1/n_\psi$  for  $K_t$ .

### The **Free** Hydrogen Atom

This section will present the structure of the three innermost sets of orbits and their total momenta (including spin) and magnetic moments for a hydrogen atom **free** of any *external* electric or magnetic fields. This is something *that no present textbook can do* because of the non visualizability of the QM ensemble approach. Whenever modern textbooks try to describe the various orbital states, they are forced to immerse the atom in some form of external field. The ensuing complication completely obscures the simplicity of a **free** atom. Here the task is to *visualize a single, deterministic atom in a field free region*.

So far, nothing has been said of the atom's *magnetostatic* field, although it plays a significant role in both the atom's structure and in its radiation process. The magnetostatic field of a circular filament of current is sometimes used as a starting point for the description (see



Maximum flow surface  
Figure 32

Figure 32). All that must be said at this point is that the orbiting electron in each orbit creates a vortex magnetic field, roughly dipole in form. When the atom radiates a photon, an electron is falling from one orbit to another, generally smaller. Since the smaller orbit has a smaller magnetic field, the difference in magnetic moment is carried away by the emitted photon along with the difference in angular momentum.



As discussed earlier,  $n$  is the usual quantum number that fixes orbit size  $a$  and energy  $E$ ,

$$a = \frac{n^2 h^2}{\pi m_0 e^2} \quad (\text{A}) \quad , \quad E = -\frac{e^2}{8\pi a} \quad (\text{B}) \quad . \quad (209)$$

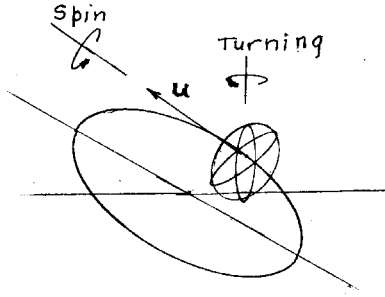


Figure 33  
Orbiting electron turning and spin

Orbit *shape* is set by  $n_\psi$ . The electron is spread out *laterally*, because of its kinetic energy, and has an oblate spheroid shape. Also, in the electric field of the proton, it "turns" (in addition to the spin) so its shape axis is along the orbit. The *spin* aligns itself with the electron *shape* axis. Figure 33 shows the electron, moving in orbit at velocity  $\mathbf{u}$ , turning and spinning.

Total vector angular momentum  
The basic *orbital* angular momentum

is given by Eq.(167),

$$\mathbf{p}_\psi = m_0 a^2 \omega \quad , \quad (210)$$

as predicted by Newton's laws. However, because the electron's shape "turns", in the plane of the orbit, one turn per electron period, this "turning" angular momentum adds to  $\mathbf{p}_\psi$  to give a total angular momentum,

$$\mathbf{p} = \mathbf{p}_\psi + \mathbf{p}_t = (1 + K_t) \mathbf{p}_\psi \quad . \quad (211)$$

When atoms are *quiescent*, the turning factor  $K_t$  is related to the orbit shape through,

$$K_t = \frac{1}{n_\psi} \quad . \quad (212)$$

Combining Eqs.(210), (211) and (212), the total angular momentum, *before adding spin* is (see Eq.(207)),

$$\mathbf{p} = \sqrt{n_\psi(n_\psi + 1)} \frac{h}{2\pi} \quad . \quad (213)$$

At this point, before discussing the total vector angular momentum,  $\mathbf{J}$ , and in order to be close to the conventional notation, the substitutions  $\mathbf{S} = \sigma = \frac{1}{2} \hbar$  ( $\hbar = h/2\pi$ ) and  $\mathbf{L} = \mathbf{p}$  can be made. It is customary, in *ensemble* quantum physics, to use the same *form* that appears in Eq.(213) for  $\mathbf{S}$  and  $\mathbf{J}$ ; i.e.  $\sqrt{s(s+1)}\hbar$  and  $\sqrt{j(j+1)}\hbar$ . However, from the present point of view, *there is no physical justification for this*, because  $\mathbf{S}$  and  $\mathbf{J}$  do not have any extra turning components. Therefore, the vector spin and total vector angular momentum become,

$$\mathbf{S} = \hat{\mathbf{S}}\mathbf{S} = \hat{\mathbf{S}} \frac{1}{2} \hbar \quad , \quad \mathbf{J} = \hat{\mathbf{J}}\mathbf{J} \quad ; \quad (214)$$

and there are no magnetically induced precessions of these vectors involved in the *free atom*.

It is clear from Figure 33 that *the spin vector and the orbit vector are always perpendicular to each other*; so, from Eqs.(213) and (214), the total vector angular momentum  $\mathbf{J} = \mathbf{L} + \mathbf{S}$  has a magnitude,

$$J = \sqrt{L^2 + S^2} = \sqrt{n_\psi(n_\psi + 1) + \frac{1}{4}} \hbar \quad . \quad (215)$$

This very simple equation for J will not be found in the literature, since it depends on the free atom analysis not available to modern physics.

Eqs.(209) and (213) give the energy and angular momentum for each orbit. Referring again to Figure 31, Table X lists some of the values related to those orbits. The radii are given in terms of the *Bohr radius*,

$$a_0 = 5.2918 \times 10^{-9} \quad , \quad \text{cm} \quad (216)$$

a convenient unit. The atomic vortex is observed as the atom's magnetic moment,

$$\mu = n_\psi \mu_B \quad , \quad (217)$$

where  $\mu_B$  is the Bohr magneton ( $3.287553 \times 10^{-20}$  ergs/hlG). Values of  $\mu$  for the inner orbits of hydrogen are listed in Table XI.

TABLE XI

n	$n_\psi$	a	$\omega$	$p_\psi$	L = p	J	$\mu$
		cm	$s^{-1}$	g-cm/s	g-cm/s	g-cm/s	$\frac{\text{ergs}}{\text{hlG}}$
1	1	$a_0$	$2.9233 \times 10^{16}$	$0.7071\hbar$	$1.4142\hbar$	$\frac{3}{2}\hbar$	$\mu_B$
2	1	$4a_0$	varies	$0.7071\hbar$	$1.4142\hbar$	$\frac{3}{2}\hbar$	$\mu_B$
	2	"	$4.2194 \times 10^{15}$	$1.6330\hbar$	$2.4495\hbar$	$\frac{5}{2}\hbar$	$2\mu_B$
3	1	$9a_0$	varies	$0.7071\hbar$	$1.4142\hbar$	$\frac{3}{2}\hbar$	$\mu_B$
	2	"	varies	$1.6330\hbar$	$2.4495\hbar$	$\frac{5}{2}\hbar$	$2\mu_B$
	3	"	$1.3260 \times 10^{15}$	$2.5981\hbar$	$3.4641\hbar$	$\frac{7}{2}\hbar$	$3\mu_B$

## XXII RODS, CLOCKS AND PLUMB BOBS

The most fundamental law of physics is the Principle of Identical Environments (P.I.E.), which can be stated: *Any Measurements made in identical environments, performed with identical instruments, will yield identical results*<sup>19</sup>. Whether or not such experiments can ever be carried out is a moot point; but such is the basis of physics. The principle of

19. J.E.McGuire & M.Tammy, Certain Philosophical Questions: Newton's Trinity Notebook, Cambridge University Press (1983); J.C.Maxwell, Matter and Motion, p13, Dover Publications, N.Y.; R.L.Kirkwood, On The Theory of Relativity, Thesis, Stanford U. Phys. Dept. (1950).

identical environments (P.I.E) applies anywhere, any time; e.g. in inertial systems, accelerating systems, rotating systems, etc. *Without the P.I.E. there could be no physics.*

In modern textbooks, the discussion of measurement usually begins and ends with a description of Einstein's Special Relativity; but even today, there are literally hundreds of *dissidents*, some knowledgeable, some not, who are confused by the non-intuitive explanation of the observations and calculations SR is used for. Although it is clear to almost any practicing physicist that the Lorentz transformation is an essential tool in any quantitative study, it is equally clear that, for 104 years the explanation of the meaning of the observations and calculations continues to be disturbing to many.<sup>20</sup> The present section is an attempt to reconcile the successful formalism of the Lorentz transformation with an intuitive, non-paradoxical explanation of the physics based on cause and effect.

A proper examination of The Special Theory should begin with the question, "Why did Einstein write his 1905 paper? What was he trying to do?" A clue to the answer can be found in the paper's title, "On the Electrodynamics of Moving Bodies". *He was trying to save Maxwell's equations.* To understand this, it is necessary to go back to Maxwell himself.

By the 1870's Maxwell had completed his equations for the behavior of electromagnetic fields in laboratories *at rest in the ether*, but he was disturbed about their application in laboratories *moving* through the ether (e.g. earth labs). It is important, at this point, to realize just what Maxwell did **not** know. For example, he did not know about *rod shortening* experiments, starting with the Michelson-Morley (1880's) and running beyond. He knew nothing of *clock slowing* experiments, most of which came over 60 years later, and the Lorentz transformation was 25 years in the future. Keeping this in mind, the following is a variation on what was bothering him.

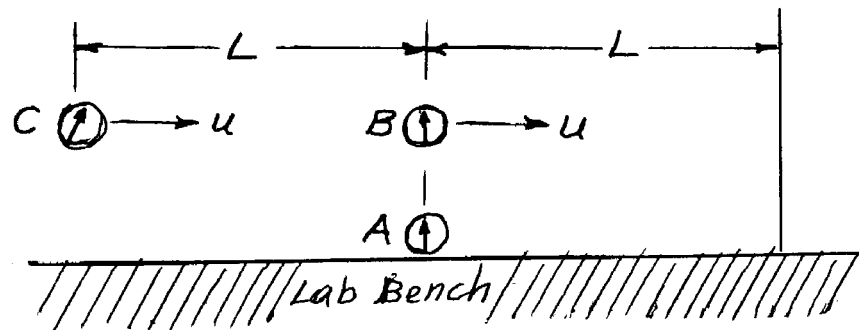


Figure 34.

20. A. Ungar, Am. J. Phys. **56**, 814 (1998) and R. W. Brehme, 811. These also have important references.

Figure 34 illustrates a laboratory set up involving a lab bench to which is attached a clock A. Two other clocks B and C, identical to A, are attached to the ends of a rod of length L and moving at velocity u to the right. If B and C are synchronized, and they simultaneously send out light pulses toward each other, because C is approaching B's pulse and B is moving away from C's pulse, B and C measure different arrival times. If, now, the B-rod-C combination is regarded as a separate inertial lab with two observers, then B and C have found the velocity of light to be different in opposite directions, one  $c_0 + u$  and one  $c_0 - u$ . But, *Maxwell's equations have only the single propagation velocity  $c_0$ , so they can't be used in the B-rod-C lab.* Maxwell died before he could straighten this out.

The Michelson-Morley was performed to check Maxwell's problem, but added a decade of confusion. Finally, Lorentz and Fitzgerald independently deduced, what now seems obvious, that *rods shorten when moving through the ether.* That explains the M-M results.

### Rod Contractions

As first described by Lorentz, a practical measuring rod consists of a number of particles laid end to end, but always in neutral pairs or groups in the form of atoms. These have their inner dimensions established by their balance of motions and deformations. Likewise, the "forces" between the atoms are balanced to determine the length of the rod. Similarly, a real clock is composed of many layerons arranged in various ways. The fact that there is no "matter", other than these very flexible bulk layeron constructs in the ether, accounts for all the changes in the rods and clocks when they move relative to the medium.

When a rod is at rest, its internal "forces" are determined by the negative gradient of  $\bar{\phi}$ ; but when the rod is in motion with constant velocity, the negative dynamic gradient,

$$\mathbf{E} = - \left( \nabla \bar{\phi} + \frac{1}{c_0^2} \frac{\partial(\bar{\phi}_a \mathbf{V})}{\partial t} \right) , \quad (218)$$

conventionally called the *electric field intensity*, determines the "force". Earlier it was shown that  $\bar{\phi}$  in layerons *expands laterally* to their direction of motion, yet, if  $\mathbf{E}$  is calculated from Eq.(218) it is found to *contract longitudinally*. So Lorentz was able to demonstrate<sup>21</sup> (using a "point" charge field) that when the rod moves at constant velocity, the dynamic gradient (field intensity,  $\mathbf{E}$ ) contours contract in the direction of motion by  $1/\gamma$ . Here, *the finite layer  $\bar{\phi}$  gives the same result.*<sup>22</sup> On the

21. H.A.Lorentz, Proc.Acad.Sci.Amsterdam, 6, 809 (1904). Reprinted in The Principle of Relativity, Dover Publications Inc. Also see Lectures on Theoretical Physics, Vol 3, Macmillan Co. Ltd., London (1931).

22. R.H.Dishington, Physics, Beak Publications, Pacific Palisades, CA (1989).

....., Advances in Fundamental Physics, p. 187, M. Barone & F. Selleri Eds., Hadronic Press, Palm Harbor, FL (1995).

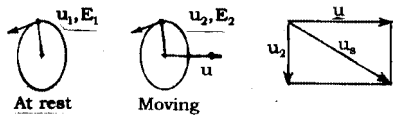
basis of this contraction of the particle  $\mathbf{E}$  field, Lorentz argued correctly that the total rod length  $L$ , when a rod *moves* parallel to its length, would contract to,

$$L_m = \frac{L}{\gamma} \quad . \quad (219)$$

Being made of particles that are solutions of the same field equations as the electron/positron, *all material objects contract in the direction of their motion with respect to the ether.* This is not a mathematical nor philosophical contraction, but *a real physical shortening of the rod moving through the ether.* Cause and effect are acting through the behavior of the particles. The reality of this shortening is obscured in present day texts by introducing transformation equations. *It should be quite clear that only one observer is so far involved.*

Clock Slowing

Clocks moving relative to the ether run slower than clocks at rest in it. This is true for all types of clocks, mainly because clocks are made of particles just as rods are. Because there are many kinds of time measuring devices, it is not as easy to prove the general statement as it was for rods; but if each type is examined, it always turns out to be true. Most texts describe simple photon clocks, where a photon is sent out to a mirror and back, detected, and another photon sent, etc. There, the time interval of the moving clock is increased because the photon path length is longer.



Another elementary form of clock involves a mass circling on the end of a string or fine wire of negligible mass, as exhibited in Figure 35. When the clock is at rest, the energy of the circling mass is,

Figure 35 Circling mass clock.

$$E_1 = E_0 / \sqrt{1 - \frac{u_1^2}{c_0^2}} \quad ; \quad (220)$$

where the relationship to its rest energy  $E_0$  is taken from Section XVIII. Now the clock is moved at constant velocity  $u$  in a direction perpendicular to the orbit (this is not necessary, but simplifies the discussion). It is assumed that the motion has been inaugurated without disturbing the orbiting mass, so that its momentum perpendicular to the clock's direction of motion is *conserved*. The mass now executes a spiral motion through the ether, and its new total energy is,

$$E_2 = E_0 / \sqrt{1 - \frac{u_s^2}{c_0^2}} \quad , \quad (221)$$

where,  $u_s^2 = u_2^2 + u^2$  as seen in Figure 35. Using the conservation of

momentum,

$$\frac{E_2}{c_0^2} u_2 = \frac{E_1}{c_0^2} u_1 \quad ; \quad (222)$$

which can be combined with Eqs.(220) and (221) to yield,

$$\frac{u_2}{\sqrt{1 - \frac{u_2^2}{c_0^2}}} = \frac{u_1}{\sqrt{1 - \frac{u_1^2}{c_0^2}}} \quad . \quad (223)$$

Squaring both sides, cross multiplying and canceling like terms, Eq.(223) becomes,

$$u_2 = u_1 \sqrt{1 - \frac{u_1^2}{c_0^2}} = \frac{u_1}{\gamma} \quad . \quad (224)$$

This result reintroduced into Eq.(222) shows that,

$$E_2 = \gamma E_1 \quad . \quad (225)$$

Thus, the orbital speed of the mass particle *decreases*, to compensate for its energy increase due to the motion at velocity  $u$ , and just enough to preserve its momentum, which has no reason to change. At rest with respect to the ether, the period of the clock is,

$$T = \frac{2\pi r_1}{u_1} \quad ;$$

while, in motion with respect to the ether, its period is,

$$T_m = \frac{2\pi r_2}{u_2} \quad .$$

So, the period in motion is related to the period at rest by ( $r_1 = r_2$ ),

$$T_m = \frac{r_2}{r_1} \frac{u_1}{u_2} T = \gamma T \quad ; \quad (226)$$

i.e. the clock runs slower. Again, this is *not an hypothetical change, but a true slowing of its rate*; because it moves relative to the ether and its changes in deformation and speed produce the effect. All clocks behave in the same way. Spring clocks, for example, involve length contractions, energy changes, velocity changes and numerous interactions of these, yet they follow Eq.(226). So far, no one has ever found a clock that did not follow Eq.(226) when moving through the ether at constant velocity.

#### Rod, Clock and Mass Changes

Rod, clock and mass changes are now *experimentally measured* physical effects; but in 1893, when Lorentz and Fitzgerald proposed rod shortening to explain the null Michelson-Morley result, rod shortening was suspect. By 1904, it appeared to Lorentz to account for many of the numerous null experiments. In particular, the failure to detect ether motion in inertial labs.

*The rod and clock changes are what make the Lorentz Transformation*

*equations necessary.* Except in ultra-high speed particle experiments, they usually represent *extremely small changes*. Compared with the much larger, first order velocity difference in Maxwell's problem, they are negligible. **They have nothing directly to do with the purpose or solution in Einstein's 1905 paper.**

#### Poincare's Relativity Principle

In 1899, based on numerous experiments, Poincare' deduced a new physical principle:

Electro-optical phenomena depend only on relative motion of material bodies, radiation sources, and electro- optical apparatus.

In 1900 he said that precise observations cannot reveal more than relative displacements, implying *that detection of datum ether motion in inertial labs was not possible*. His position can be summed up by the **correct** statement:

Identical *experiments*, carried out in all inertial labs, yield identical results.

In 1904, he named it *The Principle of Relativity*; but, unfortunately, he replaced it with the idea that the *laws of physics are the same in all inertial labs*. If, by laws of physics is meant the equations of physics, that statement is not generally true. *It depends critically on how the clocks are set.*

The correct form of Poincare's Relativity Principle, in terms of **experiments**, is only coincidentally related to the old Newtonian concept of relativity. Instead, it is a sub-part of the most basic principle of physics, The Principle of Identical Environments (P.I.E.). **The latter, and Poincare's Sub-Principle have nothing directly to do with the purpose or solution in Einstein's 1905 paper.**

#### Lorentz' Transformation

In April 1904, Lorentz published a set of complete transformations, from one moving lab to another, for Maxwell's *equations* (not quite the exact form now known as the Lorentz transformation). He discussed the role of ether in rod shortening but probably didn't think the clocks truly ran slow. What he was offering was a way to make the calculations on moving bodies taking the ether into account.

#### Einstein's Solution of Maxwell's Problem

Apparently Einstein was unaware of Lorentz' 1904 paper. Although he was aware of the failure of the Michelson-Morley and numerous other attempts to detect motion through the ether, he still didn't know about the clock-slowness measurements to be made 32 years later and beyond, and he probably didn't know of the particles' shape change. At least he didn't appear to think of the variations in length and time as is possible now, armed with years of experimental data.

Going back to Maxwell's problem, there *are several different ways to set the clocks*. As described in PHYSICS 2001Rev, Section 8.7, the most

*fundamental way to synchronize* two identical clocks is by *contact set*. As long as two clocks remain in contact, no matter how they move about, they are truly synchronized. If, as in Figure 34, one is fixed and one moves at constant velocity, because of experimentally demonstrated clock slowing, once contact-set, the two clocks are geared together, and the times of each one, although they differ, are known exactly. *Thus, clocks B and C can be truly synchronized in the usual sense of the word using contact-set, and Maxwell's problem is real.* If the B and C clocks are synchronized this way, **two different propagation velocities will be observed.**

Einstein realized that to use Maxwell's equations in moving systems, there must be only **one** propagation velocity  $c_0$  in all directions, just as in the labs *at rest*. His brilliant insight was to see that, *if all the clocks are two-way light set*, there is just one calculated velocity  $c_0$  in all directions.

Einstein's artificial forcing of the two clocks, B and C, to be set by two-way light or the equivalent actually *de-synchronizes* them. In their de-synchronized state, they allow the use of Maxwell's equations and the Lorentz Transformation. The Special Theory thus solves Maxwell's problem in a very practical, but arbitrary, way. The **space-time** justification for this violates real world logic, and experiment, by ignoring intuition, visualization, cause and effect (the motivation provided by the ether), and the evidence of shape changing effects in acceleration.

*This solution has immense practical value.* But, to use **space-time** to *explain* the physics causes the confusion that has been evident for over 100 years. The ether makes the physics clear. **Einstein's solution is simply a clock setting technique and has nothing to do with the metaphysical nature of time.**

#### Maxwell's first Order Experiment

A formal analysis of Maxwell's experiment (see figure 34) appears in PHYSICS 2001Rev, Section 8.7, where the two different propagation velocities are  $c_B = \gamma^2(c_0 + u)$  and  $c_C = \gamma^2(c_0 - u)$ . The first order measurement is in the  $\pm u$  term, and the (in this case) negligible second order effect is in the  $\gamma^2$  factor. This experiment is extremely difficult to do in the form shown; because of the large distance requirements imposed by the high speed of light. It has not been done this way. However, there are other indications that the outcome is stated correctly. For example, Sagnac<sup>23</sup> mounted four mirrors on a rotating platform and sent two light beams in opposite directions around the loop they formed. The interference fringes showed that their propagation velocities matched the amounts predicted. Later larger loops were used, and Michelson<sup>23</sup> built a huge outdoor circuit of mirrors and evacuated pipes and

---

23. H. P. Robertson, T.W. Noonan, Relativity and Cosmology, pg.38, Sagnac, pg. 40, Michelson, W. B. Saunders Company, Philadelphia (1968).





relates a unique set of three numbers to each point in the lab.

In primary labs, clock setting is also simple. One can imagine, although it is not practical, having a tiny clock *at each point* in the lab space, wall to wall and floor to ceiling. When doing experiments, in any and all labs, the observer in each lab always assumes that *all the clocks in the lab have been set to read exactly the same time at any given instant*. He thinks that he has used a clock set procedure that ensures this. In secondary labs this is most often not true, but in primary labs *it can always be true if the clocks are properly set*.

The *simplest* procedure, for primary labs, is *light set*. This involves one master clock at rest in the ether, which is at rest in the lab. Light signals are sent from the master clock to all the other lab clocks. There are two versions of light set, one way and two way. In one way, when the signals arrive, the clocks are set to the master clock's time by correcting for the signal time delay, based on the constant velocity of light  $c_0$  in the ether, and the known distance to each point. In two way, each clock sends back a pulse to the master, and the outlying clocks are set to half the round trip time.

A third more difficult method uses a particular form of *contact set* by carrying a clock from the master clock to all the others at a known constant speed and making the proper corrections.(see Eq.(226)).

All of *these methods produce the same true clock synchronization* of any primary inertial lab's clocks, because the ether is at rest everywhere, and all light pulses propagate in any direction at the same velocity  $c_0$ .

### Secondary Inertial Labs

It has been demonstrated here, that in secondary labs with *truly synchronized clocks*, the laws of physics take on complicated forms that must include the different propagation times caused by the constant velocity of propagation relative to the ether. The way out of this dilemma is narrow, but intuitively satisfying.

It is likely that most inertial lab experiments ever done have been done in secondary labs. As depicted in Figure 36, in secondary labs with

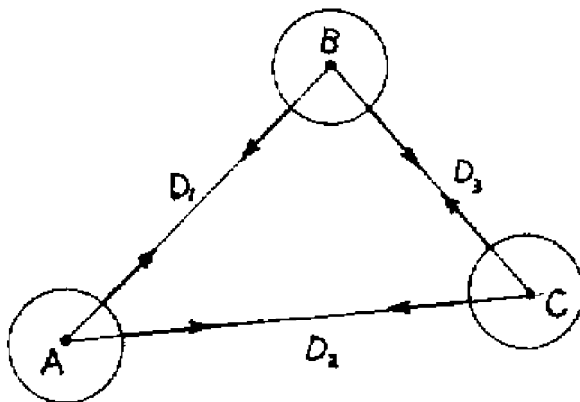


Figure 36 Three points in a secondary lab.

*truly synchronized* clocks, each *pair* of points in the space has *two* propagation velocities associated with it due to the constant ether flow through the lab (not shown in the Figure). Light pulses going in opposite directions between the points have different speeds. Thus, using a clock set procedure that would *truly synchronize* the secondary lab's clocks

would be a very bad choice, with ferociously complicated equations.

The proper approach to secondary lab clock set is to find a way to de-synchronize the clocks so that both directions of propagation between two points have the same *calculated* velocity, using the incorrect clock time. *This is done by first giving up the contact clock set used for true synchronization. One-way light set from a master clock also fails.* Special Relativity actually gets the desired result, but its methods are so abstract and unmotivated that many of its users and advocates are unaware that the clocks are deliberately *de-synchronized*.

The correct method for clock setting in *secondary* inertial labs is found as follows. Referring to Figure 36, it is seldom necessary to actually set the time at every point in the 3D lab space. Often, only a few clocks are placed about the lab, and the significant propagation is along just those few paths. As an example, in Figure 36, only three paths and three clocks are shown. The latter are represented by the three black dots at the centers of the spherical wave fronts shown propagating away from the point clocks, which are at any three points in the lab. The constant velocity ether flow through the lab is not shown, because it cannot be known to the lab workers. As derived in PHYSICS 2001 Rev, Section 8.7, given *truly synchronized* clocks, there were *two* actual propagation velocities caused by the *constant* ether velocity in the secondary lab. However, in that example, the ether flow was along the line between the two clocks being set. In the general case of Figure 36, if the constant velocity ether flow happened, by huge coincidence, to be along one of the paths, then it would surely cut across the other paths.

Figures 37 and 38, illustrate two very *special* flow configurations between any pair of clocks, and Figure 39 covers all others. The first, Figure 37, represents the example given earlier, where the ether flow is along the line of propagation. It was shown that the *absolute observer* sees the out-back propagation times as,

$$t_1 = \frac{L}{c_0 + u} \quad , \quad t_2 = \frac{L}{c_0 - u} \quad ,$$

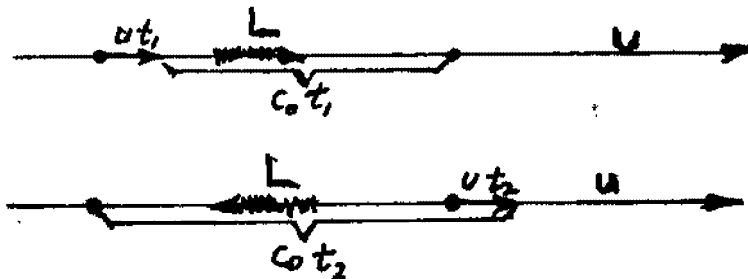


Figure 37 Ether flow  $u$  parallel to  $L$ .

where  $u$  now represents the secondary lab's ether flow to the right, and the clocks and  $L$  are fixed. Clock slowing makes the lab's times,

$$t_{l1} = \frac{L}{\gamma(c_0 + u)} \quad , \quad t_{l2} = \frac{L}{\gamma(c_0 - u)} \quad .$$

If the rod's length in a primary lab is  $\gamma L$ , then rod shortening causes the lab observer to measure the propagation velocities,

$$c_{\ell 1} = \frac{\gamma L}{t_{\ell 1}} = \gamma^2(c_0 + u) \quad , \quad c_{\ell 2} = \frac{\gamma L}{t_{\ell 2}} = \gamma^2(c_0 - u) \quad .$$

In this particular secondary lab, the proper way to set the clocks is to force the one way velocity of propagation to be the same, and equal to  $c_0$ . This is done, using Einstein's **solution**, by setting,

$$\boxed{t_{\ell} = \frac{1}{2}(t_{\ell 1} + t_{\ell 2})} \quad . \quad (227)$$

The result is,

$$t_{\ell} = \frac{1}{2} \left[ \frac{L}{\gamma(c_0 + u)} + \frac{L}{\gamma(c_0 - u)} \right] = \frac{L}{\gamma} \left[ \frac{c_0}{c_0^2 - u^2} \right] = \frac{\gamma L}{c_0} \quad ,$$

so the lab worker measures the propagation velocity  $c_{\ell} = \gamma L/t_{\ell} = c_0$  both ways.

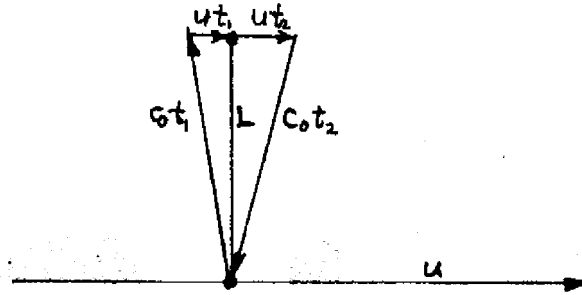


Figure 38 Ether flow Perpendicular to L.

If, by another rare coincidence, the datum flow through the lab was at right angles to the line between two clocks, the timing (as seen by an absolute observer) would be as illustrated in Figure 38. The ether is

flowing to the right in the lab and the absolute observer finds the light pulse transit times to be,

$$t_1 = \frac{L}{\sqrt{c_0^2 - u^2}} = \gamma \frac{L}{c_0} \quad , \quad t_2 = \frac{L}{\sqrt{c_0^2 - u^2}} = \gamma \frac{L}{c_0} \quad .$$

In this case, *there is no rod shortening*, because the rod length is at right angles to the ether velocity  $u$ , but clock slowing makes the lab's times,

$$t_{\ell 1} = \frac{L}{c_0} \quad , \quad t_{\ell 2} = \frac{L}{c_0} \quad .$$

Substituting the lab times in the two way clock set Eq.(227), the result is,

$$t_{\ell} = \frac{1}{2} \left( \frac{L}{c_0} + \frac{L}{c_0} \right) = \frac{L}{c_0} \quad ,$$

so the lab worker measures the propagation velocity  $c_{\ell} = L/t_{\ell} = c_0$  both ways.

The general case, depicted in Figure 39, requires a more elaborate derivation that need not be repeated here, because the derivation of the

Lorentz transformation gives the same result later on. Einstein's Special Relativity postulate about the constancy of the velocity of light is nothing more than a statement that two way light set, using Eq.(227), *de-synchronizes* the clocks and, *effectively converts a secondary inertial lab into the equivalent of a primary inertial lab, with calculated propagation velocity  $c_0$  in all directions.*

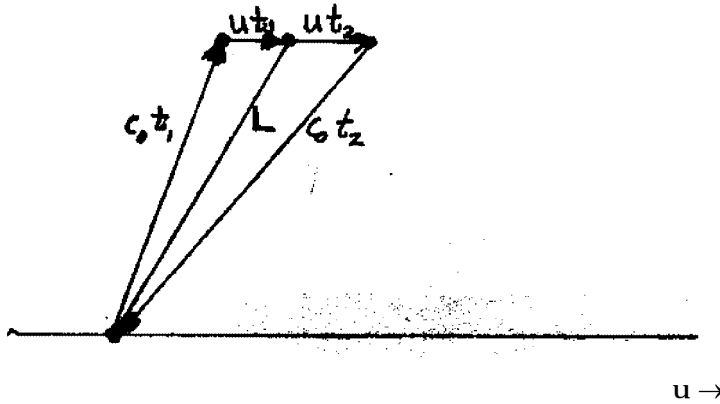


Figure 39 Ether flow in any direction relative to L.

### Actual Ether Experiments

There are two classes of ether experiments that have been conducted since around 1887:

1. Measurements to determine
  - a. Two way velocity of light
  - b. Clock slowing
  - c. Rod contraction
2. Measurements to detect constant velocity motion relative to the datum

All accurate *measurements of the velocity of light* have been *two way* measurements. The presently accepted value is regarded as well established. Until an experiment equivalent to the one described on page 98 is achieved, the one way velocity must be deduced.

*Clock slowing* was first measured directly as late as 1938.<sup>24</sup> Even then it was a very difficult measurement involving the frequency shift of radiating hydrogen atoms moving in a beam. The time dilation had to be separated from a much larger doppler shift component. Later, the lifetimes of decaying unons and bions both in cosmic rays and finally in large accelerators gave convincing support to the fact<sup>25</sup>. A reasonable interpretation of the Hafele-Keating experiment also concurs<sup>26</sup>.

It is true that *rod contraction* has never been measured *directly*, but that hardly takes away from the fact of its existence. Certainly the notorious Michelson-Morley experiment led both Fitzgerald and Lorentz to accept the contraction as the most reasonable explanation of the

24. H.E. Ives, G.E. Stilwell, J.Opt.Soc.Amer. **28**, 215 (1938); **31**, 369 (1941).

25. B. Rossi, D.B. Hall, Phys.Rev. **59**,223 (1941). Durbin, Loar & Havens, Phys.Rev. **88**, 179 (1952).

J. Bailey et al, Nature, **268**, 301 (1977).

26. J. Hafele, R. Keating, Science, **177**, 166 (1972).

results. Many examples of so called relativistic experiments depend upon rod shortening as well as the two preceding characteristics in such a way that it would require a fantastic coincidence for all of them to come out as observed.

Referring to Item 2 above, it is well known that *no experiment has yet determined the constant velocity of the ether relative to any inertial system.* From numerous examples in the literature and several in PHYSICS 2001, it should be clear that this will always be the case. On the other hand, everyone has performed an experiment that shows the acceleration of the ether.

### The Ether Observer

Strong arguments have been advanced here to preserve visualization, cause and effect, intuition and determinism, using an ether, while at the same time avoiding metaphysics at the physical level. However, certain experiments have been described that have caused physicists no end of soul searching and mysticism in resolving the results obtained. For example, though the laws (equations) of physics are in simplest form in primary inertial labs, apparently no one is able to say which inertial labs are primary.

It was stated in section III that an *absolute* observer is one with respect to whom the ether is everywhere at rest in a field free lab. Since no constant velocity lab (non-accelerating) observer has any indication of his velocity relative to the ether, it might seem reasonable to assume that none of those observers, with a range of velocities, could identify whether or not they were the *absolute* observer with  $u = 0$ . Conventionally, the inability of inertial system observers to detect their motion relative to the ether has been used to argue against the ether's existence; but *a far more useful conclusion can be drawn.*<sup>27</sup> Based on the *Principle of Identical Environments*, it would seem just as reasonable for any one of them to *assume he is the absolute observer, and the results he observes are exactly what the ether observer would see doing the same experiment.* Now, since the phenomena discussed earlier are intuitively obvious in terms of an ether observer, that is how the physics should always be *explained*. Assume the ether observer is doing the experiment. All other inertial observers will see the same thing. This is true *without* using the two way light set procedure of special relativity. It is also true using the light set procedure, or any other reasonable procedure.

### The Lorentz Transformation Without Space-Time

What is the future role of the Lorentz transformation and of special relativity? Space-time offers nothing to the physicist. SR consists of two postulates; the basic Relativity principle, which is just a limited form of the Principle of Identical Environments, and correct; and the constancy of the velocity of light, generally incorrect. *The second postulate only holds true for the arbitrary setting of clocks by two way light set.* For two-

---

27. R. H. Dishington, PHYSICS, Beak Publicatios, Pacific Palisades, CA (1989).

clock contact setting the one way velocity of light is different in opposite directions, so *the second postulate is wrong as presently stated*. Thus, Einstein's form of special relativity must be used with great care and an appreciation of its non-metaphysical nature is indispensable. All that will be retained is the basic "relativity" postulate.

Conversely, the Lorentz transformation has a utilitarian value. This is because two way light set is generally the simplest process available. When it is used, and rods are read by moving observers carrying them along, then the Lorentz transformation does give the proper method for *calculating* the readings of the moving clocks and rods in terms of those of the assumed ether observer, and vice versa. In order to explain away the last vestiges of paradox or confusion associated with the Lorentz transformation, it will be derived here in its usual form, but with a slightly different emphasis, inasmuch as the ether will be tacitly assumed as the basis of its validity.

#### Lorentz Transformation and Simultaneous Synchronization

Before carrying out the derivation, a crucial difference between the two-clock contact and light-set experiments must be indicated. Referring back to Figure 34, notice that *the methods used by the two sets of clocks for synchronization were not the same*. That is, during the experiment, *the experiences of the two inertial observers were not symmetrical*. There is nothing about the relativity postulate that requires it. The only reciprocal requirement imposed by relativity is that if the whole procedure is repeated with the roles of the clock pairs reversed, then the results must be indistinguishable from the first experiment.

A well known derivation of the Lorentz transformation, described by Robertson,<sup>28</sup> implies that the transformation follows from two postulates:

1. Relativity
2. The Fitzgerald-Lorentz matter contraction.

Unfortunately, *this is not quite true*. It is shown, in PHYSICS 2001Rev, that rod contraction coupled with the clock slowing, *cause* the relativity postulate to be true, *even in systems where the Lorentz transformation and the constancy of the velocity of light are not directly applicable*. Actually, Robertson's derivation is much more restrictive. It invokes the implicit assumption that both systems are "de-synchronized" in the same way at the same time. In other words, that everything happening to the two inertial observers is mutually symmetrical, simultaneously. *This is a much more restrictive condition than the Lorentz contraction and relativity impose*. It is this very tight restriction that is responsible for much of the confused intuition. Once the implications of this implicit restriction are understood, much of the mystery vanishes.

---

28. H.P.Robertson & T.N.Noonan, Relativity and Cosmology, p 43, W.B. Saunders Company, Philadelphia, PA (1968).

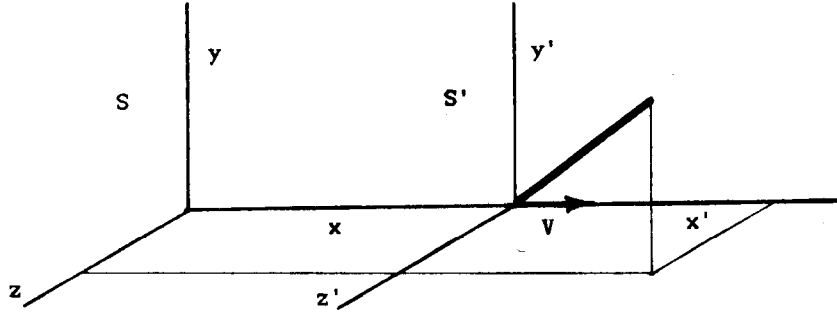


Figure 40. Inertial systems in relative motion.

Continuing with Robertson's derivation, Figure 40 displays the usual pair of observer systems in relative motion, at constant velocity  $V$  as seen by the ether observer  $S$ . A rod at rest in  $S'$ , with one end at the origin and the other at  $(x', y', z')$ , will appear to  $S$  to have its ends at  $(Vt, 0, 0)$  and  $(x, y, z)$  respectively. The matter contraction with motion through the ether requires that,

$$x - Vt = \frac{1}{\gamma} x' \quad , \quad y = y' \quad , \quad z = z' \quad , \quad (228)$$

where,

$$\gamma = \frac{1}{\sqrt{1 - \frac{V^2}{c_0^2}}} \quad .$$

Next, Robertson writes,

$$x' + Vt' = \frac{1}{\gamma} x \quad , \quad y' = y \quad , \quad z' = z \quad , \quad (229)$$

on the basis of the relativity postulate; i.e. inertial observers performing the same experiment see the same results. This is acceptable from the ether viewpoint because it is known that the time slowing of clocks and the contraction work together to ensure that result.

At this point Robertson says that Eqs.(228) and (229) may be solved for the Lorentz transformation:

$$x' = \gamma(x - Vt) \quad , \quad y' = y \quad , \quad z' = z \quad , \quad t' = \gamma \left( t - \frac{V}{c_0^2} x \right) \quad , \quad (230)$$

and,

$$x = \gamma(x' + Vt') \quad , \quad y = y' \quad , \quad z = z' \quad , \quad t = \gamma \left( t' + \frac{V}{c_0^2} x' \right) \quad . \quad (231)$$

*This is the step that imposes the simultaneous transformation not required by Relativity or the Fitzgerald-Lorentz matter contraction. As Robertson points out, this is equivalent to the adoption of the postulate of the constancy of the velocity of propagation. Earlier that postulate was shown not to be true in general, but to result from the very arbitrary and*



restrictive two way method of setting the clocks. That is what results when the Lorentz transformation is used.

In spite of the severely restrictive character of the Lorentz transformation, with its two way light-set clocks and its constant calculated velocity of light in all inertial systems, its utility in setting up experiments and in certain types of problem solving make its use logical and practical. *It should never be used to try to explain the physics.* The simple ether picture is better for that purpose, basic and correct. Almost all of the intuitional difficulties of special relativity came from the unreal philosophical decoration of "space-time" and from the simultaneously symmetrical imposition of the Lorentz transformation.

#### Implications of the Lorentz Transformation

Going back to Figure 40 and Eq.(230), which are used by S to find out what S' measures; if S wants to know of the origin of S', he sets  $x' = 0$  into the first equation and finds it satisfied by  $x/t = V$ . If S' wants to know of the origin of S, he uses the inverse Eq.(231), setting  $x = 0$  and finds it satisfied by  $x'/t' = -V$ . *S and S' both measure their speeds as equal, with opposite velocities.* By simply reversing the sign and making the primes unprimed and vice versa, S' and S will be interchanged, with the original S' system now the ether observer equivalent and the original S system now the moving observer equivalent. With this arbitrary clock set arrangement, the two are completely symmetrical, simultaneously. It is in this connection that the greatest philosophical or metaphysical confusion enters the conventional approach. The ether eliminates this.

To the question, "which rod is really shorter or which clock truly slower?", common conventional answers are that question has no meaning<sup>29</sup>, irrelevant<sup>30</sup>, the space-time manifold<sup>31</sup>. Since 1960, it has become popular to just omit such questions, as though intuition is in the way, and should be ignored. In fact, the question is perfectly valid. So is the answer. *In every case, the rod or clock moving fastest relative to the ether, is the shortest or slowest.* The fact that it is not possible to determine how the ether is flowing external to any inertial system does not invalidate that answer. The previous sections have explained clearly and intuitively why the ether flow cannot be measured by an inertial observer. The intuitive difficulty was artificially introduced by an arbitrary choice of the simultaneously symmetric transformations. The Lorentz transformation is used as a general formalism, but should not be used to obtain an intuitive grasp of any given experiment, a number of at first sight strange results can be deduced through its use. There are numerous expositions of these effects available.

The following summarizes the gains in understanding using the ether as a motivation for the many choices made in clock setting.

---

29. A.Sommerfeld, Electrodynamice, p 227, Academic Press, N.Y.N.Y. (1952).

30. R.B.Lindesy & H.Margenau, Foundations of Physics, p 340, John Wiley & Sons, N.Y. (1936).

31. I.S.Sokolnikoff, Tensor Analysis, p 267, John Wiley & Sons, N.Y. (1951).

## INERTIAL LAB MEASUREMENT SUMMARY

The Principle of Identical Environments (Relativity Principle) holds between *all* inertial labs:

Identical experiments in **any** two inertial labs yield identical results.

### Primary Inertial labs:

*No inertial observer can determine that he is in a primary inertial lab; but, (before he sets his clocks) any inertial observer can assume he **is** in a primary inertial lab, and the experimental results he observes (now including his choice of clock setting) will be exactly what a primary observer would see doing the **same** experiment (with the same clock setting).*

### Secondary Inertial Labs:

*There are two types of secondary inertial labs of particular interest: Those with truly contact synchronized clocks and those with two way light set de-synchronized clocks.*

#### TRULY SYNCHRONIZED CLOCKS

1. The secondary lab clocks are set with difficulty
2. The clocks are truly synchronized *in the most fundamental way*
3. The principle of the constancy of light propagation velocity is **not** generally true
4. The *equations (laws)* of physics do **not** generally have the same form as in the inertial lab used to set the clocks
5. The Lorentz transformation does **not** generally apply between the truly synchronized lab and the inertial lab used to set the clocks

#### TWO WAY LIGHT SET CLOCKS

1. The secondary lab clocks are easily set
2. The clocks are *deliberately de-synchronized* to ensure  
3. below
3. The one way calculated velocity of light is always the same,  $c_0$
4. The equations (laws) of physics are exactly the **same** in all two way light set inertial labs
5. The Lorentz transformation applies between two-way light set inertial labs

## XXIII C-PARTICLES

### Introduction

In Section XVIV, the dichotomy dividing fundamental particles into layerons (electric) and c-ons (magnetic) was described, but only the layerons were analyzed there. Now, enough background has been established so that an attempt to describe the c-ons can be made. It will be less formal than the layeron analysis, but will establish a useful visualization. The following is mainly qualitative.

The key to understanding detailed, deterministic c-on structure is the *profound difference between free space antenna radiation and atomic radiation*. Antenna radiation is completely described by Maxwell's macroscopic equations (see Section IV), and no case has ever been found where the free space radiation did not *spread out* following a geometrical energy reduction proportional to  $1/r^2$ . There is no reason to believe that the radiation caused by moving an electron in an antenna is anything more than *the simple wave motion in the ether* described by Maxwell's equations.

Atomically generated photons, on the other hand, travel for untold light years without changing in any way except for a small shift in their wavelength. *This is a profound difference*.

The behavior of antenna radiation is similar to all simple physical wave motions, which exhibit the geometrical spreading. The spreading is essentially independent of any particulate property of the wave medium. On the other hand, *photons behave like particles*. An electron, for example, can travel long distances and still retain its essential properties. Conventionally, photons are treated as point particles, and all transverse wave radiation, including antenna radiation, is assumed to be carried by photons. Here, *this concept is abandoned*. In the present work, for reasons to be discussed in the following, c-on structure applies only to photons and neutrinos; and antenna radiation is seen to be completely free of any photons. It was described in Section IV.

### C-ons

Although these ether configurations have wave properties, *they are true particles*, i.e., stable entities that can maintain their identity only if they move at the velocity  $c_0$  relative to the ether. They come in two basically different varieties, photons and neutrinos; but they are very similar, and both appear to endure forever unless they interact physically with other particles. For many years very little was known about them. For example, they were both thought to have zero rest energy, zero net charge and zero magnetic moment; only differing in spin, 1 for the photon and 1/2 for the neutrino. Recently there has been speculation that their rest energies and magnetic moments are not zero. However, numerous astounding experiments have only established that these properties are not greater than certain very small maxima.

The first hints as to c-on structure come from the conversion processes that produce them. Table V (pg.57) lists several, such as the  $\mu$  and  $\tau$  decays, the  $\pi^\pm$  decay and the neutron decay, all of which produce neutrinos. Also listed there are the  $\pi^0$ ,  $\eta$  and  $\Sigma^0$  decays which generate photons. Of course, the most common sources of photons are atomic and molecular transitions.

Although photons and neutrinos are, in some respects, almost twins, their differences dictate that the proper study of c-ons begins with a detailed examination of *photon* generation.

### Photon Generation

As far as is known, all photons are generated by *orbiters*. Certainly electrons orbiting in atoms are the primary sources; but the outside orbiter bions are also clear examples. Still questionable are the rare instances where even non-orbiting, concentric bions such as  $\pi^\pm$  or  $K^\pm$  have one or two photons as decay products. In these cases the chance of occurrence is less than  $10^{-3}$ , so they probably represent accidental configurations that coincidentally produce an orbiting effect.

In an atom generating a photon, the nucleus absorbs the momentum of the back push as the photon leaves, so a *single* photon can be pushed out on an axis perpendicular to the orbit. The choice of which of the two possible directions it takes is made by slight differences in the phase fronts of the  $\ell$ -wave caused by datum fluctuations. In the orbiter bion case, there is no nucleus to absorb the kickback, so *two photons* are generated, going in opposite directions, again on a line perpendicular to the orbit plane.

It should be emphasized that most of the present discussion will be about the simplest photons produced by *free* atom radiation. Other conditions can result in the production of much more complicated photons; particularly when the radiating atom is part of a more elaborate environment, such as being immersed in a high pressure gas, a solid or a liquid. Though even these complex photons are still roughly similar to the ones to be analyzed, since they result from more violent dumping of energy in a shorter time, they are physically shorter and have larger amplitude waves.

### The Photon Generator

To keep the discussion simple, the Hydrogen atom is chosen as the photon generator. Here the task is to visualize a *single, deterministic atom in a field free region*. The basic analysis applies Newton's laws to a "planetary" electron orbiting a proton nucleus. This is not a temporary crutch to be abandoned as the derivation proceeds, but the actual physical mechanism operating. The inner orbit Hydrogen characteristics were shown in Figure 31 (pg.92) and listed in TABLE X (pg.93).

A single orbiting electron generates an ether vortex with a dipole type magnetic field, as depicted in Figure 32 (pg.95), that is the crucial element in photon generation. TABLE XI (pg.97) lists the magnetic

moments of the inner Hydrogen orbits. The values listed in the above tables indicate the principal factor in photon generation.

### The Radiation Orbit

In a quiescent Hydrogen atom the electron is circling the innermost orbit  $(n, n_\psi) = (1, 1)$ . If that atom is excited to the  $(2, 2)$  state, the electron is circling the  $(2, 2)$  orbit (see Figure 31). After a relatively short delay time the datum fluctuations perturb the orbit and cause the electron to start the decay back to the  $(1, 1)$  orbit. When a downward transition occurs, the electron is suddenly out of lock-step with the initial pseudo-stable orbit. It spirals inward to the final orbit, releasing energy, but the program it executes is not simple.

As explained in Section XV (pg.90), many orbit cycles are required to generate the photon. *It is assumed that the radiated energy per cycle is small compared to the total photon energy.* The energy radiation rate is proportional to how much of  $\Delta E$  remains, so that the electron's orbital energy during photon generation is,

$$E = \Delta E \varepsilon^{-t/\tau_p} + E_f \quad .$$

where  $\tau_p = 1.59 \times 10^{23} / \omega_p^2$ ,  $\omega_p$  is the photon angular frequency and  $E_f$  is the energy of the electron in the final orbit. When  $t = 5\tau_p$ , 99.3% of  $\Delta E$  has been radiated.

All photons appear to have certain well known characteristics, such as: very small or zero rest energy, zero net charge and zero magnetic moment. They also have spin 1, in agreement with the  $1\hbar$  reduction in the radiating atom's total vector angular momentum. A few other photon characteristics appear well founded. For example, in the  $(2, 2) \rightarrow (1, 1)$  transition, the photon produced is a long, narrow particle ( $L/a > 10^8$ ) because it takes time to generate it *and it is propagating away from the atomic orbit at velocity  $c_0$* . It has a circularly polarized, energy carrying t-wave; and also, because the radiation process is a disturbance, an energyless, plane  $\ell$ -wave propagating at velocity  $c_0$ .

Of all *atomic photons*, the smallest diameter particle is produced by the  $(2, 2) \rightarrow (1, 1)$  hydrogen transition. It is roughly  $10^{-8}$  cm across. Its *effective* length  $L \cong 5c_0\tau_p$  is 99.5 cm, containing  $8.2 \times 10^6$  cycles of the radiated wave, or 99.3 % of  $\Delta E$ .

This meager collection of photon attributes is a relatively simple extension of the *conventional* concept of a photon. One further photon property can be invoked to improve that concept considerably.

### The Photon Vortex

The proper approach to photon structure is to find the physical mechanism, that antenna radiation does **not** have, by which the photon is held in *particle* form. The backbone of a photon's particle structure is a long tubular vortex. It is pushed out perpendicularly to the electron's

orbit, probably because the orbit radius decreases during radiation. Because of this, the ether vortex has a form close to that of a very long, needle thin solenoid; with ether rotating as a solid body inside, and slipping outside (zero curl field outside). Figure 41 is greatly compressed lengthwise and expanded in diameter.

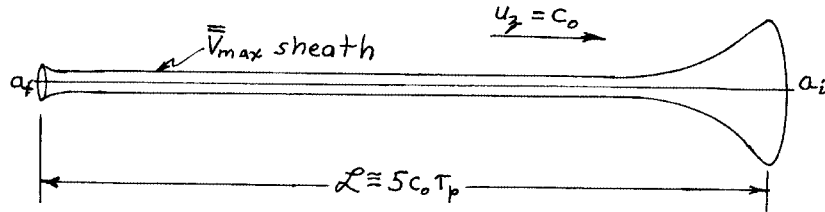


Figure 41 Photon vortex (compressed in length 10 times and expanded in diameter  $10^8$  times)

Although originally there is a circulating charge (the orbiting electron *generating* the photon vortex), once the vortex leaves the atom it is a *free* vortex, moving at velocity  $c_0$ , *with no attached circulating charge*. This indicates that it is an *energyless magnetic field* (see Section IV, pg.12). It also explains why a photon has no magnetic moment. It is well known that vortices can travel considerable distances without significant change. The photon vortex has the advantage that *the ether is a frictionless fluid*, and thus the vortex is essentially indestructible. Only when it finds a compatible particle that unwinds it can it vanish.

Any disturbance in the ether causes the formation of  $\ell$ -waves (longitudinal waves), so it is assumed that an  $\ell$ -wave propagates inside the vortex and moves along with it. Photons are also known to exhibit circularly polarized t-wave (transverse wave) characteristics, so there is also a t-wave propagating inside the vortex and moving along with it. Without the vortex, these waves would behave like antenna radiation and would exhibit no particle properties. Both waves propagate, in the direction of the vortex axis, *inside* the rigid body region. Outside, the slip prevents coherent wave propagation.

No complete quantitative analysis of the complicated ether flow pattern during the radiation exists. Moreover, no complete quantitative description of the photon is available. However, some progress has been made (see PHSICS 2001Rev, Chapter 10).

#### The Neutrino

*None of the sources available, that discuss the neutrino, indicate the size or shape of that elusive particle.* It is often illustrated as a small sphere. The neutrino was first *postulated*, in connection with the conversion of a free neutron into a proton and electron, in order to save the conservation of energy law. However, with hindsight, *its most important function is to allow spin conversion*. This is understood by considering the decay of the  $\mu^-$  unon, first described in Table V, pg. 57.

The conversion process, in its simplest form, starts with the  $\mu^-$  at rest, buffeted by the datum fluctuations. After a certain delay time, the  $\mu^-$  begins to ooze outward from the 2<sup>nd</sup> layer position; and, at the end of the conversion, an electron with its maximum electric energy at the 1<sup>st</sup> layer position is formed. Almost all of the rest energy of the  $\mu^-$  must be carried away as kinetic energy, and the fact that the  $\mu^-$  vortex velocity distribution is much more compact than the final  $e^-$  vortex velocity distribution means that some process of *circulation reconfiguration* must also take place. The method nature uses to do the latter is to simply remove the  $\mu^-$  spin vortex ( $v_\mu$ ) from the conversion region, and generate an electron neutrino/antineutrino pair of spin vortices, one ending up inside the electron and the other ( $\bar{\nu}_e$ ) also leaving the conversion region. All three final particles can carry kinetic energy away with them.

#### The Neutrino Vortex and $\ell$ -Wave

The neutrino has almost the same structure as the photon, *but it has no transverse wave*. It is most often generated by a spinning unon. As described in Section V, pg.12, the unon spin velocity forms an energyless dipole field that turns as a rigid body in a small central region but slips outside. There is no orbiting electron as in photon generation. During  $\mu^-$  decay, for example, it is the expansion of the particle to the lower energy electron that causes the spin field to leave the  $\mu^-$ . Here as in photon generation, the vortex is stretched out, but it is much smaller in cross section ( $\leq 0.06 r_e$ ) than the photons. The neutrino vortex and its plane  $\ell$ -wave are depicted in Figure 42.

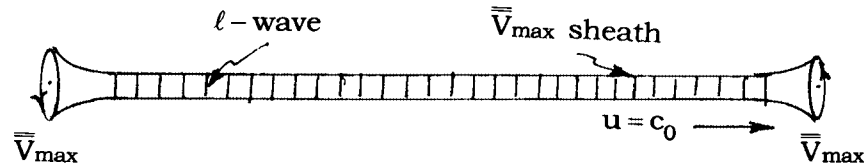


Figure 42  $\ell$ -wave inside the propagating  $v_\mu$  vortex.

The more formal photon analysis in PHYSICS 2001Rev, Chapter 10 is directly applicable to the neutrino also. It does not appear that there is any *recoverable* magnetic energy associated with the neutrino. Since all of its distributed charge is in the end structures, the chance that it has any significant magnetic moment is slight. Nevertheless, it does have the external slip field of  $\bar{V}$ , so some miniscule magnetic effect might be measurable. Again, this is an open question.

At the present time, there is much speculation that the neutrinos oscillate from one type ( $\nu_e, \nu_\mu, \nu_\tau$ ) to another and back. Since nature was

forced to remove the  $\nu_\mu$  and replace it with the  $\nu_e$  in the  $\mu$  decay, and since it seems to be the rule that one whole spin structure must be replaced with another whole spin structure, it is unlikely that the individual neutrinos can oscillate.

At this point, very little more is known about these untouchable particles; but the visualization presented here does help to understand many of the odd situations that involve neutrinos.

## XXIV THE GRAVITIC FIELD

### Introduction

Around 1590, Galilei measured the acceleration of falling bodies. In 1687, after thinking about the problem on and off for about twenty years, Newton published his Principia, which expounded the Law of Universal Gravitation (attraction between large neutral bodies). To explain *why* neutral bodies attracted each other, Einstein "geometrized" space-time in his 1916 General Theory of Relativity. From that time to this, investigators have been trying to combine that space-time geometrization with a theory of electricity and magnetism; but this has failed. In the 1950's Kirkwood<sup>32</sup> adopted the ether as the gravitic medium, and succeeded in developing a gravitic field theory that has the correct properties. The present section is essentially an elaboration of Kirkwood's gravitic field theory with minor modifications. The full importance of his theory is not recognized at present<sup>33</sup>, but its influence is strong in every chapter of PHYSICS 2001Rev(2009).

### The Gravitic Field

Layerons have gravitic fields, c-ons do not. In Section XV, the gravitic field of the most elementary layeron, the electron, was shown to be a *standing*  $\ell$ -wave with density  $\phi_s$  and velocity  $V_s$  (coexistent with the *traveling*  $\ell$ -wave) that just *quivers in and out* at frequency  $\omega_e$ . All the other layerons also have similar standing wave fields varying at their own characteristic frequencies. The travelling  $\ell$ -wave fields of *charged* layerons produce bulk distortions that interact so strongly with other charged layerons that the gravitic forces are negligible. However, in neutral layerons, neutral atoms and larger neutral composites, the *traveling*  $\ell$ -waves go directly from the negative to the positive layers, and so *only a short distance away from the neutral combination, the standing gravitic wave is dominant*.

Conventionally, gravitation is approached as a "force" between neutral bodies. The ether view is that, since there is no "force", the interaction is just a condition of acceleration of the primary inertial system at each

---

32. Kirkwood, R.L., PhD Thesis, *Stanford U. Physics Dept.*, (1950).

....., *Phys. Rev.*, **92**, 1557 (1953). *Phys. Rev.*, **95**, 1051 (1954).

33. ...., *Project RAND*, D-7210, (1960). *The RAND Corp.*, RM-3146-RC, (1962). *J. Math. Phys.*, **11**, 2983 (1970). *Int. J. Theor. Phys.*, **6**, 133 (1972). *Loc.cit.* **7**, 391 (1973).



point in the field. Establishing the motion of the primary inertial system about a neutral body is the key to the problem.

### Gravitostatics

Here the emphasis will be on the field around a "large", spherical, neutral (uncharged) body at rest relative to the absolute observer. The conditions for a gravitostatic field are:

$\overline{\mathbf{V}} = \overline{\phi} = 0 \quad , \quad \overline{\phi}_a = \overline{\phi}_d \quad , \quad \frac{\partial \overline{\mathbf{V}}}{\partial t} = \frac{\partial \overline{\phi}}{\partial t} = 0$ <p style="text-align: center; margin-top: 10px;">All higher time partials of <math>\overline{\mathbf{V}}</math> and <math>\overline{\phi}</math> are zero.</p>	<p style="text-align: center;">Conditions for Gravitostatics</p>
--	--

(232)

When these conditions are substituted into the standing  $\ell$ -wave Eq.(89), that equation reduces to,

$$\nabla^2 \overline{\mathbf{V}}^2 = 0 \quad . \quad (233)$$

It was shown, in Section XV (pg. 39), that Eq.(233) has a solution,

$$\mathbf{V}_\cdot = \hat{\mathbf{r}} \sqrt{\frac{K_g}{r}} \cos \omega t \quad , \quad (234)$$

where  $K_g$  and  $\omega$  are, as yet, *unspecified* and  $r$  is greater than the source mass radius. Again, from Section XV,

$$\phi_\cdot = \frac{3\phi_d}{2\omega} \sqrt{\frac{K_g}{r^{3/2}}} \sin \omega t \quad ,$$

and as discussed there, this standing  $\ell$ -wave has a time average acceleration,

$$\overline{\mathbf{a}} = \overline{\mathbf{V}_\cdot \cdot \nabla \mathbf{V}_\cdot} = - \hat{\mathbf{r}} \frac{K_g}{4r^2} \quad ,$$

where  $K_g$  is not the same as that of the electron. Here again, it is the time average acceleration of the neutral body standing  $\ell$ -wave that produces the gravitic effect on other bodies.

### Sources of the Gravitic Field

A hydrogen atom is composed of a proton and an electron. To act together as a single object they must adjust their individual frequencies  $\omega_p$  and  $\omega_e$  to a single composite  $\ell$ -wave frequency that is slightly greater than  $\omega_p$  ( $E_{p0} = 1.50328 \times 10^{-3}$  ergs) because of the added electron rest energy ( $E_{e0} = 0.00082 \times 10^{-3}$  ergs). The negative interaction energy ( $E_{ep} = - 4.3574 \times 10^{-11}$  ergs) is so small that the reduction from  $\omega_h = 1.42626 \times 10^{24}$  rad/sec is not measurable. If another hydrogen atom is added to the first, the two often combine to form a molecule, and *all the particles must adjust to a new  $\ell$ -wave frequency*, roughly twice the original  $\omega_h$ , because of the increased energy. However, when many

atoms are joined in a large neutral body, they don't appear to go to higher frequencies, but simply combine their fields. The exact cutoff is not yet understood.

Nevertheless, it is well known that the time average acceleration field of a composite body is,

$$\bar{\mathbf{a}} = -\hat{\mathbf{r}} \frac{GM}{4\pi r^2} \quad , \quad (235)$$

where M is just the sum of the rest masses of all the components. So, working back to Eq.(234), the  $\ell$ -wave velocity field is then,

$$\mathbf{V}_\ell = \hat{\mathbf{r}} \sqrt{\frac{GM}{\pi r}} \cos \omega t \quad .$$

If the body consists of N hydrogen atoms, then,

$$\mathbf{V}_\ell = \hat{\mathbf{r}} \sqrt{\frac{NK_g}{r}} \cos \omega t \quad ,$$

where  $K_g$  is the constant for a single atom.

### The Gravitic Primary Inertial Systems

Earlier sections have provided characteristics of particles, e.g., rest energy, frequency, charge, etc., as seen in inertial systems or by an absolute observer. In 2001Rev, Chapter 12, the technique for dealing with bodies moving in *non-inertial* regions, e.g. inside the vortex of a solenoid, was examined. It used the fact that, at any point in the flow, *laws of physics held in the differential inertial system that translated and rotated with the fluid at the point.* Then, the motion in that differential system was transformed to the absolute system by a *Galilean* transformation.

In considering particle/field interactions, particularly neutral particle/field interactions, one controlling influence is the particle's motion factor (or distortion factor),

$$\gamma = \frac{1}{\sqrt{1 - \frac{(\mathbf{u} - \bar{\bar{\mathbf{V}}}_e)^2}{c_0^2}}} \quad , \quad (236)$$

where  $\bar{\bar{\mathbf{V}}}_e$  is the *effective* velocity of the differential primary inertial system at the particle's location and  $\mathbf{u}$  is the particle's velocity, both as seen by the absolute observer conducting the measurements. From another viewpoint, the absolute observer can find the primary inertial system at any point in the field by finding a test particle's velocity that results in a  $\gamma$  of unity (only rest energy in the particle). In Section XVIII,  $\bar{\bar{\mathbf{V}}}_e = \bar{\mathbf{V}} = 0$  because the datum ether is at rest relative to the absolute

observer. In Section XXII (Rod contractions), the same conditions applied. However, in 2001Rev (Section 12.4),  $\overline{\overline{\mathbf{V}}}_e = \overline{\overline{\mathbf{V}}} \neq 0$ . *In most cases, the time average ether velocity  $\overline{\overline{\mathbf{V}}}$  establishes the primary inertial system velocity.*

One outstanding exception to this is the gravitic field of a large neutral body, because there  $\overline{\overline{\mathbf{V}}} = 0$  and the test particle distortion that establishes  $\overline{\overline{\mathbf{V}}}_e$  is caused by *opposing* the acceleration  $\overline{\overline{\mathbf{a}}}$ . In 2001Rev (Section 13.3), several figures show various accelerated particles and the asymmetrical bunching distortion in their fields due to acceleration. The gravitic acceleration produces just such distorted particles if their motion in step with  $\overline{\overline{\mathbf{a}}}$  is *impeded* or *augmented*. To determine the primary inertial system in a spherical gravitic field, allow a free-space test particle at very large distance from the source body to free-fall toward it. As it falls, its velocity  $\mathbf{u} = \overline{\overline{\mathbf{V}}}_e$  increases. At each point in the field, the primary inertial system *inward* velocity can be found by integrating  $\overline{\overline{\mathbf{a}}}$  from  $r = \infty$  to  $r$ , with the result,

$$\overline{\overline{\mathbf{V}}}_e = - \hat{\mathbf{r}} \sqrt{\frac{GM}{2\pi r}} \quad . \quad (237)$$

Any test body that moves at that inward velocity is in free-fall *and is at rest in the differential primary inertial system*. It feels no acceleration and has only its rest distortion ( $\mathbf{u} = \overline{\overline{\mathbf{V}}}_e$ ,  $\gamma = 1$ ).

One of the strangest facts about the gravitic field is that *at each point there appear to be only two primary inertial systems*. To see this, start a test body at the source surface with the *outward escape* velocity given by,

$$\overline{\overline{\mathbf{V}}}_e = + \hat{\mathbf{r}} \sqrt{\frac{GM}{2\pi r}} \quad , \quad (238)$$

and let it free-fall to infinity where its velocity will be zero. All during that *outward* free-fall, *the test body is at rest in the differential primary inertial system*. It feels no acceleration and has only its rest distortion ( $\mathbf{u} = \overline{\overline{\mathbf{V}}}_e$ ,  $\gamma = 1$ ).

In practical problem solving, the velocity  $\mathbf{u}$  is not always along a radius, but varies both in magnitude and direction as the body moves through the  $\overline{\overline{\mathbf{a}}}$  field. Since  $\overline{\overline{\mathbf{V}}}_e$  appears in Eq.(236), that applies to the test body's motion, at any given point the proper sign of  $\overline{\overline{\mathbf{V}}}_e$  must be selected (see 2001Rev). It is determined by the sign of the  $r$  component of  $\mathbf{u}$ , i.e. by  $u_r = dr/dt$ . *The sign of  $\overline{\overline{\mathbf{V}}}_e$  must always be chosen to be the same as the sign of  $u_r = dr/dt$ .* For example, in elliptic orbit problems, for the half of the orbit where  $r$  is increasing,  $\overline{\overline{\mathbf{V}}}_e$  is positive; but, for the other half,  $r$  is decreasing and  $\overline{\overline{\mathbf{V}}}_e$  is negative.

### Test Body Mass in a Gravitic Field

Once the primary inertial system motion field is established, Eq.(236) leads directly to the energy and mass relationships,

$$E = \gamma E_0 \quad , \quad m = \gamma m_0 \quad , \quad (239)$$

where  $E_0$  and  $m_0$  are the tests body's *rest* energy and mass. The concept of a body's *rest* energy, in all preceding sections, was fixed by its energy distortion content when it was at *rest* in the datum ether. That definition still applies in a gravitic field. However, a semantic problem arises when a test body is at "rest" ( $\mathbf{u} = 0$ ) in a gravitic field, since Eqs.(236) and (239) indicate that its *rest* mass is augmented by its motion relative to the primary inertial system in the field. Here, to avoid confusion, *a test body with zero velocity, as seen by the absolute observer, will be described as "fixed" in the gravitic field.*

Notice that, when a body is "fixed" in the field ( $\mathbf{u} = 0$ ), Eq.(236) gives the *same* value of  $\gamma$  for both the inward and outward inertial system values of  $\bar{\bar{\mathbf{V}}}_e$ ,

$$\gamma = \frac{1}{\sqrt{1 - \frac{GM}{2\pi c_0^2 r}}} \quad . \quad (\mathbf{u} = 0) \quad (240)$$

Eq.(239) then indicates that a test body held fixed at smaller distances from the source has greater mass. It is smallest at  $r \rightarrow \infty$ ,  $m = m_0$ ; and increases, when it is fixed at the surface, to,

$$m = m_0 \left( 1 - \frac{GM}{2\pi c_0^2 r_s} \right)^{-\frac{1}{2}} \quad , \quad (241)$$

where  $r_s$  is the source body radius.

### Clock Rate in a Gravitic Field

Now it is possible to understand the observed slowing of clocks in a gravitic field. Just as in Section XXII (pg.100), only one simple circling mass-on-a-string clock will be analyzed. In the gravitic case, for simplicity, the circling is in a plane perpendicular to the  $\bar{\mathbf{a}}$  field, so that the only effect of the field on the mass particle is the change in energy and momentum. Figure 43 shows the physical layout. At  $r \rightarrow \infty$ , the circling mass has energy  $\gamma_1 E_0$  and momentum  $u_1 \gamma_1 E_0 / c_0^2$ . If the clock is moved toward the source body, and held fixed at the distance  $r_2$ , the energy of the circling mass changes to  $E_2 = \gamma_2 E_0$ , but its momentum  $u_1 \gamma_1 E_0 / c_0^2$  remains the same, since no force was applied in the plane of the

The diagram illustrates a 'Circling mass clock' in a gravitic field. At the bottom, a 'source body' is represented by a shaded, semi-circular area. Above it, at a distance  $r_2$ , a mass particle is shown in a circular orbit. The orbit is in a plane perpendicular to the radial direction. Labels for this orbit include 'At  $r = r_2$ ' and ' $\bar{\mathbf{V}}_{e2}$ '. The energy and momentum of the mass at this distance are labeled as  $E_2$  and  $u_2 E_2$  respectively. Above the orbit at  $r_2$ , there are two vertical arrows pointing downwards, representing the radial direction. At the top of the diagram, at a distance  $r \rightarrow \infty$ , another mass particle is shown in a circular orbit. Labels for this orbit include 'At  $r \rightarrow \infty$ ' and ' $\bar{\mathbf{V}}_e = 0$ '. The energy and momentum of the mass at this distance are labeled as  $u_1 E_0$ .

Figure 43  
Circling mass clock.

orbit. Therefore,  $\mathbf{u}_2 \mathbf{E}_2 = \mathbf{u}_2 \gamma_2 \mathbf{E}_0 = \mathbf{u}_1 \gamma_1 \mathbf{E}_0$  and, because  $\mathbf{u}_i$  is perpendicular to  $\overline{\mathbf{V}}_e$ ,

$$\frac{\mathbf{u}_1}{\sqrt{1 - \frac{\mathbf{u}_1^2}{c_0^2}}} = \frac{\mathbf{u}_2}{\sqrt{1 - \frac{\mathbf{u}_2^2}{c_0^2} - \frac{\overline{\mathbf{V}}_e^2}{c_0^2}}} .$$

This can be solved to show that,

$$\mathbf{u}_2 = \frac{\mathbf{u}_1}{\gamma} , \quad T_2 = \gamma T_1 ,$$

where,

$$\gamma = \frac{1}{\sqrt{1 - \frac{\overline{\mathbf{V}}_e^2}{c_0^2}}} = \frac{1}{\sqrt{1 - \frac{GM}{2\pi c_0^2 r}}} ,$$

so the clock runs slower, closer to the source body. This is true of all types of clocks.

If this process is reversed, that is, start the clock at the surface and then move it far from the source ( $r \rightarrow \infty$ ), the clock runs *faster* at greater distances.

The lowered clock rate at the surface of a star, for example, explains what is known as the "gravitational red shift". A photon emitted at the star surface has a lower frequency than the value measured on the less massive earth (red shifted), and that frequency remains constant as the photon travels outward from the source body because  $\overline{\phi}_a = \phi_d$  and  $c = c_0$ .

#### A Test Body Held Fixed in a Gravitic Field

An external force is required to hold a test body fixed ( $\mathbf{u} = 0$ ) against the acceleration of a source body gravitic field. The field is assumed to be irrotational ( $\overline{\mathbf{w}} = 0$ ), and because  $\mathbf{u} = 0$  and  $r$  is fixed, Eq.(240) indicates that  $\gamma$  is constant and it follows that  $dm/dt = 0$ . Thus, the equation of motion reduces to,  $\mathbf{F} = -m\overline{\mathbf{a}}$ . Taking the value of  $\overline{\mathbf{a}}$  from Eq.(235),

$$\mathbf{F} = \hat{\mathbf{r}} \frac{GMm}{4\pi r^2} = \hat{\mathbf{r}} \gamma \frac{GMm_0}{4\pi r^2} . \quad (242)$$

This is the external force that must be exerted on any body of mass  $\gamma m_0$  held fixed in the gravitational field of a source body. More fundamental is the acceleration of the object when that support is removed.

#### Gravitic Energy

In educational institutions the gravitic field is presented in two completely different ways. Undergraduates are given a simple picture of "force" and "work" that leads directly to the concept of "potential energy" in the *field*. The farther apart two neutral objects are, the greater the potential energy stored between them. On the other hand, graduate

students are introduced to the General Theory of Relativity, and bombarded with such a horde of math symbolisms that the fact that the experimental evidence precludes gravitic energy stored in the field is lost. The ether theory allows this to be demonstrated quite simply.

Since the gravitic field is just an acceleration in a standing  $\ell$ -wave field, and since  $\ell$ -waves carry no energy, it appears, right from the start, unlikely that there can be energy stored in the field. In the following it will be shown that all energy observed in gravitic field experiments appears to be electric or possibly magnetic.

#### Force and Work in a Gravitic Field<sup>33</sup>

The nature of gravitic energy can be pursued by studying a small, neutral test body moving *radially* in the field of a large mass M, where  $\overline{\mathbf{w}} = 0$ . In 2001Rev the motion is described by the reduced equation,

$$\frac{d(\gamma m_0 \mathbf{u})}{dt} = - \hat{\mathbf{r}} \left( \frac{GMm_0}{4\pi r^2} \left( \frac{1}{\gamma} \right) - \left( \frac{1}{\gamma^2} + \frac{1}{c_0^2} \sqrt{\frac{GM}{2\pi r}} \left| \dot{\mathbf{r}} \right| \right) F_{\text{ext}} \right) . \quad (243)$$

where  $F_{\text{ext}}$  is radially outward. Only three specific cases are needed to describe the gravitic energy problem.

The first is a test body fixed in the Earth's field. Eq.(242) indicates that the external upward force required to hold the body fixed is,

$$\mathbf{F}_{\text{ext}} = \hat{\mathbf{r}} \gamma \frac{GMm_0}{4\pi r^2} . \quad (244)$$

Present day interpretations of energy in relativity are a strange mix of Newtonian ideas and "relativistic" motion factors. Conventionally, the work (energy) required to *slowly* raise such a test body from the Earth's surface to infinity is defined as,

$$W = \int_{r_{\text{ea}}}^{\infty} F_{\text{ext}} dr = m_0 c_0^2 \left( \frac{\gamma_s - 1}{\gamma_s} \right) , \quad (245)$$

where  $\gamma_s$ , is the value at the Earth's surface.

In gravitic energy situations,  $\gamma_s$  is usually so close to unity that it is useful to introduce the increment  $\delta = \gamma - 1$  instead. To get some idea of the amounts of the energies involved, Eq.(245) becomes  $W \cong \delta_s m_0 c_0^2 = \delta_s E_0$ , where  $\delta_s \cong 7 \times 10^{-10}$ . Thus, energies involved in test body motion are smaller than the body's rest energy by a factor of about  $10^{-9}$ , and essentially a negligible fraction of the source body energy. With this in mind, if a test body is slowly *lifted* from the Earth's surface to outer space, using an hypothetical elevator attached to Earth, work or energy  $\delta_s E_0$  (Newtonian) or slightly *less* than  $\delta_s E_0$  (relativistic, Eq.245) is required conventionally. Actually the test body energy is *lowered* from  $\gamma_s E_0$  to  $E_0$ , and the elevator gives  $\delta_s E_0$  back to the source (Earth).

---

33. R.H.Dishington, Apeiron, 5, 1 (1998). Presented at Symposium *The Present Status of the Quantum theory of Light*, York University, Toronto, Canada, August (1995).

The second case is that of a test body free-falling in the field from  $r \rightarrow \infty$  to the Earth's surface, neglecting air friction. Since  $F_{\text{ext}} = 0$ , if the initial velocity is  $\mathbf{u} = 0$ , *then the test body remains at rest in the primary inertial system all the way down*, so that  $\mathbf{u} = \overline{\overline{\mathbf{V}}}_e$  and, from Eq.(236),  $\gamma = 1$ . This reduces Eq. (243) to,

$$\frac{d\mathbf{u}}{dt} = -\hat{\mathbf{r}} \frac{GM}{4\pi r^2} \quad . \quad (246)$$

Just before making contact with the Earth's surface, the test body velocity is,

$$\mathbf{u}_s = -\hat{\mathbf{r}} \sqrt{\frac{GM_{\text{ea}}}{2\pi r_{\text{ea}}}} \quad . \quad (247)$$

In test body cases, the slick Newtonian approximation obscures the true problem. It describes a free-falling mass as converting "potential" to "kinetic" energy and carrying the latter to the source body, which ultimately absorbs the "kinetic" energy as heat. However, in connection with Eqs.(246) and (247), the free-falling body ( $E_0$  at  $\infty$ ) is at *rest* in an inertial system, its  $\gamma = 1$ , *undergoing no physical change all the way to the ground*. After the inelastic collision with the Earth, the test body's energy is  $\gamma_s E_0$  (See Eq.241), so it has **gained** energy  $\delta_s E_0$ . This is borne out by the observed change-of-clock-rate and red-shift in a gravitic field. In addition, there is an *equal* amount of heat generated, so a total of  $2\delta_s E_0$  *suddenly* appears in the collision. Clearly *it comes from the source, not the test body*, meaning that all of these energies are electric, localized in the bodies and conserved. Since the "binding" energy is just that lost to heat, it also is localized and electric in nature. So, the "kinetic" and "potential" energies of Newtonian theory are just artificial bookkeeping tricks to allow easy calculation of the heat energy generated, ignoring the energy increase of the body after it is stopped.

The third case is that of a test body *shot* vertically from the earth's surface with a velocity the negative of that given in Eq.(247), again neglecting air friction. With  $F_{\text{ext}} = 0$ , it follows that,

$$\mathbf{u} = \overline{\overline{\mathbf{V}}}_e = \hat{\mathbf{r}} \sqrt{\frac{GM}{2\pi r}} \quad , \quad (248)$$

$\gamma = 1$ , and the body decelerates to 0 as  $r \rightarrow \infty$ . From the instant it is free, its energy is  $E_0$  *with all other energy adjusted out through the driving mechanism*. Being at rest in the primary inertial system, it rises with neither "kinetic" nor "potential" energy change, escaping with energy  $E_0$ .

At present, most of what conventionally appear to be gravitic energy phenomena actually are localized electric energy exchanges. Without a few new solutions to certain presently intractable accelerating charge problems, the final word on localized, stored gravitic energy cannot be said.

## General Relativity

In the name of brevity, of the three famous tests for General Relativity, demonstrations of two are not included here. The "gravitational red shift" was derived above, but the "advance of the perihelion" and the "bending of a light beam" are not. They are, however, carried out in detail in PHYSICS 2001Rev, with each step visualizable and following cause and effect. No curved space, relativity or other exotic concept is used to get the well-known results.

## XXV THE CONSERVATION LAW

### Introduction

For more than 150 years, starting with mechanical systems, the fact that certain quantities such as energy, momentum, etc. are constant in physical processes has led to an increasing number of conservation laws. With the advent of quantum physics, new conserved quantities, such as baryon and lepton numbers, have been found. In these new cases, the question of just what is being conserved arises. Moreover, it is clear that the same lack of understanding applies to the "classical" laws, since no conventional theory explains just what "energy" or "momentum" really are, for example.

Recently, much emphasis has been placed on the related transformation symmetry properties, and the realization that gauge transformation symmetries are the source of certain quantum conservation laws. However, in spite of the insight this approach has provided, in no case has true understanding of "what it is" that is conserved been forthcoming.

The following account suggests that, rather than the multiplicity of conservation laws now in use, a single conservation law produces all of the effects now ascribed to the many; and further, the one quantity that is being conserved is shown to be the ether.

### The Conservation Law<sup>34</sup>

In Section VI the *conservation of ether* was described by the *kinematic* relationship known as the continuity equation,

$$\nabla \cdot (\phi_a \mathbf{V}) = - \frac{\partial \phi_a}{\partial t} \quad ; \quad (248)$$

and in APPENDIX C its separated forms are given as,

$$\nabla \cdot (\overline{\phi_a \mathbf{V}}) + \frac{\partial \overline{\phi_a}}{\partial t} = 0 \quad , \quad \nabla \cdot \{\phi_a \mathbf{V}\}_\cdot + \frac{\partial \phi_\cdot}{\partial t} = 0 \quad . \quad (249)$$

Each of these equations is a derived conservation law that holds because of the basic ether conservation law of Eq.(248). The second equation indicates that ether is conserved during the passage of any  $\ell$ -wave. The

---

34. R.H.Dishington, Apeiron, 5, p.1, Jan-Apr (1998)



first equation ensures that ether is conserved in bulk motion. It is often written as,

$$\nabla \cdot (\overline{\phi \mathbf{u}}) + \frac{\partial \overline{\phi}}{\partial t} = 0 \quad . \quad (250)$$

### Charge Conservation

The conservation of charged *particles* is well known and easily derived using Maxwell's macroscopic equations. It has an exact parallel in the microscopic case. To show that the distributed charge distortion in the ether is conserved, add the divergence of Eq.(75) to the partial time derivative of Eq.(72) and transpose the signs, with the result,

$$\nabla \cdot (\rho \mathbf{u}) + \frac{\partial \rho}{\partial t} = -\nabla^2 C + \frac{1}{c_0^2} \frac{\partial^2 C}{\partial t^2} \quad ,$$

where,

$$C = \nabla \cdot (\overline{\phi_a \mathbf{V}}) + \frac{\partial \overline{\phi_a}}{\partial t} = 0 \quad . \quad (251)$$

So because, *and only because*, ether is conserved according to Eq.(249), distributed charge distortion is conserved.

### E & B form of Maxwell's equations

It is instructive to review the conventional form of Electrodynamics. The electric field  $\mathbf{E}$  and the magnetic field  $\mathbf{B}$  are defined in terms of forces on whole charged particles. Maxwell's "force field" equations, i.e. written in terms of  $\mathbf{E}$  and  $\mathbf{B}$ , can be derived, for the case of free charges in space (absence of matter), from the bulk Eqs.(2), with the result,

$$\nabla \cdot \mathbf{E} = \rho - \frac{1}{c_0^2} \frac{\partial C}{\partial t} \quad , \quad \nabla \times \mathbf{B} = \frac{1}{c_0} \left( \rho \mathbf{u} + \frac{\partial \mathbf{E}}{\partial t} \right) + \frac{1}{c_0} \nabla C \quad , \quad (252)$$

and the identities,

$$\nabla \cdot \mathbf{B} = 0 \quad , \quad \nabla \times \mathbf{E} = -\frac{1}{c_0} \frac{\partial \mathbf{B}}{\partial t} \quad . \quad (253)$$

Eqs.(252) reduce to the usual forms *only because* ether is conserved ( $C = 0$ ). Both Eqs.(252) and (253) are valid macroscopically and microscopically.

### Energy Conservation

In contrast to the simplicity of charge conservation, energy conservation is complicated. First, energy comes in so many forms. Second, no *conventional* visualization of the internal mechanism is available in many situations. Finally, the whole conventional structure of equivalent energies in the different forms is based on "forces". As discussed in 2001Rev, Chapter 12, in the ether, there are no forces. Particles flow. Here the concept of work (force) is used as a convenience, whereas the different forms of energy have been given a visualizable mechanism (see Eqs.65 and 24). Still, *there is, as yet, no overall energy conservation equation*, and each of these different forms must be dealt with individually, as is the custom. There are still certain aspects of

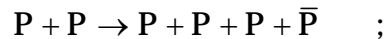
energy that are not understood, even in the context of the unified field theory.

### Other Conservation Laws

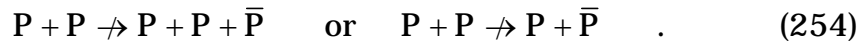
It is clear from the earlier discussion that the conventional description of the quantities being conserved required revisions. The other conservation laws can be understood by considering those same revisions. For example, as described in Section XVIII, momentum and inertia derive from the fact that it takes *time* for electric energy distortion in a particle to physically redistribute itself into another particle and be separated from the first. Ether conservation is again central to the process. *Even in cases involving presently unexplained phenomena such as baryon and lepton number conservation, it is simple to show ether conservation to be the basis.*

In particle experiments, conversion occurs when a single pseudo-stable particle redistributes to a less distorted configuration, or splatter produces a number of by-products during a cataclysmic collision in an interaction between particles (see Section XIV, pg.55). In analyzing which interactions are possible and which are not, it has been found that certain numbers assigned to particles are always conserved, leading to *baryon and lepton number conservation*. What is conserved in these interactions is ether.

A simple example of this is one used by Feynman.<sup>35</sup> Proton-proton bombardment is used to produce anti-protons by the reaction,



but not by,



Violation of baryon number conservation is the conventional explanation. However, from Section XIV, P and  $\bar{P}$  have opposite charge distortions and the  $\bar{\phi}$  ether density patterns are also opposites. Thus,  $P + \bar{P}$  represents zero net ether increment, whereas  $P + P$  represents a *large* ether increment. To conserve ether, there must be the original  $P + P$  increment and no more.  $P + \bar{P}$  adds no more. Both of the interactions of Eq.(254) violate ether conservation. In fact, if vortex conservation is included, all of the cases of baryon and lepton conservation, as conventionally described, are seen to be cases of ether conservation.

*All conservation laws can be traced back to the single conservation of ether law.* In the future, new conservation laws can be found by examining phenomena in the light of the ether physics involved. Much more is discussed in 2001Rev. Still to come will be a *total* energy conservation law, probably to be derived using a four dimensional formalism along the lines investigated by Kirkwood.

---

1. R.P.Feynman, R.B.Leighton, and M.Sands, The Feynman Lectures on Physics, 3, p 25-4, Addison-Wesley Publ. Co., Reading, Mass. (1965).

## APPENDIX A

### EQUATIONS OF THE UNIFIED FIELD

#### Maxwell's Macroscopic Equations

$$\nabla^2 \bar{\phi} - \frac{1}{c_0^2} \frac{\partial^2 \bar{\phi}}{\partial t^2} = -\rho \quad , \quad \nabla^2 (\bar{\phi} \mathbf{u}) - \frac{1}{c_0^2} \frac{\partial^2 (\bar{\phi} \mathbf{u})}{\partial t^2} = -\rho \mathbf{u} \quad , \quad \nabla \cdot \bar{\phi} \mathbf{u} = -\frac{\partial \bar{\phi}}{\partial t}$$

#### Unified Microscopic Equations

##### $\ell$ -wave equations

$$\nabla^2 \bar{\eta} - \frac{1}{c_0^2} \frac{\partial^2 \bar{\eta}}{\partial t^2} - \frac{1}{\bar{\eta}} \left( (\nabla \bar{\eta})^2 - \frac{1}{c_0^2} \left( \frac{\partial \bar{\eta}}{\partial t} \right)^2 \right) = \pm \frac{c_0 \omega}{\phi_d D} \nabla \cdot \bar{\phi} \bar{\mathbf{V}} \quad (\text{traveling})$$

$$\nabla^2 \bar{\eta} - \frac{1}{c_0^2} \frac{\partial^2 \bar{\eta}}{\partial t^2} = 0 \quad (\text{standing}) \quad , \quad \bar{\eta} = \bar{\mathbf{V}}^2$$

$$\phi_d \nabla \cdot \bar{\mathbf{V}} + \frac{\partial \bar{\phi}}{\partial t} \cong 0 \quad (\text{conservation}) \quad , \quad \omega = \mathcal{G}(\phi_m) \quad (\text{compr./osc.})$$

##### the bridge equation

$$\nabla \bar{\phi} + \frac{1}{c_0^2} \frac{\partial \bar{\phi}_a \bar{\mathbf{V}}}{\partial t} = \mathbf{b} \bar{\phi} \bar{\mathbf{V}}$$

##### bulk equations

$$\bar{\phi} \mathbf{u} = \bar{\phi}_a \bar{\mathbf{V}} \quad (\text{apparent flow}) \quad , \quad \nabla \cdot (\bar{\phi} \mathbf{u}) + \frac{\partial \bar{\phi}}{\partial t} = 0 \quad (\text{conservation})$$

$$\varepsilon_e = \frac{1}{2} \left( (\nabla \bar{\phi})^2 - \frac{1}{c_0^2} \left( \frac{\partial \bar{\phi}}{\partial t} \right)^2 \right) \quad (\text{gradient squared distortion})$$

$$\rho = - \left( \nabla^2 \bar{\phi} - \frac{1}{c_0^2} \frac{\partial^2 \bar{\phi}}{\partial t^2} \right) \quad (\text{surrounding function distortion})$$

$$\rho \mathbf{u} = - \left( \nabla^2 (\bar{\phi} \mathbf{u}) - \frac{1}{c_0^2} \frac{\partial^2 (\bar{\phi} \mathbf{u})}{\partial t^2} \right) \quad (\text{bulk flow}) \quad , \quad \nabla^2 \bar{\mathbf{V}} - \frac{1}{c_0^2} \frac{\partial^2 \bar{\mathbf{V}}}{\partial t^2} = 0 \quad (\text{vortex})$$

##### Maxwell's microscopic equations

$$\rho = - \left( \nabla^2 \bar{\phi} - \frac{1}{c_0^2} \frac{\partial^2 \bar{\phi}}{\partial t^2} \right) \quad , \quad \rho \mathbf{u} = - \left( \nabla^2 (\bar{\phi} \mathbf{u}) - \frac{1}{c_0^2} \frac{\partial^2 (\bar{\phi} \mathbf{u})}{\partial t^2} \right) \quad , \quad \nabla \cdot \bar{\phi} \mathbf{u} = -\frac{\partial \bar{\phi}}{\partial t}$$

## APPENDIX B

### UNITS

Table B.1

To obtain the quantity in HLU, multiply the MKS quantity by the factor given. To go from HLU to MKS, divide.

	HLU	MKS
Electric Potential	$\bar{\phi}$	$9.40967 \times 10^{-4}$ Volts
Magnetic Vector-Potential	<b>A</b>	$2.82095 \times 10^5$ Webers/m
Energy	$\mathcal{E}$	$10^7$ Joules
Energy Density	$\varepsilon$	10 Joules
Charge	$q$	$1.06274 \times 10^{10}$ Coulombs
Charge Density	$\rho$	$1.06274 \times 10^4$ Coulombs/m
Current	$i$	$1.06274 \times 10^{10}$ Amperes
Resistance	$\mathbb{R}$	$8.85419 \times 10^{-14}$ Ohms
Capacitance	$C$	$1.12941 \times 10^{13}$ Farads
Inductance	$L$	$8.85419 \times 10^{-14}$ Henrys
Electric Intensity	<b>E</b>	$9.40967 \times 10^{-6}$ Volts/m
Magnetic Induction	<b>B</b>	$2.82095 \times 10^3$ Teslas
Electric Displacement	<b>D</b>	$1.06274 \times 10^6$
Magnetic intensity	<b>H</b>	$3.54491 \times 10^{-3} \frac{\text{Amp Turns}}{\text{m}}$

Table B.2

Electric Energy Density	$\varepsilon_e$ (ergs/cm <sup>3</sup> ) = $10^{-1} \varepsilon_{\text{mks}}$ (Joules/m <sup>3</sup> )
Energy	$\mathcal{E}$ (ergs) = $10^{-7} \mathcal{E}_{\text{mks}}$ (Joules)

Table B.3

Starred quantities are Gaussian. Listed quantities are substituted directly. Quantities along rows are equal.

	HLU	MKS	EMU	ESU
Electric Potential	$\phi$	$\frac{10^8}{c_0\sqrt{4\pi}} \phi_{\text{mks}}$	$\frac{1}{c_0\sqrt{4\pi}} \phi_{\text{m}}$	$\frac{1}{\sqrt{4\pi}} \phi_{\text{s}}^*$
Magnetic Vector Potential	$\mathbf{A}$	$\frac{10^6}{\sqrt{4\pi}} \mathbf{A}_{\text{mks}}$		$\frac{1}{\sqrt{4\pi}} \mathbf{A}_{\text{s}}^*$
Charge	$q$	$\frac{c_0\sqrt{4\pi}}{10} q_{\text{mks}}$	$c_0\sqrt{4\pi} q_{\text{m}}$	$\sqrt{4\pi} q_{\text{s}}^*$
Current	$i$	$\frac{c_0\sqrt{4\pi}}{10} i_{\text{mks}}$	$c_0\sqrt{4\pi} i_{\text{m}}$	$\sqrt{4\pi} i_{\text{s}}^*$
Electric Intensity	$\mathbf{E}$	$\frac{10^6}{c_0\sqrt{4\pi}} \mathbf{E}_{\text{mks}}$	$\frac{1}{c_0\sqrt{4\pi}} \mathbf{E}_{\text{m}}$	$\frac{1}{\sqrt{4\pi}} \mathbf{E}_{\text{s}}^*$
Magnetic Intensity	$\mathbf{H}$	$\sqrt{4\pi}10^{-3} \mathbf{H}_{\text{mks}}$ (A.T./m)	$\frac{1}{\sqrt{4\pi}} \mathbf{H}_{\text{m}}^*$	$\frac{1}{c_0\sqrt{4\pi}} \mathbf{H}_{\text{s}}$
Electric Displacement	$\mathbf{D}$	$\sqrt{4\pi}10^{-5} \mathbf{D}_{\text{mks}}$	$\frac{c_0}{\sqrt{4\pi}} \mathbf{D}_{\text{m}}$	$\frac{1}{\sqrt{4\pi}} \mathbf{D}_{\text{s}}^*$
Magnetic Induction	$\mathbf{B}$	$\frac{10^4}{\sqrt{4\pi}} \mathbf{B}_{\text{mks}}$ (Teslas)	$\frac{1}{\sqrt{4\pi}} \mathbf{B}_{\text{m}}^*$	$\frac{c_0}{\sqrt{4\pi}} \mathbf{B}_{\text{s}}$
Magnetic Moment	$\mu$	$10^3\sqrt{4\pi} \mu_{\text{mks}}$	$\sqrt{4\pi} \mu_{\text{m}}^*$	$\frac{\sqrt{4\pi}}{c_0} \mu_{\text{s}}$
Conductivity	$\sigma$	$\frac{4\pi c_0^2}{10^9} \sigma_{\text{mks}}$	$4\pi c_0^2 \sigma_{\text{m}}$	$4\pi \sigma_{\text{s}}^*$
Resistance	$\mathbb{R}$	$\frac{10^9}{4\pi c_0^2} \mathbb{R}_{\text{mks}}$	$\frac{1}{4\pi c_0^2} \mathbb{R}_{\text{m}}$	$\frac{1}{4\pi} \mathbb{R}_{\text{s}}^*$
Capacitance	$C$	$\frac{4\pi c_0^2}{10^9} C_{\text{mks}}$	$4\pi c_0^2 C_{\text{m}}$	$4\pi C_{\text{s}}^*$
Inductance	$\mathbb{L}$	$\frac{10^9}{4\pi c_0^2} \mathbb{L}_{\text{mks}}$	$\frac{1}{4\pi c_0^2} \mathbb{L}_{\text{m}}$	$\frac{1}{4\pi} \mathbb{L}_{\text{s}}^*$

## APPENDIX C

### SEPARATION EQUATIONS

$$\phi = \bar{\bar{\phi}} + \phi, \quad \mathbf{V} = \bar{\bar{\mathbf{V}}} + \mathbf{V}, \quad \mathbf{a} = \bar{\bar{\mathbf{a}}} + \mathbf{a}.$$

$$\phi_a = \phi_d + \phi = \phi_d + \bar{\bar{\phi}} + \phi = \bar{\bar{\phi}}_a + \phi.$$

$$\bar{\bar{\mathbf{a}}} = \frac{\partial \bar{\bar{\mathbf{V}}}}{\partial t} + \bar{\bar{\mathbf{V}}} \cdot \nabla \bar{\bar{\mathbf{V}}} + \overline{\mathbf{V} \cdot \nabla \mathbf{V}}, \quad \mathbf{a} = \frac{\partial \mathbf{V}}{\partial t} + \bar{\bar{\mathbf{V}}} \cdot \nabla \mathbf{V} + \mathbf{V} \cdot \nabla \bar{\bar{\mathbf{V}}} + \{\mathbf{V} \cdot \nabla \mathbf{V}\}.$$

$$\overline{\phi_a \mathbf{V}} = \bar{\bar{\phi}}_a \bar{\bar{\mathbf{V}}} + \overline{\phi \cdot \mathbf{V}} \quad (\text{bulk}), \quad \{\phi_a \mathbf{V}\} = \bar{\bar{\phi}}_a \mathbf{V} + \phi \cdot \bar{\bar{\mathbf{V}}} + \{\phi \cdot \mathbf{V}\} \quad (\ell\text{-wave})$$

$$\bar{\bar{\mathbf{V}}} = -\frac{\overline{\phi \cdot \mathbf{V}}}{\bar{\bar{\phi}}_a} \quad \text{if } (\bar{\bar{\phi}}_a \bar{\bar{\mathbf{V}}} = 0), \quad \bar{\bar{\mathbf{a}}} = \overline{\mathbf{V} \cdot \nabla \mathbf{V}} \quad \text{if } (\bar{\bar{\mathbf{V}}} = 0)$$

$$\nabla \cdot (\overline{\phi_a \mathbf{V}}) + \frac{\partial \bar{\bar{\phi}}_a}{\partial t} = 0 \quad (\text{bulk}), \quad \nabla \cdot \{\phi_a \mathbf{V}\} + \frac{\partial \phi}{\partial t} = 0 \quad (\ell\text{-wave})$$

$$\nabla \cdot (\bar{\bar{\phi}}_a \bar{\bar{\mathbf{V}}}) + \nabla \cdot (\overline{\phi \cdot \mathbf{V}}) + \frac{\partial \bar{\bar{\phi}}_a}{\partial t} = 0 \quad (\text{Bulk})$$

$$\nabla \cdot (\bar{\bar{\phi}}_a \mathbf{V}) + \nabla \cdot (\phi \cdot \bar{\bar{\mathbf{V}}}) + \nabla \cdot \{\phi \cdot \mathbf{V}\} + \frac{\partial \phi}{\partial t} = 0, \quad (\ell\text{-wave})$$

## APPENDIX D

### TRUNCATION INTEGRALS

1.  $\int_0^x \varepsilon^{-1/y} dy = T(x)$     The truncation integral.
2.  $\int_0^x \varepsilon^{-a/y} dy = a T\left(\frac{x}{a}\right)$
3.  $\int_0^x y \varepsilon^{-a/y} dy = \frac{x^2}{2} \varepsilon^{-a/x} - \frac{a^2}{2} T\left(\frac{x}{a}\right)$
4.  $\int_0^x y^2 \varepsilon^{-a/y} dy = \left(\frac{x^3}{3} - \frac{ax^2}{2 \cdot 3}\right) \varepsilon^{-a/x} + \frac{a^3}{2 \cdot 3} T\left(\frac{x}{a}\right)$
5.  $\int_0^x y^3 \varepsilon^{-a/y} dy = \left(\frac{x^4}{4} - \frac{ax^3}{3 \cdot 4} + \frac{a^2 x^2}{2 \cdot 3 \cdot 4}\right) \varepsilon^{-a/x} - \frac{a^4}{2 \cdot 3 \cdot 4} T\left(\frac{x}{a}\right)$
6.  $\int_0^x y^n \varepsilon^{-a/y} dy = \left(\frac{x^{n+1}}{n+1} - \frac{ax^n}{n(n+1)} + \frac{a^2 x^{n-1}}{(n-1)n(n+1)} - \dots \dots \dots \right. \\ \left. \dots \dots \dots \pm \frac{a^{n-1} x^2}{(n+1)!}\right) \varepsilon^{-a/x} \mp \frac{a^{n+1}}{(n+1)!} T\left(\frac{x}{a}\right)$
7.  $\int_0^x \frac{\varepsilon^{-a/y}}{y^2} dy = \frac{\varepsilon^{-a/x}}{a}$
8.  $\int_0^x \frac{\varepsilon^{-a/y}}{y^3} dy = \frac{\varepsilon^{-a/x}}{a^2} \left(1 + \frac{a}{x}\right)$
9.  $\int_0^x \frac{\varepsilon^{-a/y}}{y^4} dy = \frac{2\varepsilon^{-a/x}}{a^3} \left(1 + \frac{a}{x} + \frac{a^2}{2x^2}\right)$
10.  $\int_0^x \frac{\varepsilon^{-a/y}}{y^n} dy = \frac{(n-2)! \varepsilon^{-a/x}}{a^{n-1}} \left(1 + \frac{a}{x} + \frac{a^2}{2! x^2} + \frac{a^3}{3! x^3} + \dots \dots + \frac{a^{n-2}}{(n-2)! x^2}\right)$
11.  $Q(x) = \varepsilon^{1/x} T(x)$     ,     $T(x) = \varepsilon^{-1/x} Q(x)$
12.  $\frac{dQ(x)}{dx} = 1 - \frac{1}{x^2} Q(x)$

x	T(x)	x	T(x)
0.05	$4.7024 \times 10^{-12}$	7.00	4.5615
0.10	$3.8302 \times 10^{-7}$	7.50	4.9971
0.15	$2.2539 \times 10^{-5}$	8.00	5.4365
0.20	$1.9929 \times 10^{-4}$	8.50	5.8794
0.25	$7.9955 \times 10^{-4}$	9.00	6.3254
0.30	$2.1277 \times 10^{-3}$	9.50	6.7742
0.35	$4.4403 \times 10^{-3}$	10.0	7.2254
0.40	$7.9190 \times 10^{-3}$	11.0	8.1345
0.45	$1.2674 \times 10^{-2}$	12.0	9.0512
0.50	$1.8767 \times 10^{-2}$	13.0	9.9743
0.55	$2.6207 \times 10^{-2}$	14.0	10.9029
0.60	$3.4990 \times 10^{-2}$	15.0	11.8362
0.65	0.04508	16.0	12.7737
0.70	0.05645	17.0	13.7149
0.75	0.06903	18.0	14.6593
0.80	0.08279	19.0	15.6067
0.85	0.09766	20.0	16.5567
0.90	0.11361	25.0	21.3385
0.95	0.13057	30.0	26.1594
1.00	0.14850	35.0	31.0076
1.20	0.2288	40.0	35.8759
1.40	0.3214	45.0	40.7595
1.60	0.4241	50.0	45.6552
1.80	0.5351	55.0	50.5608
2.00	0.6532	60.0	55.4746
2.50	0.9734	65.0	60.3952
3.00	1.3207	70.0	65.3216
3.50	1.6881	75.0	70.2531
4.00	2.0709	80.0	75.1890
4.50	2.4660	85.0	80.1287
5.00	2.8710	90.0	85.0719
5.50	3.2842	95.0	90.0181
6.00	3.7044	100.0	94.9671
6.50	4.1304	$x \rightarrow \infty, T(x) \rightarrow x - \log_e x$	